

Chlorination of Sulfonamide Antibiotics:
Products, Proposed Pathways, and Putative Mechanisms

A Thesis

Presented to the Faculty of the Graduate School of

Cornell University

In Partial Fulfillment of the Requirement for the Degree of

Master of Science

by

Mian Wang

August 2015

© 2015 Mian Wang

ABSTRACT

During drinking water treatment, micropollutants can react with free available chlorine (FAC) resulting in the formation of potentially toxic disinfection byproducts (DBPs). Sulfonamide antibiotics are a group of micropollutants commonly detected in drinking water resources and their occurrence pose threats to public health. Previous researchers have reported on structures of disinfection byproducts of sulfamethoxazole in reactions with FAC. However, relatively few products were found and little is known about products of reactions between other sulfonamide antibiotics and FAC. The objective of this research was to investigate three sulfonamide antibiotics to address the following questions: (1) what are the structures of the DBPs formed in the sulfonamide-FAC reaction?; (2) what are the likely oxidation reaction pathways?; and (3) what reaction mechanisms are common to the three sulfonamide antibiotics? The micropollutants were spiked individually into batch reactors infused with a range of FAC concentrations. Samples from the reactors were separated with HPLC and the residual sulfonamide antibiotic concentrations were measured with UV-VIS to observe products. To determine the products of the reaction, samples from same reactors were separated with HPLC and analyzed by quadrupole-orbitrap mass spectrometry. A non-target screening workflow was developed using the Sieve software and applied to analyze high-resolution mass spectrometry acquisitions for potential chlorination products. Structures were proposed for 16, 18, and 16 DBPs of sulfamethoxazole, sulfadimethoxine, and sulfathiazole, respectively. The structures are supported with both analytical data and a discussion of chlorine reaction mechanisms reported in the literature. Common reactions that were

observed for all three sulfonamide antibiotics include N-chlorine substitution, hydrolysis initiated by S-N bond cleavage, hydrolysis initiated by S-C bond cleavage, hydroxylation, and SO₂ extrusion. These observations are important in extrapolating this work to other sulfonamide antibiotics that have not yet been studied.

BIOGRAPHICAL SKETCH

I am truly grateful for all the luck that I have ever been blessed with. Being born as the child of my parents and becoming a student of Dr. Helbling's are the greatest luck I have ever had.

Growing up as the daughter of my parents, I am always a happy child. Seeing how much my parents love and support each other, I grow up believing in love. My eventual goal in life is to become a person that has the ability to protect people that she loves.

Becoming a student of Dr. Helbling is the best thing that ever happened to me in years. No one could expect a better advisor than Dr. Helbling. The advice, support and care I got from Dr. Helbling are the most precious treasures I have ever received. Being super devoted and dedicated into research and into helping his students, Dr. Helbling is not only my advisor, but also my role model. I wish one day, over effort of a life-time, I could become someone like Dr. Helbling— being truly genuine and respectful to people, work, and science; being curious about the wonderings in nature and in life; and being super cool.

I hope one day, through endless effort, I could become a beautiful woman, who has a deep understanding of what she does, and is capable of loving herself and loving others. I hope I could live my life to the fullest, yet being responsible to people that love and care about me. And this thesis, in which effort, logic and innovation are valued, is the start.

ACKNOWLEDGEMENT

First of all, I would like to thank Dr. Helbling for all the help he gives me. Dr. Helbling is the best advisor a student could ever imagine. Words are too pale to describe how much I appreciate the help that Dr. Helbling offers to me: the in-person demonstrations he provides in operating HPLC-UV and HPLC-MS, the inspirations and instructions he gives me in the research, the patience and encouragements he has for me: instead of telling me answers, he leads me into thinking on my own. Dr. Helbling not only teaches me facts, answers to questions, but also how to think about questions. And above all, he made my graduate school experience very delightful and enjoyable. The help and care Dr. Helbling gives me has far exceeded what I expected from an advisor. I am truly, truly grateful. And I think after graduation, I would miss this experience so much. In fact, I am already nostalgic about the happy times I had when Dr. Helbling was in lab doing experiments by my side. Going to lab was the happiest thing to do in a day over that summer.

Secondly, I would like to thank Dr. Gossett for being my minor advisor. I truly enjoyed every minute in the Biological Processes class and I learned a lot from it.

Last but not least, I would like to thank my family, my friends and everyone in my research group. Maybe years later when I recall these two years, I would not remember what grades I got, what projects I did, but I would always remember those happy times: warm street lights, pouring midnight rain, soft moonlight, red wine, cold beer, waterfalls, our laughter and the hot summer nights.

致谢

首先，我要感谢我的导师，赫博林博士 (Dr. Helbling) 给予我的无私帮助。我的导师达冕·赫博林是一个学生所能祈盼的最好的导师。语言已经无法形容我对他的帮助的感激之情：在实验室，他亲自为我示范如何使用高效液相色谱-紫外光度检测和高效液相色谱-质谱仪；在研究中，他从不吝惜给我启示和指导。他对我是那样的有耐心——他不仅授我以鱼，更授我以渔，指引我如何去独立思考。而我的两年的研究生生涯也因为我的导师赫博林博士而十分美好。赫博林博士给我的帮助已经远远超出了我对一个导师所有的期待。我想，毕业之后，我将会无比怀念这两年的时光——事实上，我已经开始怀念在我的导师赫博林博士身边做实验的那些日子，那些幸福时光。那年夏天，去实验室是每天中最快乐的事情了。

其次，我要感谢我的另一位导师，高赛特博士 (Dr. Gossett)。我诚挚地爱着他所教授的生物过程这门课程的每一分钟。从这门课里，我学到了很多知识。

最后，我要感谢我的家人，朋友，和我实验室的每一个人。也许很多年后，在我再次回想起这两年的时光，我并不会记得我考了多少分，我做了什么项目。但是，我想我永远都会记得那些快乐时光：暖色的街灯，午夜倾盆而下的雨，暖纱般的月色，红酒，冰啤酒，瀑布泠淙，你的眼神我的笑语，和那些暖暖的，伊萨卡的夏夜。

Table of Contents

ABSTRACT.....	III
BIOGRAPHICAL SKETCH.....	V
ACKNOWLEDGEMENT.....	VI
致谢	VII
LIST OF FIGURES	XI
LIST OF TABLES	XIV
CHAPTER 1 INTRODUCTION.....	1
1.1 Context.....	1
1.2 Objectives	3
CHAPTER 2 BACKGROUND.....	4
2.1 Micropollutants	4
2.1.1 Occurrence of micropollutants in ground and surface water resources	5
2.1.2 Occurrence of micropollutants in finished drinking water	6
2.1.3 Toxicity of micropollutants in drinking water	7
2.2 Chlorination and disinfection byproducts	8
2.2.1 Chlorination	8
2.2.2 Conventional disinfection byproducts	9
2.2.3 Emerging disinfection byproducts	9

2.3 Sulfonamide antibiotics	10
2.3.1 Sulfamethoxazole, sulfadimethoxine, and sulfathiazole.....	11
2.3.2 Kinetics of chlorination of sulfonamide antibiotics.....	12
2.3.2 Chlorination products of SMX.....	13
2.3.2.1 Chlorination products, reaction pathways and mechanisms of SMX proposed by Dodd	14
2.3.2.2 Chlorination products, reaction pathways and mechanisms of SMX proposed by Gao et al.	15
CHAPTER 3 MATERIALS AND METHODS.....	17
3.1 Standards and reagents.....	17
3.2 Experimental procedures	17
3.3 Analytical methods	21
3.4 Disinfection byproduct identification	22
3.4.1 Identification of peaks observed by HPLC-UV-VIS	22
3.4.2 Identification of other masses	23
CHAPTER 4 RESULTS AND DISCUSSION.....	29
4.1 Product identification.....	29
4.1.1 Identification of peaks observed by HPLC-UV-VIS	29
4.1.2 Identification of masses observed by HPLC-MS.....	33
4.1.3 Comparing peaks from UV to MS	37
4.2 Proposed reaction pathways and putative mechanisms	39
4.2.1 Reaction pathways of SMX-FAC	39

4.2.2 Reaction pathways of SDM-FAC	45
4.2.3 Reaction pathways of STZ-FAC.....	50
4.3 Reaction mechanisms proposal.....	54
4.4 Environmental relevance	55
CHAPTER 5 CONCLUSION.....	57
REFERENCES.....	61

LIST OF FIGURES

Figure 1: Chlorination products and reaction pathways of SMX proposed by Dodd and Huang. Compounds in brackets are proposed intermediates. $[M+H]^+$ is the nominal mass. RT is the reported retention time of each product.	14
Figure 2: Chlorination products and reaction pathways of SMX proposed by Gao et al. (2014). Compounds in brackets are proposed intermediates or end products. Compounds in brackets are proposed intermediates. $[M+H]^+$ is the mass acquired by LC-MS. RT is the reported retention time of each product.	16
Figure 3: Summary of procedures of chlorination reaction experiments.	20
Figure 4: Sieve workflow developed for candidate DBP identification.	24
Figure 5: Workflow in product identification using the Sieve software. Numbers here show general reduction of candidate DBP frames. Real numbers of frames of candidate DBP will be given for each compound later in the thesis.	26
Figure 6: Reconstructed ion chromatograms in sieve: a) a real peak b) not a real peak..	27
Figure 7: Separation of DBPs at six chlorination levels observed by HPLC-UV: a) full DBP peaks in SMX-FAC, b) full DBP peaks in SDM-FAC, c) full DBP peaks in STZ - FAC; d) partial DBP peaks in SMX-FAC, e) partial DBP peaks in SDM-FAC, f) partial DBP peaks in STZ-FAC.	30

Figure 8: Peak area trend of each DBP of three sulfonamides as a function of initial FAC level: a) SMX-FAC, b) SDM - FAC, c) STZ – FAC.....	32
Figure 9: Product identification workflow for SMX, SDM and STZ in reaction with FAC in positive mode.....	33
Figure 10: Sieve integrated intensity graph, XIC, and MS spectra, for SMX 298 ($m/z = 298.0488$ for MH^+).	35
Figure 11: Sieve integrated intensity graph, extracted ion chromatogram (XIC), and MS spectra for SDM379 ($m/z = 379.0026$ for MH^+).	37
Figure 12: Matching peaks observed on HPLC - UV and masses/frames obtained by HPLC-MS.	38
Figure 13: Proposed products and pathways for reactions of SMX with FAC. Red arrows show pathways that are initiated directly from SMX. Blue arrows show pathways following initial pathways. Products shown in parentheses are proposed intermediates or products based on putative reaction mechanisms.	40
Figure 14: Proposed products and pathways for reactions of SDM with FAC. Red arrows show pathways that are initiated directly from SDM. Blue arrows show pathways following initial pathways. Products shown in parentheses are proposed intermediates or products based on putative reaction mechanisms.	46

Figure 15: Proposed products and pathways for reactions of STZ with FAC. Red arrows show pathways that are initiated directly from STZ. Blue arrows show pathways following initial pathways. Products shown in parentheses are proposed intermediates or products based on putative reaction mechanisms. 51

LIST OF TABLES

Table 1: Physical chemical properties of SMX, SDM, and STZ.	12
Table 2: Calculated volumes of reagents for each experiment.	18

CHAPTER 1 INTRODUCTION

1.1 Context

Drinking water is one of the most precious natural resources on Earth. Degraded water quality or dwindling water quantity can have negative effects on the environment.

Unfortunately, the quality and quantity of drinking water has been constantly jeopardized by anthropogenic activities, which have released a wide range of pollutants into water systems, posing threats on public health¹⁻³

Pollutants frequently occurring in water resources can be divided into two groups: traditional pollutants which include nitrogen, phosphorous, or petroleum constituents and “emerging” pollutants. Emerging pollutants are characterized here as polar to semi-polar chemicals that are frequently found in drinking water resources in the ng/L to µg/L range⁴ and are consequently referred to as micropollutants. Sulfonamide antibiotics are a group of micropollutants that are widely used in human and veterinary medicine. Sulfonamide antibiotics have the potential to alter the composition of environmental bacterial communities⁵ and to cause or promote antibiotic resistance in bacteria and pathogens⁶. Moreover, some of the sulfonamide antibiotics are proved to be toxic⁷ or carcinogenic⁸.

Drinking water treatment plants are designed to remove contaminants from surface and ground water resources and to protect the public. Whereas conventional drinking water treatment processes are designed to remove traditional pollutants, their ability to remove emerging micropollutants is often inefficient and incomplete.⁴

Disinfection is a critical drinking water treatment process that protects consumers against pathogens and microorganisms. Free available chlorine (FAC) is among the commonly used disinfectants in drinking water treatment. Upon free chlorination, pathogens are inactivated through oxidation of cell membranes and other vital macromolecules.

Meanwhile, other organic matter can also react with FAC and result in the formation of disinfection byproducts (DBPs). Two major classes of DBPs are the trihalomethanes (THMs) and the haloacetic acids (HAAs). Studies have shown that long-term exposure to THMs and HAAs can have toxic effects^{9, 10} and the concentration of these DBPs in drinking water are regulated by the Safe Drinking Water Act¹¹.

Micropollutants are generally persistent through conventional drinking water treatment plants; any observed removal is likely the result of oxidation reactions with disinfectants such as FAC.⁴ However, there are a limited number of studies that explore the reactions that could occur between micropollutants and FAC in drinking water treatment plants and distribution systems. Therefore, major knowledge gaps include understanding which types of micropollutants may undergo oxidation reactions in drinking water treatment plants, understanding the types of reactions and products that may be formed in drinking water treatment plants, and whether or not the products are of concern. It is particularly interesting to study the oxidation of sulfonamide antibiotics as recent evidence has shown that transformation products for a model sulfonamide antibiotic (sulfamethoxazole) may exhibit even more toxicity than sulfamethoxazole itself¹².

1.2 Objectives

Experiments described in this thesis were designed to improve our incomplete understanding of potential DBPs formed in reactions between sulfonamide antibiotics and FAC. Three sulfonamide antibiotics were selected that are representative of the general group of compounds. Specific questions were addressed as follows:

- (1) What are the structures of the disinfection byproducts formed in the sulfonamide-FAC reaction?
- (2) What are the likely oxidation reaction pathways?
- (3) What reaction mechanisms are common to the three sulfonamide antibiotics?

CHAPTER 2 BACKGROUND

2.1 Micropollutants

Abundant, clean, and safe drinking water is among the most essential foundations upon which society lies. The quality and quantity of drinking water could be largely depleted by natural processes, for example, droughts, as well as anthropogenic activities. Along with urbanization and industrialization, anthropogenic activities consume a tremendous amount of fresh water and also release pollutants into fresh water resources through agricultural activities, excretion of human and animal urine and feces, flushing of unused medication, and other household activities.¹³ Contamination of water resources, as a result, could have great impact on human health, ecology, and the economy.

Contaminants in water resources can be divided into two groups: “traditional” pollutants and “emerging” pollutants. “Traditional” pollutants include a broad range of inorganic and organic contaminants whose sources and fate in the environment have been studied for decades. These include nitrogen and phosphorus species, chlorinated solvents used in industry, and petroleum constituents, among others. “Emerging” pollutants include a broad range of chemical and microbiological entities whose sources, fate, and effects in the environment have only been recently elucidated or remain poorly understood. As a result, few or no regulations exist for many emerging pollutants that define monitoring requirements or maximum contaminant limits.¹³

As many emerging contaminants are polar or semi-polar organic chemicals with reported environmental concentrations in ng/L to µg/L concentration range¹⁴, “emerging” pollutants are also referred to as micropollutants⁴. Micropollutants include pesticides¹⁵, pharmaceuticals and personal care products (PPCPs)^{16, 17}, endocrine disrupting compounds (EDCs)¹⁸, ionic liquids¹⁹, artificial sweeteners²⁰, nanomaterials²¹, microorganisms²², perfluorinated compounds²³, flame retardants²⁴, and other anthropogenic compounds²⁵. Given the wide range of micropollutant types, the U.S. Environmental Protection Agency (EPA) has considered addressing micropollutants as groups rather than individual pollutants. This approach is analogous to the way disinfection byproducts (DBPs) and radionuclides have been previously regulated by the EPA.

Clearly, there are many types of micropollutants of concern. The focus of this thesis is on a class of pharmaceuticals known as sulfonamide antibiotics.

2.1.1 Occurrence of micropollutants in ground and surface water resources

Many recent studies have confirmed that micropollutants are widely found in ground and surface water resources. Occurrence of micropollutants has been reported increasingly over the years due to improvements in instrumental analysis including gas chromatography–mass spectrometry (GC-MS), high performance liquid chromatography – UV detection (HPLC-UV), and high performance liquid chromatography - mass spectrometry (HPLC-MS). Benner et al. (2014), compiled data from 27 published studies reporting on the occurrence of 133 pesticides, pesticide transformation products,

pharmaceuticals and other wastewater-derived pollutants in drinking water resources.

This study emphasizes the wide occurrence of a variety of micropollutants in ground and surface water resources all around the world.⁴ In the past few decades, occurrence of micropollutants has been frequently reported in Africa²⁶, Asia²⁷, Australia²⁸, Europe²⁹, and North America³⁰. With these collected data, it is clear that micropollutants affect water quality in water resources around the world.

2.1.2 Occurrence of micropollutants in finished drinking water

We rely on drinking water treatment processes to remove micropollutants from raw water prior to distribution to consumers. Although conventional drinking water processes, which consist of coagulation, flocculation, sedimentation, filtration, and disinfection, have been long employed to reduce turbidity, remove nutrients, and improve the taste and odor of finished drinking water, often the removal of micropollutants by conventional drinking water treatment processes is incomplete and inefficient.⁴ For example, the majority of pesticides and pharmaceuticals are expected to remain partitioned in the aqueous phase during coagulation, flocculation, and sedimentation³¹. Indeed, it has been reported that the removal of certain micropollutants was less than 10% during coagulation, flocculation, and sedimentation.³²⁻³⁴ Experiments have shown that biologically active sand filters can contribute to the removal of some micropollutants.³⁵⁻³⁸ However, many chemicals remain recalcitrant through biofiltration.³⁷

Due to the inefficiency of removing micropollutants by conventional drinking water treatment processes, occurrence of micropollutants in finished water has been frequently

reported.^{39, 40} Common antibiotics, for example, carbadox, sulfachlorpyridazine, sulfadimethoxine, sulfamerazine, sulfamethazine, sulfathiazole, and trimethoprim, could not be removed by conventional drinking water treatment processes effectively or thoroughly^{4, 32}. Concentrations of micropollutants measured in finished water vary from 0.2 ng/L (the non-steroidal anti-inflammatory drug naproxen) to 1413 ng/L (the antibiotic Lincomycin).⁴¹

2.1.3 Toxicity of micropollutants in drinking water

The micropollutants existing in finished water raise concern. Although much is unknown about the potential effects that micropollutants could have on humans, a small subset of micropollutants has been reported to lead to significant developmental, reproductive, endocrine disrupting, and other chronic health effects.⁴²⁻⁴⁴ Many other micropollutants have been shown to have adverse effects on aquatic organisms¹⁸ which should be at least cautionary with respect to human exposure. Effects on aquatic organisms include endocrine disruption⁴⁵, antibiotic resistance⁴⁶, inhibition of primary productivity⁷, among others⁴⁷⁻⁵¹. Therefore, the threats that micropollutants pose on public health call for attention. Studies on micropollutants are essential.

2.2 Chlorination and disinfection byproducts

2.2.1 Chlorination

Disinfection processes protect public health by inactivating parasites, bacteria, and viruses from drinking water. Commonly used disinfectants include FAC, chloramines, chlorine dioxide, ozone, and UV light. FAC, highly oxidative, is widely used as a cost effective disinfectant to stabilize the biological quality of drinking water. Applied as Cl_2 gas or solid NaOCl salts, FAC is defined as the sum of the hypochlorous acid (HOCl) and the hypochlorite ion (OCl^-) concentrations. Reactions that generate HOCl are shown in Equations (1) and (2), and the speciation reaction of HOCl in water is shown in Equation (3). Mechanisms of how FAC inactivates pathogens may involve oxidation of microbial membranes⁵² or inactivation of the electron chain or enzymes⁵³.



However, chlorination has its drawbacks. Chlorine-based disinfectants are persistent in water as long as they are not consumed by either inactivation or competitive reactions.⁵⁴ FAC is a non-selective oxidant that can inactivate a broad range of pathogens⁵⁵, but simultaneously oxidizes natural organic matter⁵⁶, as well as anthropogenic emerging organic matter, leading to the formation of DBPs.

2.2.2 Conventional disinfection byproducts

Formation of DBPs results from both natural organic matter (NOM) and synthetic organic compounds (SOCs). DBPs formed from NOM when in reaction with a disinfectant, usually chlorine, are considered as conventional DBPs. They are of health risk concern⁵⁷ and are regulated under Safe Drinking Water Act¹¹. Currently, U.S. EPA has regulated 11 DBPs for occurrence in drinking water: 5 THMs, 4 HAAs, bromate, and chlorite.

Generally, the toxic effects of chlorinated DBPs are thought to be the result of the chlorine atom(s) on the DBP. Conventional DBPs were observed to be genotoxic and carcinogenic⁵⁸⁻⁶¹; for example, association between exposure to THMs and adverse reproductive outcomes has raised concern.⁶²⁻⁶⁴

2.2.3 Emerging disinfection byproducts

Given that micropollutants widely exist in ground and surface waters and that chlorination is commonly applied in drinking water treatment, the questions of how micropollutants react upon chlorination and whether chlorinated products are formed are important. To address the interaction of micropollutants with chlorine, studies on products of those reactions have been carried out in recent years. To acquire an overall understanding of what has been studied so far, a database summarizing previous studies on chlorination products of micropollutants is provided in Appendix A of this thesis.

A total of 33 compounds that have been found to be parent compound of chlorination products are included in Appendix A. Oxidation reactions, substitution reactions, addition reactions, decarboxylation/hydroxylation reactions, and hydrolysis reactions were commonly observed in reactions between a variety of micropollutants and FAC. Some of the DBPs formed in these reactions were studied with respect to toxicity and several were shown to have toxic effects. For example, in reactions with FAC, salicylic acid could produce halogenated organics with putative toxicity.⁶⁵ Bedner et al. (2006) found that by chlorination processes, acetaminophen could lead to formation of a toxic product, 1,4-benzoquinone.⁶⁶ N-chloro-*p*-benzoquinoneimine, which was found to be a product of sulfamethoxazole in reaction with FAC, might possess higher acute toxicity than its parent substrates.⁶⁷

2.3 Sulfonamide Antibiotics

Consisting of 36 total chemicals⁶⁸, sulfonamide antibiotics are synthetic antimicrobial agents that contain a sulfonamide functional group. Sulfonamide antibiotics are active against a wide range of Gram-positive and -negative bacteria, and they have been extensively used to promote growth rate and weight gain of food animals and are prescribed for treating bacterial infections.⁶⁷ Sulfonamide antibiotics have been detected with maximum concentration up to 110 ng/L in raw drinking water, with maximum concentration of 23 ng/L in finished drinking water, and with concentrations in wastewater orders of magnitude higher.⁴ The frequent occurrence of these antibiotic compounds are possibly due to their extensive usage in agriculture^{69, 70}, their usage in

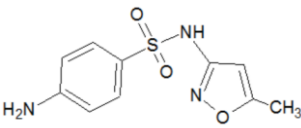
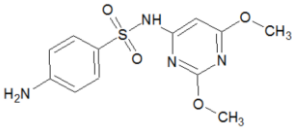
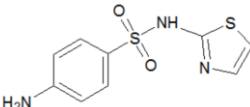
human and veterinary medicine⁷¹, their poor elimination in conventional wastewater treatment plants⁷²⁻⁷⁴, and their relative persistence in the aquatic environment.⁷⁵

The existence of sulfonamide antibiotics poses potential threats to public health. The residues of sulfonamide antibiotics in water resources enhance the risk of developing resistant bacteria and promote the spread of antibiotic resistance genes among bacteria⁴⁶. Moreover, some of the sulfonamide antibiotics are toxic⁷ or carcinogenic⁸.

2.3.1 Sulfamethoxazole, sulfadimethoxine, and sulfathiazole

Among the micropollutants that frequently occur in ground and surface water resources and can be removed by chlorination, three sulfonamide antibiotics, sulfamethoxazole (SMX), sulfadimethoxine (SDM), and sulfathiazole (STZ), especially came to our attention for the following four reasons: 1) SMX, SDM and STZ were all detected in ground and surface water resources^{4, 31, 76}; 2) upon chlorination, their removal rates were all above 50%⁴; 3) they are structurally similar compounds that may enable generalization of results to other sulfonamide antibiotics; 4) some previous research reported the kinetics of reactions between sulfonamide antibiotics and FAC, but only few considered the formation of emerging DBPs. Therefore, we targeted SMX, SDM and STZ in this research and aimed to determine their chlorination products, propose reaction pathways, and discuss chlorination mechanisms. The structures and physical chemical properties of each sulfonamide antibiotic are provided in Table 1.

Table 1: Physical chemical properties of SMX, SDM, and STZ.

Compound	Structure	Molecular Weight, Da	pK _a	logK _{ow} ^a	Water Solubility ^a
SMX		253.0518	pK _{a1} =1.6 pK _{a2} =5.7 ^{77, 78}	0.89	3942 mg/L
SDM		310.0728	pK _{a1} =2.4 pK _{a2} =6.0 ⁷⁹	1.63	433.1 mg/L
STZ		255.0136	pK _{a1} =2.2 pK _{a2} =7.2 ⁷⁸	0.05	20030 mg/L

a. logK_{ow} and water solubility were predicted using EPISuite. Data were acquired on www.chemspider.com.

2.3.2 Kinetics of chlorination of sulfonamide antibiotics

Chamberlain and Adams (2006) studied the kinetics of reactions between FAC and a variety of sulfonamide antibiotics under the assumption of second-order kinetics, that is, first-order with respect to both sulfonamide antibiotic and oxidant concentration.⁸⁰ The second-order kinetics model was previously used to model reactions of caffeine⁸¹ and triclosan⁸² with FAC and was shown to be a good fit to the experimental data. In this model, the overall reaction rate in a batch system for FAC and a sulfonamide was described as in Equations (4) to (7). $C_{Tot,Cl}$ is the concentration of total FAC; $C_{Tot,AB}$ is the concentration of total antibiotic (M); and k is second-order rate constant, ($M^{-1}s^{-1}$):

$$rate(M \cdot s^{-1}) = \frac{dC_{Tot,AB}}{dt} = -kC_{Tot,Cl}C_{Tot,AB} \quad \text{Equation (4)}$$

In which,

$$C_{Tot,Cl} = [HOCl] + [OCl^-] = C_{Tot,Cl} (\alpha HOCl + \alpha OCl^-) \quad \text{Equation (5)}$$

In which,

$$\alpha HOCl = (1 + (10^{-7.6} \times 10^{pH}))^{-1} \quad \text{Equation (6)}$$

$$\alpha OCl^- = 1 - \alpha HOCl \quad \text{Equation (7)}$$

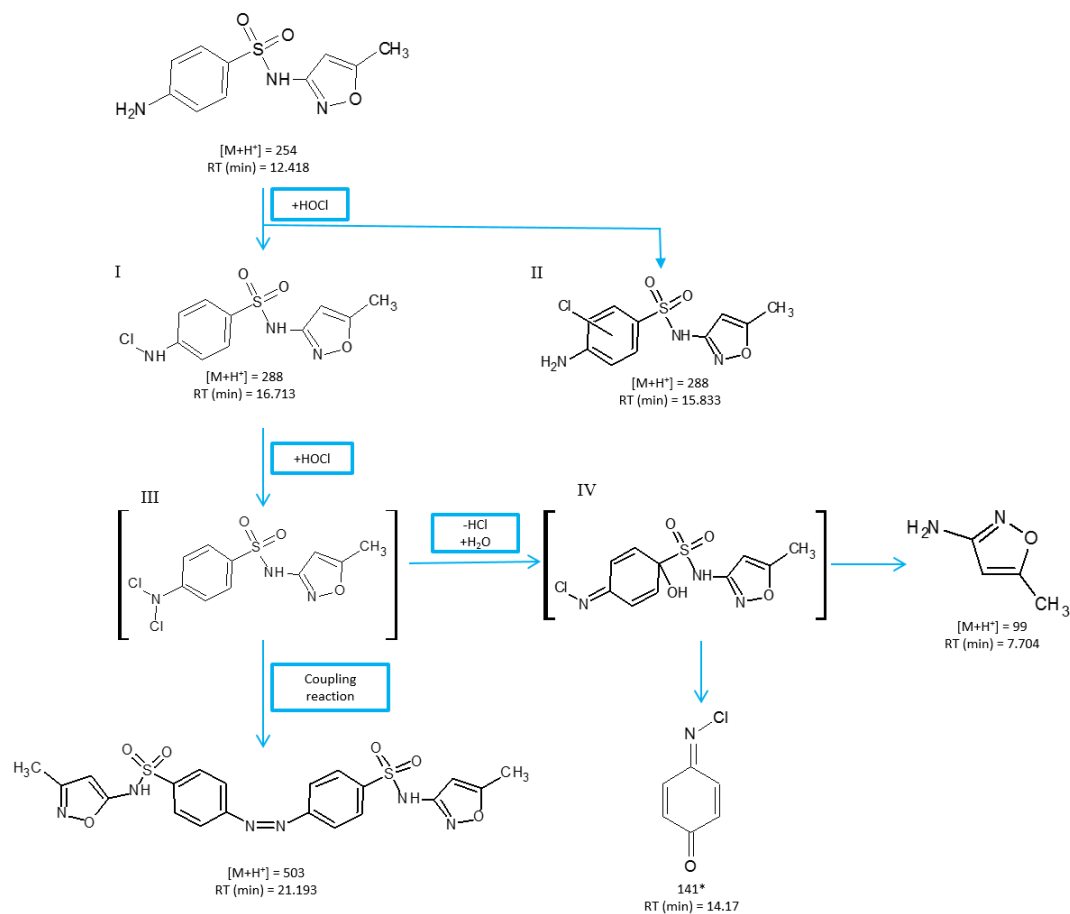
According to the experimental data from Chamberlain and Adams, at pH = 7.6, the experimental second-order rate constants ($k_{exp} (M^{-1}s^{-1})$) for SMX, SDM, and STZ were 924, 19710, and 5986, respectively.⁸⁰ Dodd and Huang also studied the kinetics of SMX in reaction with FAC.⁶⁷ Results from two research groups were in agreement with each other.

2.3.2 Chlorination products of SMX

No previous studies regarding the chlorination products of SDM or STZ were found at the time of the writing of this thesis. For SMX, Dodd and Huang proposed chlorination byproducts pathways and reaction mechanisms in 2004.⁶⁷ Moreover, Gao et al. proposed reaction pathways and mechanisms for SMX when oxidized by chlorine in 2014 as well.⁸³

2.3.2.1 Chlorination products, reaction pathways and mechanisms of SMX proposed by Dodd

A total of five products were identified by Dodd and Huang (2004)⁶⁷ in chlorination reactions with SMX as shown in Figure 1. In under-chlorinated systems, two products were identified. The major one, N-chlorinated SMX288 (I), and the minor one, ring-



* 141 yielded no mass spectrum in their LC/MS, but was detected by GC/MS.

Figure 1: Chlorination products and reaction pathways of SMX proposed by Dodd and Huang. Compounds in brackets are proposed intermediates. $[M+H]^+$ is the nominal mass. RT is the reported retention time of each product.

chlorinated SMX288 (II). In over-chlorinated systems, a prominent product, SMX99, was identified as 3-amino-5-methylisoxazole (AMI). Though with low yield, compounds formed in coupling reactions were also detected. Among those, they were able to identify a dimeric product, SMX503, as azosulfamethoxazole. Though not detected in LC/MS, a major product, SMX141, N-chloro-p-benzo-quinoneimine (NCBQ) was observed with HPLC-UV, isolated via fractionation methods, and analyzed by GC/MS and ¹H NMR.⁶⁷ Reaction pathways of the five identified products and predicted intermediate products were proposed accordingly, as illustrated in Figure 1.

2.3.2.2 Chlorination products, reaction pathways and mechanisms of SMX proposed by Gao et al.

Another study on chlorination products of SMX was published by Gao et al. (2014).⁸³ A total of seven oxidation products were detected and identified. Similar to Dodd's findings, AMI, N-chlorinated SMX, and azosulfamethoxazole were also detected and identified. They did not find NCBQ which was determined as a major product by Dodd et al. (2004), while they found new products. For example, SMX27 was a hydroxylated product formed via the addition of a hydroxyl group to the SMX structure⁸³; SMX282 was produced when the aniline moiety on SMX was oxidized to a nitrobenzene moiety.⁸³ Pathways and reaction mechanisms were proposed accordingly, as shown in Figure 2.

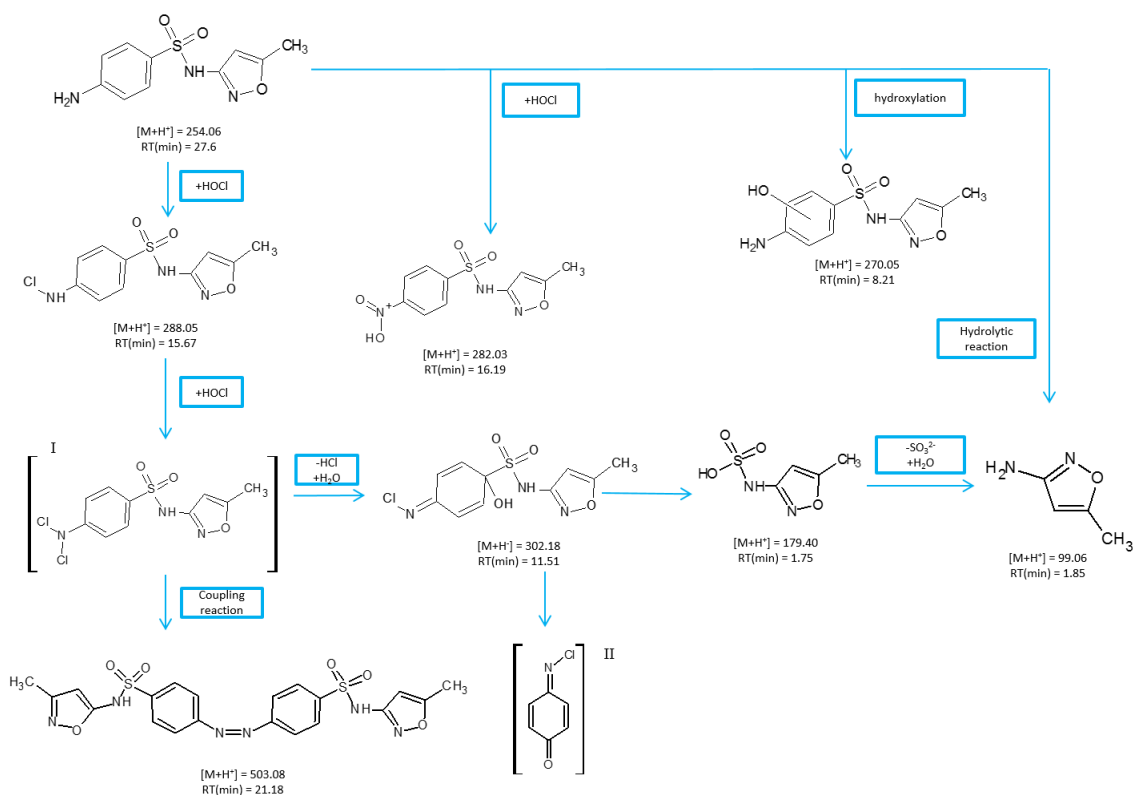


Figure 2: Chlorination products and reaction pathways of SMX proposed by Gao et al. (2014). Compounds in brackets are proposed intermediates or end products. Compounds in brackets are proposed intermediates. $[M+H]^+$ is the mass acquired by LC-MS. RT is the reported retention time of each product.

The objective of this work was to identify products in reactions involving FAC and three sulfonamide antibiotics, propose reaction pathways, and discuss mechanisms of these reactions. By understanding the reaction pathways and mechanisms of sulfonamide antibiotics and FAC, we contribute to filling a knowledge gap in understanding the DBPs of these micropollutants and — with their subsequent, proper regulation — contribute to protection of public health.

CHAPTER 3 MATERIALS AND METHODS

3.1 Standards and reagents

SMX, SDM, and STZ are the three selected sulfonamide antibiotics. SDM and STZ were both obtained from Fluka (Pittsburgh, PA). SMX was obtained from United States Pharmacopeia via Sigma-Aldrich (Rockville, MD). One gram per liter SMX, SDM, STZ stock solutions (for use in HPLC-UV and HPLC-MS product characterization studies) were prepared using 100% HPLC - grade methanol. Stock solutions were stored at -20°C.

A stock solution of 0.02 M potassium phosphate buffer (pH = 7.6) was prepared by combining 86.6 mL 0.2 M K₂HPO₄ and 13.4 mL 0.2 M KH₂PO₄ solutions with 900 mL nanopure water. KH₂PO₄ and K₂HPO₄ were both obtained from Fisher Scientific (Pittsburgh, PA). Aqueous sodium hypochlorite solution (5% chlorine) was obtained from Acros Organics and was diluted to yield both 50 and 500 mg/L FAC reagents. All FAC reagents were freshly prepared before each experiment.

3.2 Experimental procedures

Experiments with FAC and each sulfonamide antibiotic were carried out at a pH of 7.6 and solutions were chlorinated to six different levels to achieve conditions of under- and over- chlorination. To ensure that chlorination products could be detected in the analytical procedure with no limitations due to detection limits, relatively high initial concentrations of sulfonamide antibiotics were investigated. We chose 10 mg/L as the initial concentration of sulfonamide antibiotics in our experiments (SMX: 0.0395

mmole/L; SDM: 0.0320 mmole/L; STZ: 0.0392 mmole/L). Although the selected initial concentration of sulfonamide antibiotics is much larger than that in drinking water resources, the experiment is still of environmental relevance because chlorine chemistry is based on stoichiometry and results are transferrable to lower concentrations. Volumes of sulfonamide antibiotic stock solution (SDM, SMX or STZ), volumes of FAC stock solution, and volumes of buffer (phosphate buffer at pH 7.6) stock solution were calculated to achieve the initial sulfonamide antibiotic concentration of 10 mg/L and initial FAC concentrations of 0, 2, 4, 8, 16, 48 mg/L, respectively. Exact calculated volumes can be found in Table 2.

Table 2: Calculated volumes of reagents for each experiment.

Desired Initial FAC Concentration, [mg/L]	0	2	4	8	16	48
Desired Initial FAC Concentration, [mmole/L]	0	0.055	0.110	0.219	0.438	1.315
Volume of SMX/SDM/STZ Stock Solution, [μ L]	100	100	100	100	100	100
Volume of Buffer Stock Solution, [mL]	9.90	9.50	9.10	8.30	9.58	8.84
Volume of 50 ppm FAC Stock Solution, [μ L]	0	400	800	1600	0	0
Volume of 500 ppm FAC Stock Solution, [μ L]	0	0	0	0	320	960

FAC concentrations were verified by the N, N-diethyl-*p*-phenylenediamine (DPD) chlorimetric method.⁵⁵ The DPD reagent reacts with FAC, resulting in color intensity change that is proportional to the FAC concentration. DPD reagents were provided by PPD–2DPD Powder Pop Dispenser (HF Scientific). FAC concentrations were read directly from the Free Chlorine Pocket Photometer (HF Scientific). The photometer has a reported accuracy of $\pm 2\%$ within the designed concentration range.

Reactions were initiated by adding calculated volumes of FAC into reactors containing the designed volumes of SMX/SDM/STZ and buffer solutions. For each reaction, no quenching agent was used and 10-minute contact time was allowed before analysis. Chlorination reactions of SMX, SDM, and STZ were considered completed after 10 minutes according to previous kinetics studies.^{32, 67, 83} Two parallel samples were collected simultaneously from each reactor. One was for use for HPLC-UV analysis and the other was for use for HPLC-MS analysis. All experiments were carried out in 10 mL clear glass reactors obtained from Fisher Scientific (Pittsburgh, PA). All experiments were conducted in triplicate. The experimental procedure is illustrated in Figure 3.

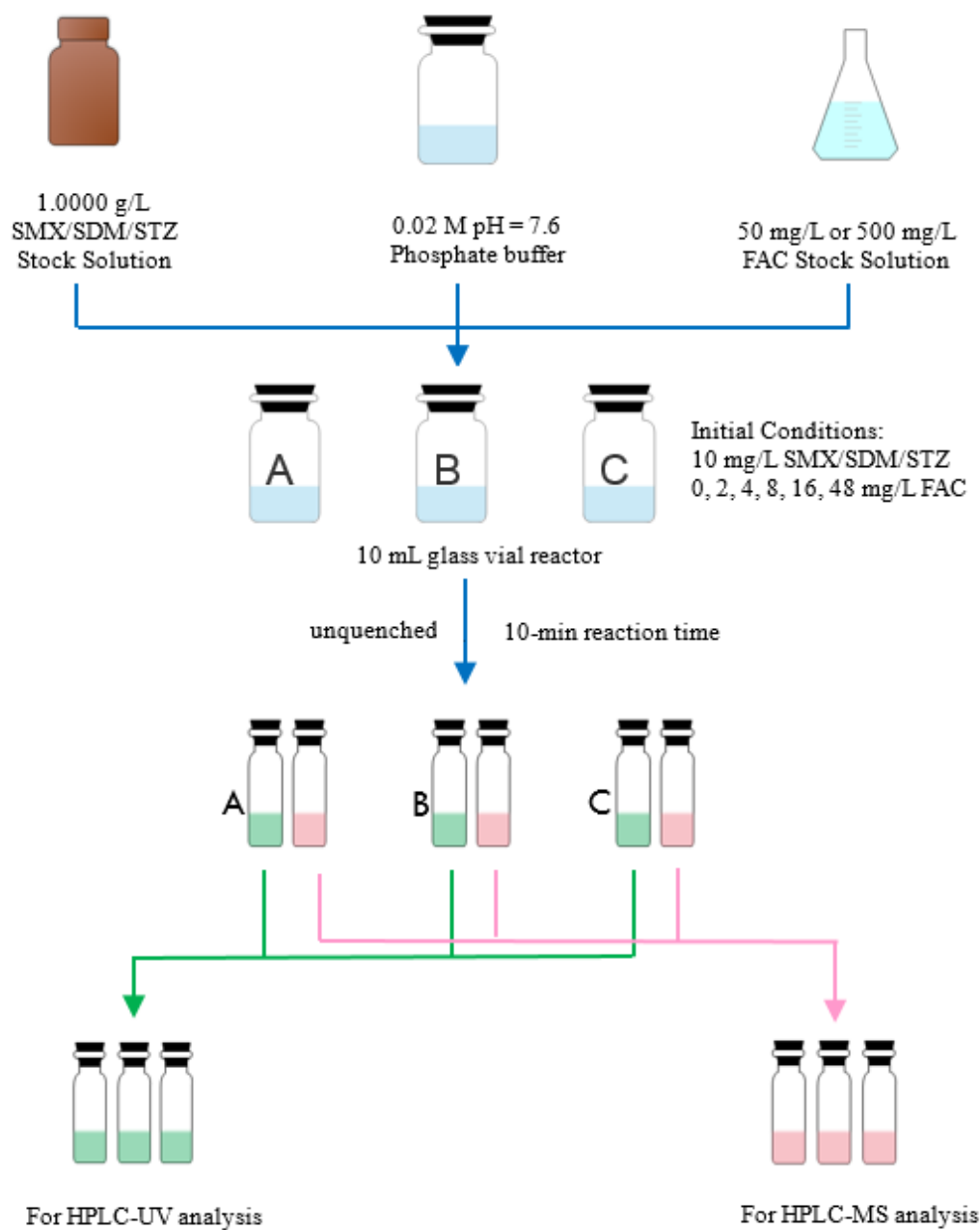


Figure 3: Summary of procedures of chlorination reaction experiments.

3.3 Analytical methods

Chemical analysis was performed on both high-performance liquid chromatography coupled to a UV detector (HPLC-UV) and a mass spectrometry detector (HPLC-MS).

In both HPLC-UV and HPLC-MS analyses, compounds were separated on an Atlantis T3 3 μ m column (150 \times 3.0 mm) at a flow rate of 300 μ L with a previously reported analytical method.^{84, 85} The constitution and gradient of mobile phase were adopted based on previously reported research^{86, 87}, consisting of nanopure water (A) and HPLC– grade methanol (Acros Organics, Geel, Belgium, B), each amended with 0.1% (volume) formic acid (98 to 100%; Acros Organics, Geel, Belgium). Samples were injected into the column at 50 μ L (UV analyses) and 20 μ L (MS analyses) with an initial mobile phase of 90:10 water/methanol and elution from the column was achieved with a final mobile phase of 5:95 water/methanol. An eluent gradient was applied to achieve separation of products. The percentage of (A) was changed linearly according to time: 0-15 min, 90%; 30 min, 30%; 33min, 30%; 36min, 90%.⁸⁷ A Figure illustrating the gradient mobile phase is provided in Appendix B. Total length of the separation method was 50 min.

HPLC-UV analyses were performed on an ultimate 3000 HPLC system (Thermo Scientific) with a WPS-3000 SL autosampler and a VWD-3400 RS dual beam detector. Injection volume for each measurement was chosen at 50 μ L. Each measurement was carried out at three wavelengths at the same time: 257 nm, 268 nm, 282 nm, which were the maximum absorption wavelengths for SMX, SDM, STZ, respectively. The maximum absorption wavelengths were previously determined by injecting 100 ppm

SMX/SDM/STZ solution directly into UV detector followed by a spectral scan. The Chromeleon Client, version 7 (Dionex), was used for chromatogram analysis and peak interpretation.

HPLC-MS analyses were performed on a high-resolution mass spectrometer (QExactive, Thermo, Waltham, MA, USA). The QExactive spectrometer was used with electrospray ionization in both positive and negative modes. Mass calibrations and mass accuracy checks were performed before each experiment; resolution was always greater than 60,000 and mass accuracy was always within ± 2 ppm. Injection volume for each measurement was chosen at 20 μ L. The QExactive acquired full-scan MS data within a mass-to-charge (m/z) range of 75-600 for each sample. XCalibur, version 2.0.7 (Thermo, Waltham, MA), was used for chromatogram analyses and interpretation.

3.4 Disinfection byproduct identification

3.4.1 Identification of peaks observed by HPLC-UV-VIS

The formation of DBPs that absorb light at the measured wavelengths can be directly observed as peaks in the HPLC-UV-VIS chromatograms. The linearity of the chromatographic responses was verified for SMX, SDM, STZ, and N-chloro-p-benzo-quinoneimine (NCBQ) using external calibration standards containing at least 6 points. R^2 values ranged from 0.9999 to 1.0000. Concentrations of SMX, SDM, STZ, and NCBQ were calculated according to the linear response of the calibration. For all the other peaks on chromatograms, a peak area was used to describe the yield of each product.

3.4.2 Identification of other masses

The mass spectrometry experiments were designed to acquire full scan mass spectra for each sample in the m/z range of 75-600. Full scan mass spectra for each sample were analyzed using the Sieve 2.0 software (Thermo Fisher Scientific). The Sieve software is designed for semi-quantitative differential analysis of complex MS datasets. Each treated sample (initial FAC concentration great than 0) is compared to the control sample (initial FAC concentration is 0) and the Sieve software identifies components with statistically significant inter-sample differences in abundance. Many parameters are adjustable in designing a Sieve workflow. The workflow used in this work was adopted from Meier et al.(2014) and is summerized in Figure 4 and briefly descibed in the following.

The Sieve software requires users to first select a domain, a signal detection algorithm, and an experiment type. For this work, small molecule, control compare trend, and chromatographic alignment and framing were selected, respectively. Control compare trend is particularly useful for the data acquired in these experiments because this enables analysis of trends over a time series of data points in a kinetic study or over a series of reaction experiments conducted to varying degrees of completion. Next, all of the raw data files from the MS are imported into Sieve and control and treated groups are defined.

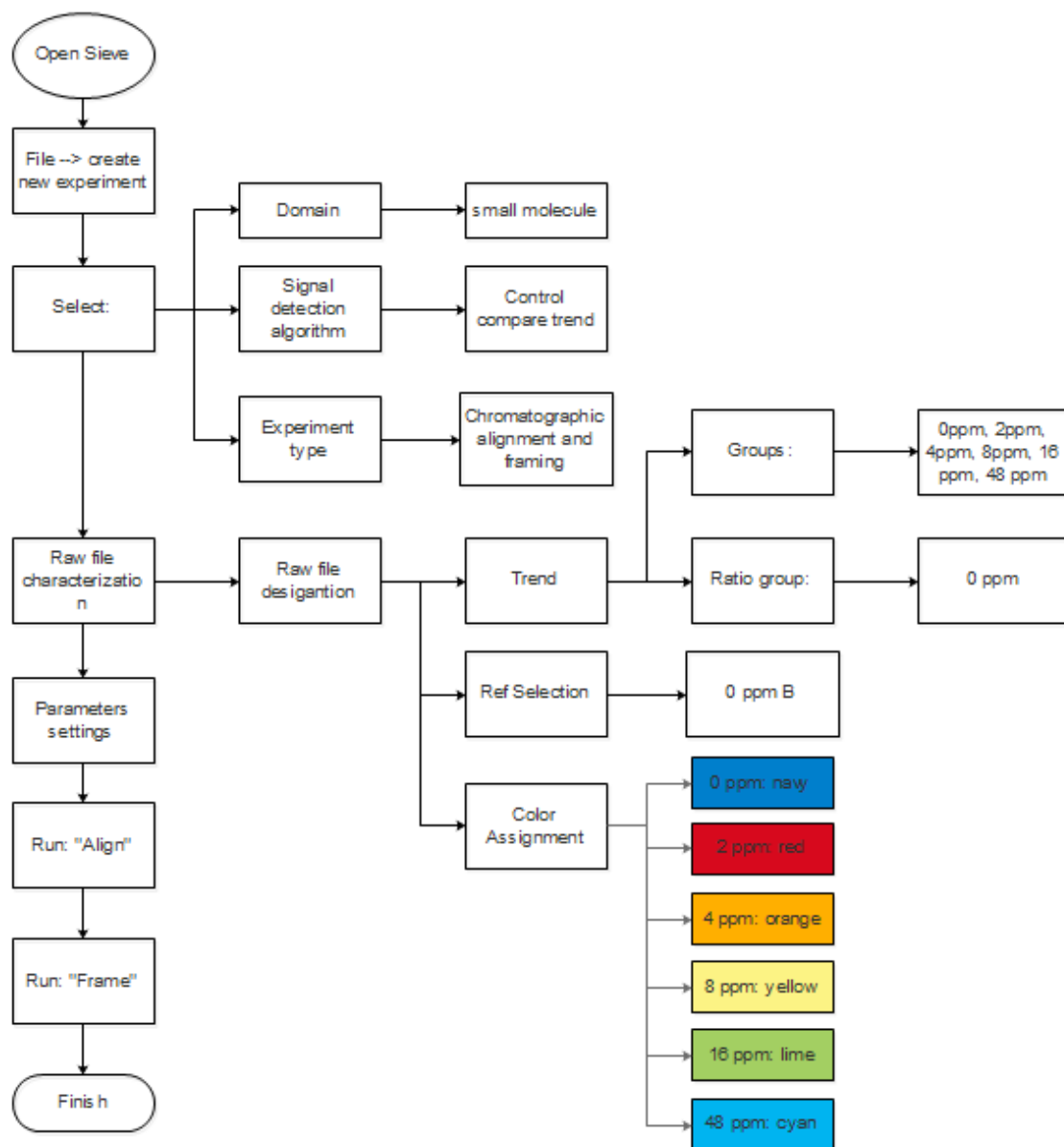


Figure 4: Sieve workflow developed for candidate DBP identification.

For each sulfonamide antibiotic, 18 raw files were generated representing the triplicate experiments conducted for the control and each of the five treated conditions. The control experiments are defined as the reference group and the remaining samples are grouped as triplicates. Finally, in the “parameters settings” step of the Sieve workflow, all

parameters were kept at software default values except for “Maximum Frames”, which was set to 15,000, and “Intensity Threshold”, which was set to 100,000. The software then runs an alignment and analysis and the output is a list of “frames”. Frames are defined as components with statistically significant inter-sample differences in abundance relative to the control group.

The resulting group of frames is expected to include DBPs, but also includes a lot of spurious data that is inherent to high-resolution MS datasets. Therefore, a series of filters were developed to narrow down the suspected products to ones that were of most interest, as illustrated in Figure 5. Three filters were applied step by step. The first filter removed frames assigned to masses that did not change appreciably in the treated groups relative to the control group. The second filter removed frames that had a maximum intensity of less than 5E4. Frames that had intensities lower than 5E4 were considered as minor products or noise and were not excluded in further study. The third filter removed frames that showed significant variance across triplicate experiments. This was justified because the formation of DBPs in oxidation reactions is expected to be highly repeatable. Approximately 90% of the candidate DBPs were removed following application of these three filters.

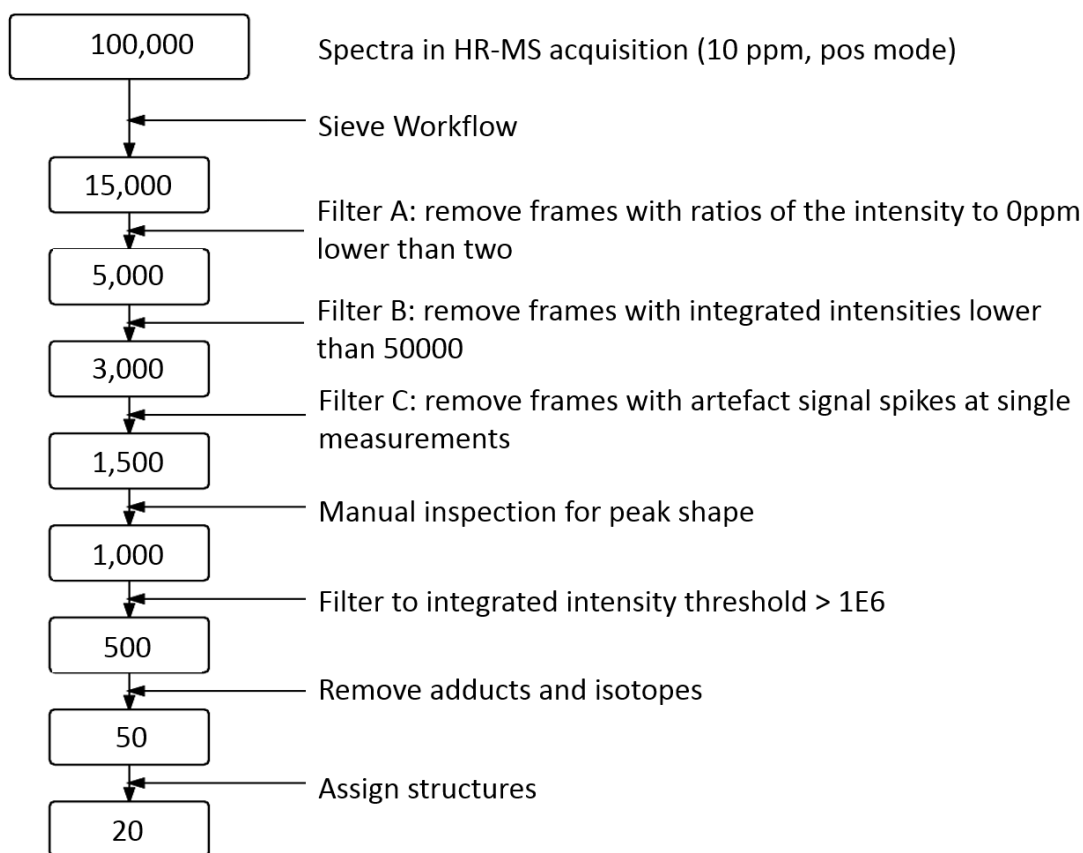


Figure 5: Workflow in product identification using the Sieve software. Numbers here show general reduction of candidate DBP frames. Real numbers of frames of candidate DBP will be given for each compound later in the thesis.

Following the filtering of the Sieve output, peak quality was assessed by manual peak inspection. To be considered as a real peak, the “reconstructed ion chromatogram” in Sieve was required to have a symmetric peak shape. For example, in Figure 6a, the frame was considered to have a symmetric peak; while in Figure 6b, the frame was not considered as a real peak. This step was rather subjective and thus a conservative approach was taken and only frames that were clearly not peaks such as shown in Figure

6b were removed. It is not clear why the Sieve software selects frames as shown in Figure 6b as candidate products.

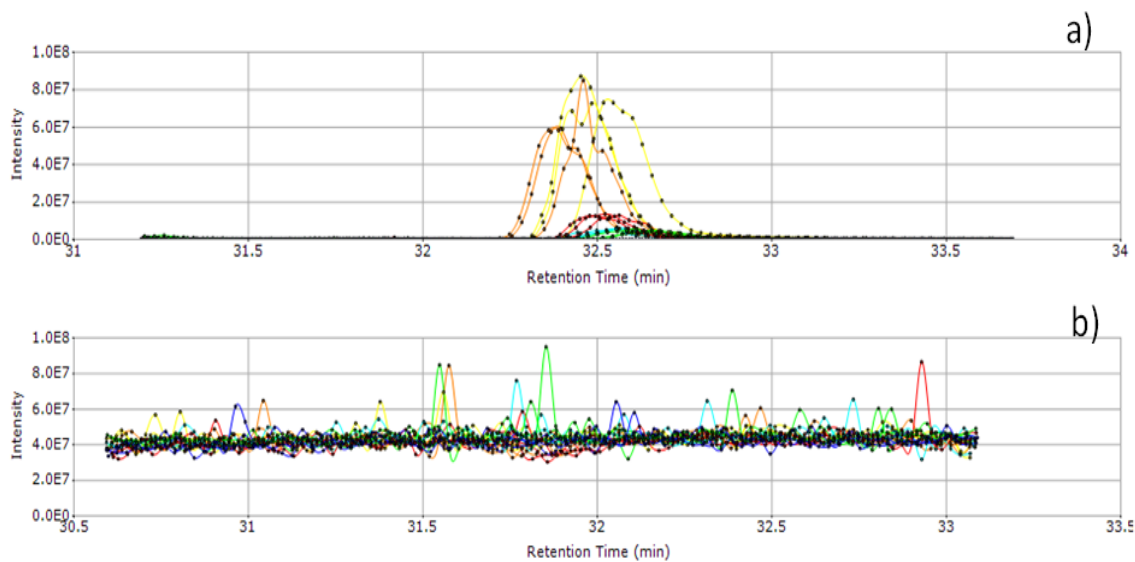


Figure 6: Reconstructed ion chromatograms in sieve: a) a real peak b) not a real peak.

Following manual inspection of peak shape, another filter was applied restricting intensities of the frames; only frames with an intensity greater than $1\text{E}6$ in at least one experimental treatment were considered for further inspection. Finally, the remaining frames were carefully manually examined to determine whether they represented masses of candidate DBPs or isotopes or adducts of candidate DBPs. Isotopes and adducts have the same retention time and peak shape as parent molecules. Isotopes are a function of the molecular formula and generally ^{13}C , ^{34}S , and ^{37}Cl isotopes were observed. Adducts form inside the mass spectrometer. The most common adducts formed were from Na^+ and CH_3O^- .

Following all of the data reduction steps outlined in the preceding, a list of candidate DBP masses was obtained and examined for structure elucidation. This process was done in both positive and negative mode. In negative mode, only unique frames that did not appear in the positive mode analyses were kept for consideration. The QualBrowser function of the XCalibur software (Thermo Fisher Scientific) was used to examine extracted ion chromatograms, exact masses, and isotope patterns. From these data, a molecular formula of the candidate DBPs was proposed. From the molecular formula, knowledge of chlorine chemistry, and reported oxidation reactions of sulfonamide antibiotics, structures of DBPs were proposed. Not every molecular formula was matched with a reasonable structure. Only frames with assigned structures were taken into consideration when proposing pathways and mechanisms of those reactions. This procedure enables a comprehensive analysis of products formed in a chemical reaction and was expected to yield an unprecedented picture of sulfonamide transformations.

CHAPTER 4 RESULTS AND DISCUSSION

4.1 Product identification

4.1.1 Identification of peaks observed by HPLC-UV-VIS

Figure 7 presents the HPLC-UV-VIS chromatograms revealing separation of DBPs for reactions between SMX, SDM, STZ and varying initial FAC concentrations after 10 minutes of RT. Figure 7 a), b) and c) were drawn to the same scale, showing initial parent chemicals as well as putative DBPs for SMX, SDM, and STZ, respectively. Figure 7 d), e), and f) were adjusted to the scale of the most prominent product in each reaction for better visualization of peaks corresponding to DBPs. In Figure 7a, the first critical observation is the preponderance of separated components in this chromatogram, with at least 9 peaks of varying size being discernible at distinct RTs. The peak at RT = 30.4 min is SMX. The remaining 8 peaks, therefore, are putative DBPs. Similarly, in Figure 7b and Figure 7c, SDM and STZ appeared at RT = 33.3 min and RT = 25.2 min, respectively; the remaining 9 and 8 peaks are DBPs formed in SDM-FAC and STZ-FAC reactions, respectively.

When initial FAC increased, the detected concentrations of parent compounds (SMX, SDM and STZ) decreased. At $C_{0,HOCI} = 2$ mg/L, SMX decreased by 32%; when $C_{0,HOCI} = 4$ mg/L, SMX decreased by 83%; when $C_{0,HOCI}$ was raised above 4 mg/L (8 mg/L, 16 mg/L, and 48 mg/L), a peak representing SMX with about 5% of its initial concentration was constantly observed. This probably indicates that a certain product of the chlorination reaction was undergoing a back-reaction, yielding the parent SMX again. The back-reaction proposal is in agreement with studies by Dodd and Huang⁶⁷, as well as

Gassman and Campbell⁸⁸. The concentration of SDM dropped to 25% of that when no FAC was added after reacting with 2 mg/L FAC. No SDM was observed when initial FAC was 4 mg/L or higher. STZ degraded by 38% at 2 mg/L HOCl and by 66% at 4 mg/L initial FAC. STZ peak was completely gone when initial FAC was 8 mg/L. Peaks corresponding to SDM and STZ disappeared in over-chlorinated experiments, exhibiting no similar back-reaction as observed with SMX-FAC. This does not necessarily indicate no back-reaction happened in SDM-FAC and STZ-FAC reactions; instead, it may still have taken place. However, given the relatively fast kinetics of the latter two reactions, parent compounds yielded by back-reaction might have been consumed by excess FAC again, and therefore were not observed on the chromatogram.

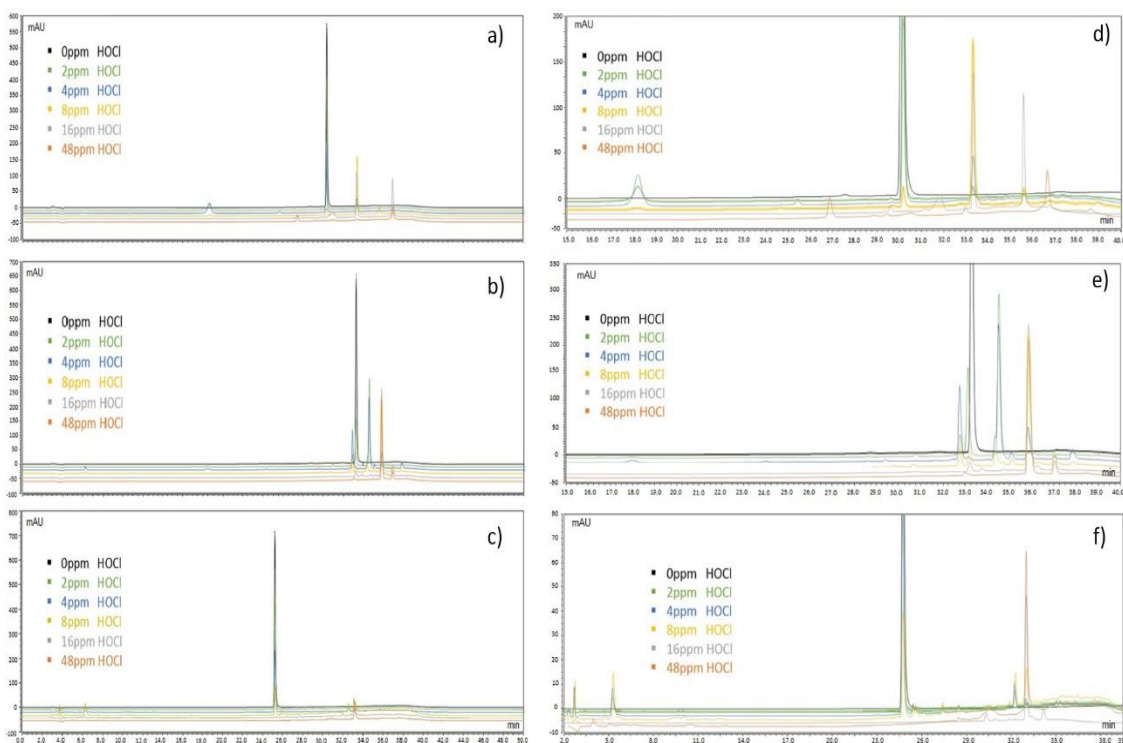


Figure 7: Separation of DBPs at six chlorination levels observed by HPLC-UV: a) full DBP peaks in SMX-FAC, b) full DBP peaks in SDM-FAC, c) full DBP peaks in STZ - FAC; d) partial DBP peaks in SMX-FAC, e) partial DBP peaks in SDM-FAC, f) partial DBP peaks in STZ-FAC.

Along with the shrinking of peaks corresponding to parent compounds, rose the peaks of putative DBPs. The peak areas of putative DBPs and the concentrations of parent compounds calculated from the external calibration are provided in Appendix C. The changes of the peak areas of putative DBPs following reactions with FAC are presented in Figure 8. This Figure provides visual information regarding the following three aspects: 1) In each reaction, some putative DBPs had larger yields than others. The putative DBP that formed at RT = 33.3 min, 36.9 min, and 30.0 min in SMX-FAC reactions, at RT = 35.8 min, 34.5 min, 32.8 min in SDM-FAC reactions, and at RT = 33.3 min, 36.9 min, and 18.6 min in STZ-SMX reactions were more prominent than peaks at other RTs. 2) The graphs clearly illustrate how peaks of each product changed with different initial FAC. 3) The graphs also show the initial FAC at which a certain product reached maximum yield. This information is useful in identifying peaks by matching them with masses obtained by HPLC-MS according to retention time. At certain retention times, more than one mass was obtained by HPLC-MS. In these scenarios, if the mass-FAC pattern from MS analysis matches the peak-FAC from UV analysis, structures can be assigned also to the matching UV peaks. All three of the criteria listed above should be met in matching processes.

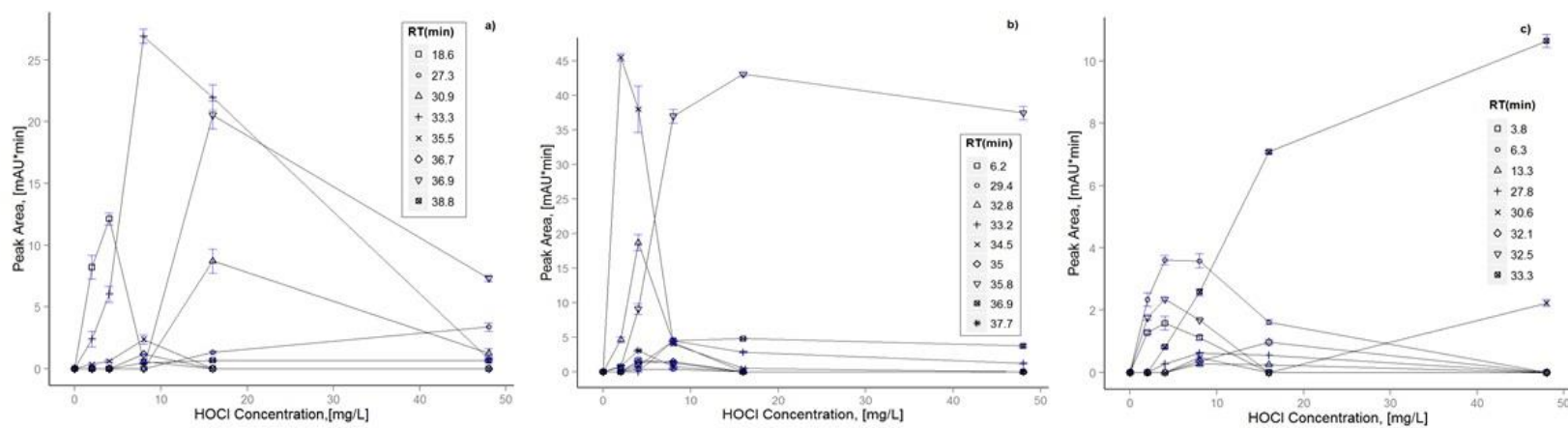


Figure 8: Peak area trend of each DBP of three sulfonamides as a function of initial FAC level: a) SMX-FAC, b) SDM - FAC, c) STZ – FAC.

4.1.2 Identification of masses observed by HPLC-MS

The Sieve workflow described in the Materials and Methods section was used to identify candidate DBPs of SMX, SDM, and STZ measured by HPLC-MS. Each sulfonamide antibiotic was examined in positive and negative ionization modes. Negative ionization measurements yielded 4, 3, and 11 unique candidate DBP masses, respectively, but no structures could be assigned using the procedures described in this thesis. The results of the candidate DBP selection procedure for each compound in positive ionization mode are presented in Figure 9. In SMX-FAC reactions, masses of 35 candidate DBPs were selected and 16 of them were proposed with structures. Among the structures proposed, 8 were previously reported^{83, 89} and 6 are believed to be reported here for the first time. In SDM-FAC and STZ-FAC reactions, a total of 18 and 16 DBPs were identified, respectively. They are believed to be firstly reported here in this study.

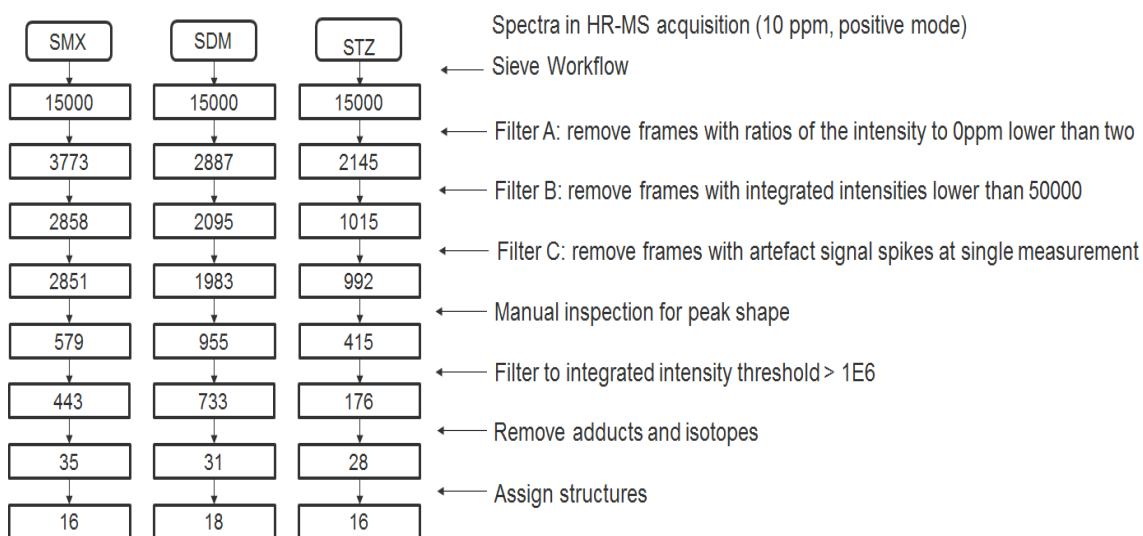


Figure 9: Product identification workflow for SMX, SDM and STZ in reaction with FAC in positive mode.

To illustrate how DBPs of the reactions investigated in this work were identified, the analytical details used to propose the structure of one of the products in SMX-FAC reactions and one of the products in SDM-FAC reactions are presented below. The analytical details and structure assignments for all products in SMX-FAC, SDM-FAC and STZ-FAC reactions are provided in Appendix D. All products were identified based on the intensity plots, the XIC, and MS spectra. However, the proposed structures cannot be confirmed until further experiments in which MS/MS data can be yielded for interpretation and complementary analytical techniques (such as NMR) can be employed. All proposed DBPs are named from the parent sulfonamide antibiotics and in accordance to their nominal masses. For example, the DBP identified for SMX at an exact mass $[M+H]^+$ of 298.0488 is referred to as SMX298.

Figure 10 shows: (a) the plot of the intensity of SMX298 in each sample; (b) the extracted ion chromatogram (XIC); and the (c) MS spectra. The intensity plot shows an increasing intensity of SMX298 from reactions where the initial FAC is 2 mg/L to reactions where the initial FAC is 16 mg/L. This evolution in the magnitude of the intensity is strong evidence that a compound with this mass is forming to varying extents upon free chlorination of SMX. The variability in the yield of this product at initial FAC concentrations of 16 ppm is higher than many other DBPs, but was within the tolerance of our filter criteria for acceptance. The XIC at the exact mass of SMX 298 reveals a clear peak at RT of 30.2 min. The MS spectra contains peaks at the exact mass of SMX298 along with those corresponding to its ^{13}C and ^{34}S monoisotopic masses. Additionally, the relative abundance of ^{13}C and ^{34}S monoisotopic masses match the

theoretical abundances for a compound containing eleven carbon atoms and one sulfur atom. Based on this evidence, a molecular formula of $C_{11}H_{12}O_5N_3S$ can be predicted. This molecular formula has a predicted exact mass that deviates -1.401ppm from the measured mass. A structure for SMX298 can be proposed.

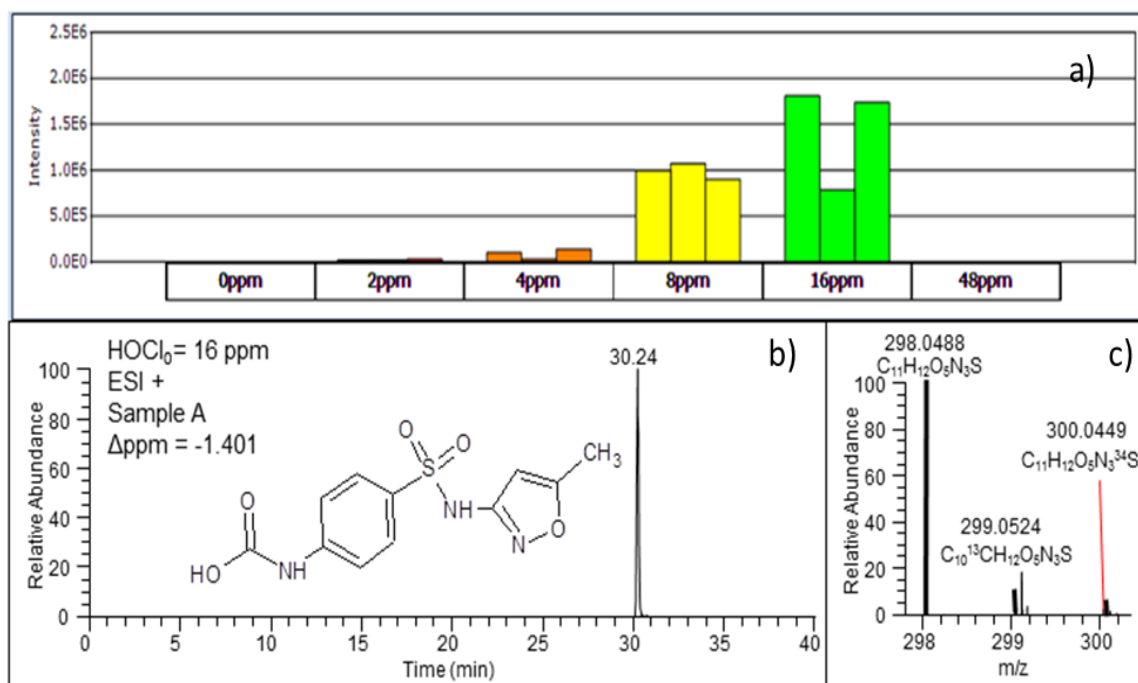


Figure 10: Sieve integrated intensity graph, XIC, and MS spectra, for SMX 298 ($m/z = 298.0488$ for MH^+).

The proposed structure is that of a carboxylation product, which is a common reaction endpoint in organic chemistry. The carboxylation is proposed to occur on the aniline nitrogen based on known reaction mechanisms, though the exact placement cannot be resolved with the analytical techniques employed. The formation of SMX298 is supported by previous transformation experiments with SMX⁶⁷ and well known chlorine

reaction pathways. The full reaction pathway and putative mechanism are discussed in more detail in the following section.

Similarly, Figure 11 shows: (a) the plot of the intensity of SDM379 in each sample; (b) the XIC; and the (c) MS spectra. The intensity plot shows an increasing intensity of SDM379 from reactions where the initial FAC is 0 ppm to reactions where initial FAC is 4 ppm, and a decreasing intensity from reactions where the initial FAC is 4 ppm to reactions where the initial FAC is 48 ppm. This evolution in the magnitude of the intensity is strong evidence that a compound with this mass is forming to varying extents upon free chlorination of SDM. The XIC at the exact mass of SDM379 reveals 2 peaks at RT = 34.79 min and 35.74 min, respectively. The MS spectra at each of those RTs contain peaks at the exact mass of SDM379 along with those corresponding to its ^{13}C and ^{37}Cl monoisotopic masses. The relative abundance of ^{13}C and ^{37}Cl monoisotopic masses suggests that SDM379 contains 12 carbon atoms and 2 chlorine atoms, theoretically. As a result, a molecular formula of $\text{C}_{12}\text{H}_{12}\text{O}_4\text{N}_4\text{Cl}_2\text{S}$ can be predicted. This molecular formula has a predicted exact mass that deviates -0.547 ppm from the measured mass. A structure of SDM379 can be proposed based on literature data and knowledge of chlorine chemistry. Considering reaction pathways of SMX-FAC proposed by Dodd and Huang (2004) and Gao et al (2014), one of these isomers could have both chlorine atoms attached at the same aniline N. In the other isomer, the second Cl atom could substitute the H atom on the ortho-C of aniline. This pathway and mechanism will be discussed in more detail in the following.

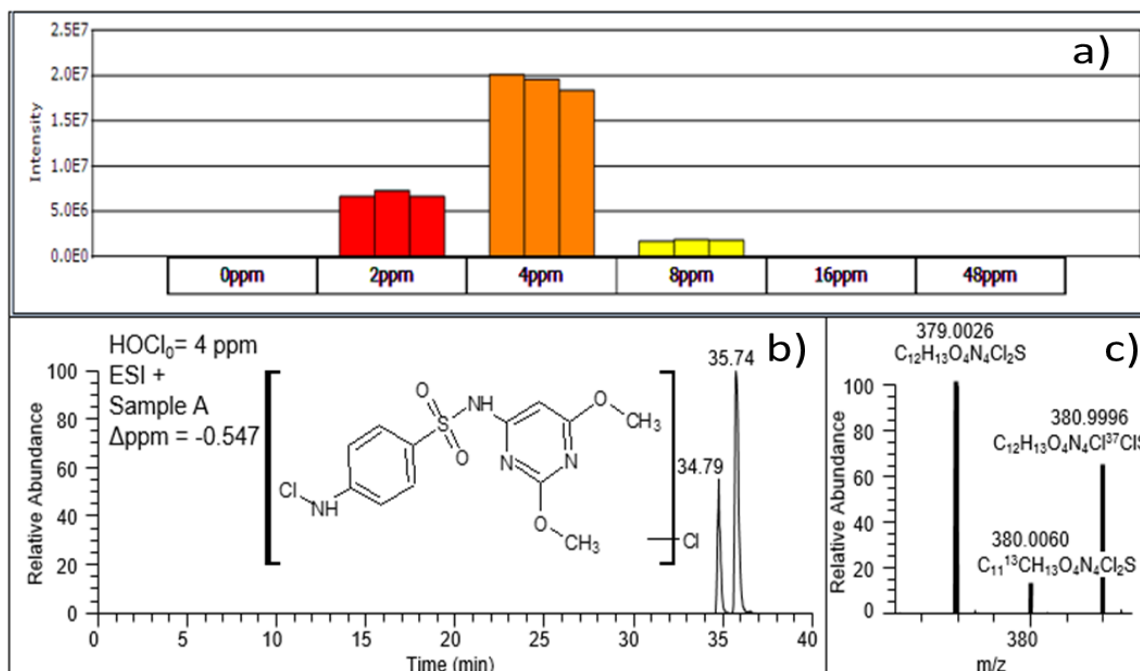


Figure 11: Sieve integrated intensity graph, extracted ion chromatogram (XIC), and MS spectra for SDM379 ($m/z = 379.0026$ for MH^+).

4.1.3 Comparing peaks from UV to MS

Matching peaks observed by HPLC-UV-Vis and masses obtained by HPLC-MS was conducted based on criteria described in 3.4.2. Since product separation was done on the same column, the order that parent compounds and products came out of the column and got detected, generating a signal on either UV-VIS inspector or MS detector should be the same. Theoretically, the RT of each chemical observed by HPLC-UV-Vis and by HPLC-MS should shift by a constant amount of time, if not exactly the same amount of time. Due to systematical errors (difference in length of capillaries connecting multiple parts of instruments), for each compound, a RT shift between the two instruments was observed. The RT shift was determined to be approximately 2.8 min for both products in SMX-FAC and SDM-FAC reactions and 2.2 min for those in STZ-FAC reactions.

The matching is illustrated in Figure 12. Structures of those masses that were matched with the UV peaks can be found in Figures 20, 26 and 27 for SMX, SDM, and STZ, respectively. Detailed descriptions of the analytical data supporting each structure are presented in Appendix D. Noticeably, the UV analysis suggested that there should be 8, 9, and 8 DBPs for SMX-FAC, SDM-FAC, and STZ-FAC reactions, respectively. However, the MS analysis yielded several more. One possible reason is that some products have lost the chromophore structure that absorbs light by such reactions as oxidative opening of the aromatic ring, thus they could not be detected by HPLC-UV. The other reason is that due to detection limit on UV, some DBPs were not detected. Moreover, not all of the UV peaks were identified in the MS analysis. This suggests that these DBPs can absorb light at the wavelengths measured, but were not ionizable or otherwise escaped our detection in MS. These observations show the importance of using multiple analytical techniques when screening for reaction products.

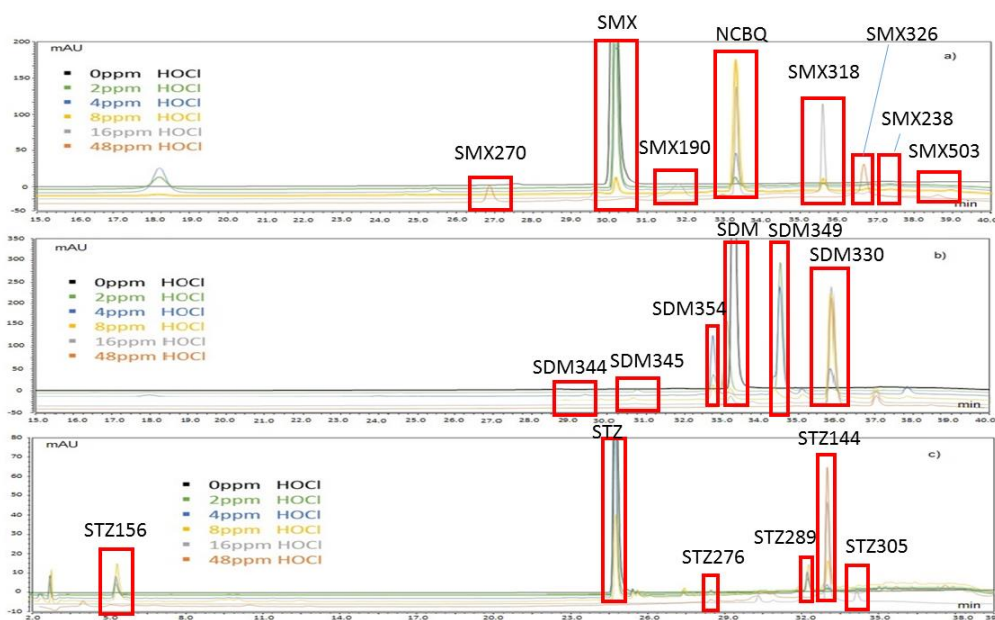


Figure 12: Matching peaks observed on HPLC - UV and masses/frames obtained by HPLC-MS.

4.2 Proposed Reaction Pathways and Putative Mechanisms

4.2.1 Reaction pathways of SMX-FAC

For chlorination of SMX, the proposed transformation pathway is provided in Figure 13. A total of 6 distinct pathways are proposed and described, as follows.

Pathway A: In reaction with FAC, a mono-chlorinated product molecule was observed (SMX288). Though the data acquired did not enable structural resolution of where the chlorine atom was added, results from prior chlorination studies with SMX and expected aniline chlorination patterns suggest chlorine addition at the amino nitrogen position or at the *ortho*- position of the aniline group.^{67, 83, 90-92} Based on the apparent high yield of SMX288 and literature data⁶⁷, it is proposed that SMX288 observed in this work is the result of a nucleophilic substitution of a chlorine atom at the amino nitrogen position of SMX, leading to the formation of SMX288. A back-reaction from SMX288 to SMX is also proposed given the existence of SMX in over-chlorinated reactions observed by HPLC-UV, which was also observed by Dodd⁶⁷. This reaction is the result of a heterolysis of the N-Cl bond to produce a phenylnitrenium ion⁸⁸, which reverts into SMX.

In the presence of excess FAC, SMX288 could be further chlorinated and is proposed to form an intermediate, N,N-dichlorinated SMX, shown as proposed intermediate a1 in Figure 13. This intermediate, though not observed in previous or the current work, can explain the formation of the following observed DBPs because it could lead to cleavage of the sulfonamide moiety. First, by heterolysis of the aromatic chloramine's N-Cl bond, proposed intermediate a1 generates an arylnitrenium cation, N-chlorinated SMX

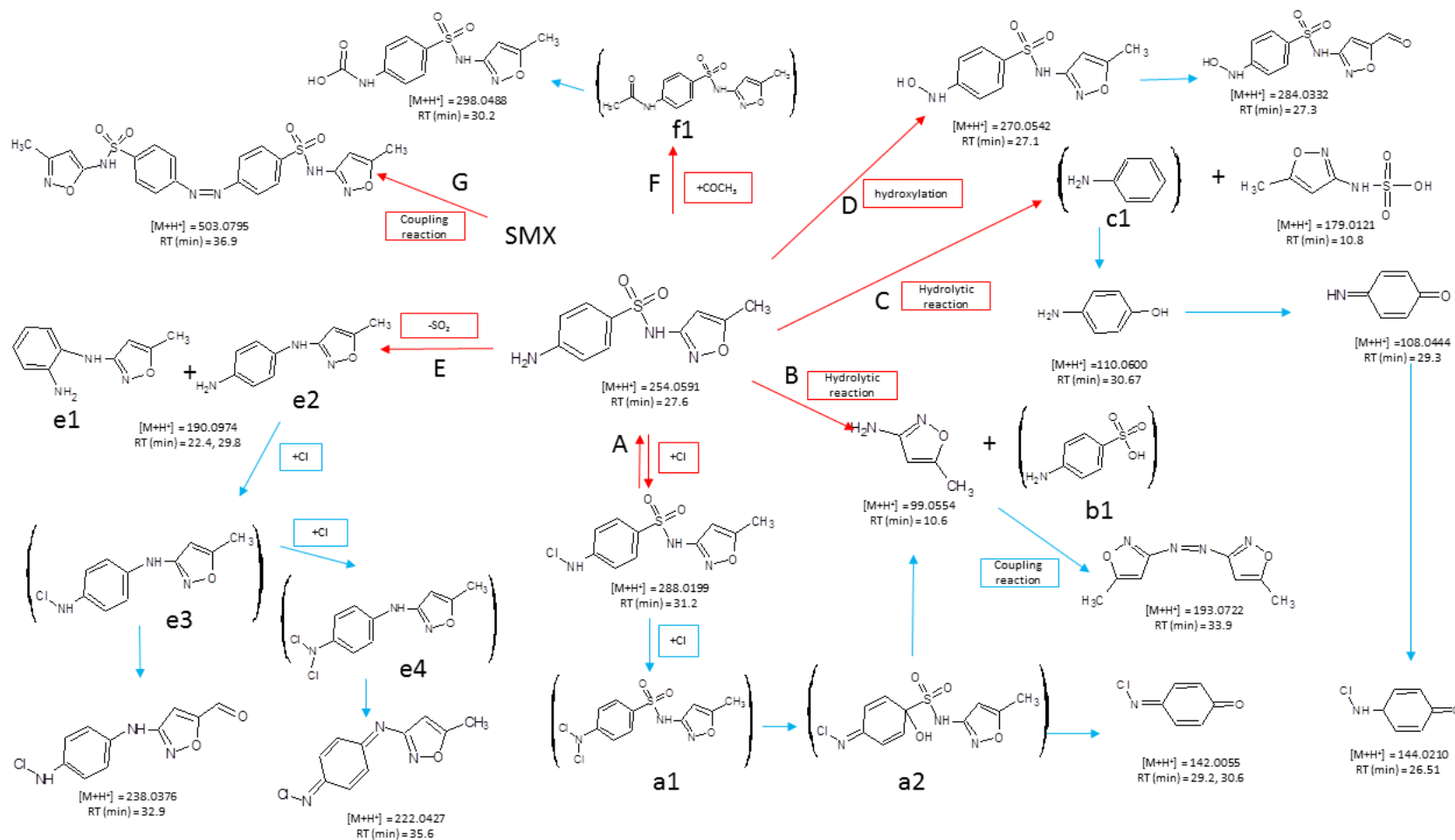


Figure 13: Proposed products and pathways for reactions of SMX with FAC. Red arrows show pathways that are initiated directly from SMX. Blue arrows show pathways following initial pathways. Products shown in parentheses are proposed intermediates or products based on putative reaction mechanisms.

nitrenium ion⁹¹, which can lead to distribution of strong electron-deficiency to the aromatic ring's *para* and *ortho* positions (see Appendix D, Figure D3). Aqueous reactions of *para*-substituted nitrenium ions lead to *p*-hydroxy intermediates^{88, 91} (shown for the case of SMX as the proposed intermediate a2 in Figure 13) that can subsequently rearrange to a *p*-benzoquinoneimine structure, SMX142 and correspondingly SMX99 while releasing sulfur dioxide (SO₂).^{67, 83} SMX142 is N-chloro-*p*-benzoquinoneimine (NCBQ), which was previously reported as a product in SMX-FAC reactions⁶⁷. An analytical standard was available for NCBQ and its maximum yield was 9.8% at an initial FAC concentration of 8 ppm. Concentrations of NCBQ and SMX in each reaction could be found in Appendix C.

Pathway B: SMX99 could also be directly formed by hydrolysis of the S-N bond in SMX⁹³, however, the expected *p*-sulfoaniline product (proposed intermediate b1) was not found in this work suggesting the nitrenium pathway (Pathway A) may be dominant. Previous studies found that direct S-N bond hydrolysis and SMX99 formation could happen when SMX was treated by ozone⁸³, permanganate⁸³, manganese oxide⁹⁴, photolysis^{95, 96}, TiO₂ photocatalysis⁹⁷, photo-fenton⁹⁸, and other processes. Whether SMX99 formed through S-N bond hydrolysis or the nitrenium pathway, SMX99 continued to react via coupling reactions, forming its dimeric compound, SMX193.

Pathway C: The observed formation of SMX179 suggests hydrolytic cleavage of the S-C bond, though the mass of the corresponding product aniline (proposed intermediate b1) was outside the range of our full scan MS acquisition and therefore not directly measured. The facile cleavage of a S-C bond was also observed by Kwart and Body (1965) in reactions of 4-quinoline sulfonyl chloride (a heterocyclic quinolone with the sulfonyl group in the *para* position relative to a nitrogen) and free chlorine.⁹⁹ This

reaction was attributed to interactions between chlorine and the nitrogen resulting in a delocalization of the electrophilic nature of the aromatic system leaving the α -carbon adjacent to the sulfur atom susceptible to nucleophilic attack.⁹⁹ Zhao et al. (1999) also found that certain groups were capable of withdrawing sufficient electron density from α -carbons adjacent to sulfonyl groups leading to cleavage of the S-C bond.¹⁰⁰ Those groups were positioned at *ortho* and/or *para* locations on aromatic or heteroaromatic rings.¹⁰⁰ The group attached to the sulfonyl group in SMX is an aromatic ring with an amino group at the *para* position, which could lead to cleavage of the S-C bond in this way.

SMX110 can be formed from proposed intermediate b1 following aniline transformation into a *para*-hydroxyl compound¹⁰¹⁻¹⁰³ which results in the formation of SMX108¹⁰⁴. This reaction pathway was also observed by Ricken, et al. (2015) in studying downstream biodegradation pathways of SMX.¹⁰⁵ (see Appendix D, Figure D4) The observed trends in the intensity-FAC patterns of SMX110 and SMX108 (see Appendix D, Figure D8 and Figure D10) also suggest that SMX108 is formed from SMX110 because the intensity of SMX108 is higher at higher FAC concentrations. Through hydrochlorination, SMX108 transforms into SMX144. A similar hydrochlorination reaction was also previously observed in the chlorination of N-acetyl-4-aminophenol.¹⁰⁶ Though the structures of SMX144 and SMX142 are quite similar, no reaction mechanisms were identified that could readily explain a reactive relationship between them. Thus, the proposed pathway in Figure 13 shows two distinct pathways resulting in the formation of these two products.

Pathway D: SMX270 suggests the formation of a mono-hydroxylated product. As with the mono-chlorinated DBP SMX288, the exact position of the hydroxylation cannot be discerned from the acquired data. Hydroxylation reactions of SMX in reaction with FAC

was also observed by Gao et al. (2014) where the hydroxylation is proposed to occur on the phenyl ring (see Figure 2), though no analytical evidence supports that structural assignment.⁸³ The structure of SMX270 in Figure 13 shows the hydroxylation on the amino group; this structural assignment is based on the known preferential nucleophilic substitution on *para*-substituted anilines as was reasoned for SMX288. The formation of SMX284 suggests further oxidation of SMX270. The oxidation is proposed as shown on the methyl group in Figure 13 because it is the only structural feature that can accept a fully oxidized oxygen atom.

Pathway E: The extracted ion chromatogram for SMX190 shows two distinct peaks at different retention times (see Appendix D, Figure D18 and Figure D19). This suggests the formation of two isomers. SMX190 is an SO₂ extrusion product of SMX. Mechanisms leading the SO₂ extrusion reaction is illustrated in Figure D20. In addition to the two product isomers, a peak representing SMX190 was also detected at RT = 27.6 in lower chlorinated solutions, which was the same RT for SMX. This suggests that SMX190 was also formed during in-source fragmentation and was an artefact of the measurement, similar to an adduct. Wang et al. (2003) also observed the loss of SO₂ in sulfonamides during in-source fragmentation and they proposed several mechanisms for the formation of the SO₂ extrusion product.⁸ According to their study, one of the aromatic carbon atoms was proposed to undergo nucleophilic attack by the lone pair of electrons on the nitrogen atom, leading to the loss of SO₂, as illustrated in Figure D20, Appendix D. The structures of the two product isomers are proposed as e1 and e2 in Figure 13. Product e2 has been previously reported as characteristic of indirect photodegradation studies of sulfonamide antibiotics^{78, 95, 96} as well as a common product in biodegradation processes¹⁰⁷. The mechanism of formation is presumed to be similar to that described by Wang et al. (2003). The structure of e1 is proposed here as a substitution at the *ortho*

position of the aniline, though no known mechanism can explain this rearrangement. Two additional products were identified following SO₂ extrusion that likely form following formation of mono- and di-chloro intermediates that were not directly measured but are shown as proposed intermediates e3 and e4 in Figure 13. Formation of SMX238 results from further oxidation of e3. The reaction is similar to that described earlier in Pathway D where SMX270 was oxidized and formed SMX284. SMX222 was formed by a nucleophilic aromatic substitution of the aniline via Aryl nitrenium ions were previously studied by Gassman et al. (1971)¹⁰⁸ The reaction was similar to that leading to the formation of a2 from a1. According to Gassman et al. (1971), the heterolytic cleavage of the N-X bond would lead to formation of a phenylnitrenium ion (anilenium ion), as illustrated in Figure 3 in Appendix D. Products of similar structure were found by Perisa et al. (2013).¹⁰⁹

Pathway F: The formation of SMX298 also suggests the formation of an intermediate structure that has been previously observed in biotransformation and photolysis reactions, but was not identified in this work.⁹⁵ N-acetyl SMX is shown as proposed intermediate f1 in Figure 13. Proposed intermediate f1 is a well characterized human metabolite and a photolysis product of SMX and it forms by substitution of an acetyl moiety on the amino group of the aniline. N-acetyl SMX is then proposed to undergo a series of base-catalyzed reactions that result in chlorinated intermediates that are expelled as trichloromethane in the final step and yields SMX298. The reaction mechanism is shown in Figure D16 in Appendix D. This suggested pathway is in compliance with mechanisms proposed by previous studies.¹¹⁰⁻¹¹² Measurement of trichloromethane was outside the scope of this research, but this finding suggests SMX could also be a source of conventional DBPs.

Pathway G: The SMX dimer identified as SMX503 was observed in the current and previous chlorination studies of SMX.^{67, 83} Dimeric compounds can be formed as artefacts in mass spectrometry, but the unique retention time observed here suggests formation of SMX503 in the chlorination experiment. One possible mechanism leading to the formation of SMX503 is through a simple coupling reaction of SMX. Others have suggested that SMX503 may form through coupling reactions of N,N-dichlorinated SMX (proposed intermediate a1, Figure 13).⁶⁷ Similar coupling reactions following N,N-dichlorination were also reported to occur during chlorination of aromatic amines.^{113, 114}

4.2.2 Reaction pathways of SDM-FAC

No previous studies have examined the formation of oxidation products of reactions between SDM and FAC. It was expected that many of the reaction mechanisms previously reported and observed in this work for SMX would likewise lead to SDM products. The product spectrum and proposed SDM oxidation pathways are provided in Figure 14 and a detailed discussion of the pathways follows. If a mechanism has been discussed with SMX-FAC reaction in the previous section, it will not be discussed again for SDM-FAC reactions. A total of 6 distinct pathways are proposed and described, as follows.

Pathway A: As with SMX, the discussion begins with the observed formation of a mono-chlorinated DBP identified as SDM345. In SDM345, the proposed N-chloroaniline group is strongly suggested as the result of a nucleophilic substitution at the amino nitrogen group of the aniline substructure. SDM361 was formed from SDM345 via a hydroxylation reaction. Hydroxylation is proposed to occur at the amino group for the same reasoning discussed in SMX-FAC reaction pathways. Unlike SMX, a di-chlorinated product was also directly measured and identified as SDM379. N,N-dichlorinated amino acids were reported to be formed with excess FAC from amino acids,¹¹⁵⁻¹¹⁷ providing evidence that this reaction is likely to happen. It is not clear whether it formed and reacted very quickly for SMX (kinetics) or it is a more favorable pathway for SDM (thermodynamics) led to the dichlorinated product being observed for SDM and not SMX. As was proposed for SMX, the N,N-dichlorinated SDM led to the formation of a proposed *p*-hydroxy intermediate^{88,91} (shown as proposed intermediate a1 in Figure 14) that subsequently rearranged to a *p*-benzoquinoneimine structure, SDM142 which is again NCBQ. Maximum yield of NCBQ was xx% at an initial FAC concentration of xx ppm. The highly similar reaction pathways between SMX-FAC reaction and SDM-FAC reaction indicate that those pathways were likely to happen as reaction mechanisms rather than coincidence.

Pathway B: Contrary to SMX, both hydrolysis products were observed following cleavage of the S-N bond leading to the formation of SDM174 and SDM156. The mechanism leading to the cleavage of S-N bonds has been described in Pathway A of the SMX-FAC reaction. A single downstream product was also observed following this

hydrolysis. SDM190 is the mono-chlorination product of SDM156. The position of chlorine atom is not fully confirmed, but N-chlorination is strongly suggested as has been discussed for the proposed structures of SMX288 and SDM345.

Pathway C: The observed formation of SDM269 suggests a hydrolytic cleavage of the S-C bond of SDM as well. However, the direct hydrolysis products were not observed and are shown in Figure 14 as proposed intermediates c1 and c2. SDM269 is then proposed as the mono-chlorination product of c2. The position of the chlorine atom is not fully resolved with the data acquired and is therefore shown as delocalized in Figure 14, though the secondary amino structure is the most likely location of a nucleophilic substitution. As with SMX, aniline (proposed intermediate c1) is a product of the S-C hydrolysis and aniline can react with chlorine to form SDM110, SDM108, and SDM 144. The proposed pathway and putative mechanism is as discussed for SMX and provides evidence that aniline substituted sulfonamide antibiotics are likely to form these products upon chlorination.

Pathway D: SDM327 was identified as a mono-hydroxylated product of SDM. As was discussed for SMX, the hydroxylation is proposed to be a nucleophilic substitution on the amino group of the aniline substructure of SDM.

Pathway E: Proposed product SDM247 was the result of a sulfonate extraction mechanism. Unlike what was discussed for SMX, only a single peak was observed for the sulfonate extrusion product for SDM and a single structure is therefore proposed as shown in Figure 14. SDM247 reacted further to form several other products. SDM281 is

the mono-chlorinated product of SDM247. The chlorination is again proposed to be a nucleophilic substitution at the amino position of the aniline substructure. Successive deamination and hydroxylation reactions provide products of SDM248 and SDM282 from SDM247 and SDM281, respectively. The deamination is likely to happen to the original sulfonamide nitrogen moiety because the same reaction happens to SDM247 and its mono-N-chlorinated product, SDM281, suggesting that the amine portion of the aniline substructure is not where deamination takes place. No known mechanism was identified to explain sulfonamide deamination. The hydroxyl group is again proposed as a nucleophilic substitution on the amino group of the aniline substructure as has been previously discussed. SDM410, a tri-chlorinated product of SDM247, suggests greater extents of chlorine substitutions on SDM than on SMX in the presence of excess FAC. The chlorines are shown as delocalized in Figure 14, but the most likely positions are dichlorination at the amino group of the Aniline substructure and at the secondary amino group of the sulfonamide.

Pathway F: The identification of SDM330 suggests one of two possible reaction mechanisms: direct substitution of the amino group with a chlorine atom or cleavage of the C-N aniline bond followed by substitution of a chlorine. Amino cleavage of *para*-substituted anilines has previously been reported in photolysis reactions of sulfonamides and is therefore a better supported proposed mechanism.^{78, 95} However, this product was not directly measured in this work and is therefore shown as proposed intermediate f1. SDM330 is therefore proposed to form via mono-chlorination of f1. The location of the

chlorine atom in the molecule is not resolved and is shown as delocalized in Figure 14, yet it is most likely to be in the *para*- or *ortho*- position of the benzene ring.^{118, 119}

4.2.3 Reaction pathways of STZ-FAC

No previous studies have examined the formation of oxidation products of reactions between STZ and FAC either. As with SDM, it was expected that many of the reaction mechanisms previously reported and observed in this work for SMX or SDM would likewise lead to STZ products. The product spectrum and proposed STZ oxidation pathways are provided in Figure 15 and a detailed discussion of the pathways follows. If a mechanism has been discussed with SMX-FAC or SDM-FAC reactions in the previous section, it will not be discussed again for STZ-FAC reactions in the following. A total of 8 distinct pathways are proposed and described, as follows.

Pathway A: Once again, Pathway A starts off with a mono-chlorinated product identified as STZ289 in Figure 15. The chlorination is expected to occur as the result of a nucleophilic substitution on the amino group of the aniline substructure of STZ. As was observed with SDM, a mono-hydroxylated product was subsequently formed and is identified as STZ305 in Figure 15. The mechanism of formation is likewise presumed to be nucleophilic substitution, as was previously discussed.

Pathway B: The S-N hydrolysis reactions observed for SMX and SDM were likewise observed for STZ, supported by the direct measurement of both hydrolysis products STZ 174 and STZ101. STZ101 reacted further with FAC to form a mono-chlorinated product as shown in Figure 15 as STZ134. It is proposed that this is a nucleophilic substitution on the primary amino group.

Pathway C: The S-C hydrolysis reactions discussed with respect to SMX and SDM were somewhat directly supported by the measurement of the resulting sulfonate product (SMX) or the mono-chlorinated sulfonate product (SDM). Neither the aniline nor the sulfonate product (or any downstream products) were directly measured for STZ. However, the downstream products of aniline oxidation were measured and provide some evidence that S-C hydrolysis was occurring with STZ as well. Therefore, the S-C hydrolysis products of STZ are shown as proposed intermediates c1 and c2 and the aniline hydroxylation product is shown as proposed intermediate c3 and its downstream rearrangement as proposed intermediate c4. Then, STZ144 forms from proposed intermediate c4 as was previously described for SMX and SDM. Contrary to SMX and SDM, a subsequent di-chlorinated product was observed as STZ177.

Pathway D: A mono-hydroxylated product was observed as STZ272 as was observed with the other sulfonamide antibiotics. The mechanism is as proposed in the preceding discussion.

Pathway E: Proposed product STZ192 was the result of a sulfonate extraction mechanism. Similar as SDM, a single peak was observed for the sulfonate extrusion product for STZ and a single structure is therefore proposed as shown in Figure 15. STZ192 reacted further to form several other products. In the presence of excess FAC, STZ192 was chlorinated and formed an intermediate, N,N-dichlorinated STZ192, shown as proposed intermediate e1 in Figure 15. STZ224 was formed from h1 by a nucleophilic aromatic substitution of the aniline via Aryl nitrenium ions. The reaction was similar to that leading to the formation of a2 from a1 in SMX-FAC reactions in Figure 13, and that leading to the formation of SMX222 from e4 in SMX-FAC reactions in Figure 13. Also, STZ192 could undergo successive deamination and hydroxylation reactions and

form product STZ193. The reaction was similar to that leading to the formation of SDM248 from SDM247, and that leading to the formation of SDM282 from SDM281.

Pathway F: The observed formation of coupling products was unique to STZ. In Pathway E, a product was formed and the analytical data supports the proposed structure of STZ351. This product appears to be a conjugation of STZ and one of the previously discussed products STZ101. Whereas a conjugation of primary amines in oxidative environments is not unusual (see discussion for SMX503), this reaction product type was not observed for the other sulfonamide antibiotics studied.

Pathway G: Another apparent coupling reaction initiates proposed Pathway G. Here, the primary amino groups in STZ interacts with the primary amino group in the free aniline from proposed intermediate b1. The result is STZ379, which is a conjugation and mono-chlorinated product. The exact location of the chlorination is unresolved and shown as delocalized in Figure 15. Two related products were also observed, STZ347 and STZ381. These products are the result of a dehydrogenation reaction and dechlorination reaction, respectively. The observed trends in the intensity-FAC patterns of STZ379, STZ347, and STZ381 (see Appendix D) suggest that SMX347 and STZ381 form from STZ379. STZ381 is a hydrogenation product of STZ379, though it is not clear which double bond becomes saturated. STZ347 is a dechlorination and hydrogenation product of STZ379.

Pathway H: Another unique product observed for STZ was cleavage of the aryl ring connected to the sulfonamide bond. This cleavage led to the formation of proposed intermediate h1 which could be subsequently hydroxylated to yield STZ216. Ring cleavage reactions are not uncommon oxidation reactions,¹²⁰ though a specific mechanism resulting in these products was not determined.

4.3 Reaction mechanisms proposal

Combing the similarities of the above three reactions, we are able to identify some underlying mechanisms behind sulfonamide antibiotics, as a group, in reactions with FAC. Only mechanisms that could be observed in all three reactions are included here.

Pathway A: chlorine substitution reactions. Pathway As in the three reactions indicate that upon free chlorination, nucleophilic substitution of a Cl atom takes place at the amino nitrogen of sulfonamides, forming a mono-N-chlorinated product. Another Cl substitution could take place in the same manner, but the di-N-chlorinated product is not stable and was only observed in SDM-FAC reaction. The di-N-chlorinated product is expected to be unstable and form downstream products analogous to work done with anilines.^{116, 117}

Pathway B: hydrolysis reactions initiated by S-N bond cleavage. Facile cleavage of the S-N bond in sulfonamides enables the potential of hydrolysis reactions; this mechanism was observed in Pathway Bs of all three reactions. The para-sulfonate aniline product was only directly measured for SDM and STZ, but the corresponding hydrolysis product was measured for all three sulfonamide antibiotics.

Pathway C: hydrolysis reactions initiated by S-C bond cleavage. Observed products formed from all three sulfonamide antibiotics with nominal masses of 110, 108, or 144 likewise suggest a direct hydrolysis of the S-C bond yielding aniline as a primary product for all sulfonamide antibiotics investigated in this thesis. This mechanism was responsible for Pathway Cs in the three reactions.

Pathway D: hydroxylation reactions. Pathway Ds in the three reactions show that reactions with FAC also yield hydroxylation products. The mechanism resulting in stable hydroxylation products is purportedly through nucleophilic substitution on the N-aniline group. This was not observed as prominently as the mono-N-chlorination products and is therefore considered perhaps to be less favorable.

Pathway E: SO₂ extrusion reactions. Reactions that form products following extrusion of SO₂ groups were also observed for all of the investigated sulfonamide antibiotics and were indicated in Pathway Es. Mechanisms that support these findings have been proposed for in-source formation of SO₂ extrusion products in mass spectrometers, though no mechanism has been proposed for chemically mediated reactions. SO₂ extrusion products have been reported for sulfonamides undergoing photodegradation and biodegradation, but this appears to be an under-reported reaction pathway in the literature.

4.4 Environmental relevance

Sulfonamide antibiotics are frequently detected in the environment and have been shown to be persistent and resistant to many environmental processes. During drinking water treatment, sulfonamide antibiotics can be rapidly removed during chlorination, but there is concern over the formation of toxic chlorination byproducts.

The antibacterial activity of sulfonamide antibiotics is believed to be linked to the sulfonamide functional group.¹²¹ In this work, the structures of a total of 45 chlorination byproducts were proposed in reactions between three sulfonamide antibiotics and FAC. Of these 45 chlorination byproducts, 18 of them were unaltered at the sulfonamide functional group. This suggests that these chlorination products may retain antibacterial

activity. Further, chlorinated organic chemicals are purportedly toxic since the halogens groups are highly electronegative — therefore, they are highly reactive and can gain an electron through reaction with other elements.¹²² A total of 24 of the proposed chlorination products contained at least one chlorine atom in its structure. These products should be considered for toxicity screening to determine if there are any effects. Finally, a total of 13 of the proposed chlorination products contained no sulfonamide functional group or no chlorine atom or atoms. From a cursory inspection, it may be considered that these chlorination products have completely or partially lost their antibacterial activity. However, some of these products have also been shown to have toxic effects. For example, N-chloro-*p*-benzoquinone imine (NCBQ) has been shown to have a higher acute toxicity than sulfamethoxazole.¹²³ NCBQ was shown to form from SDM as well as SMX, the maximum yield of which (9.8%) was from SMX. The results from this thesis suggest that more detailed study of the toxicity of sulfonamide chlorination products is warranted.

CHAPTER 5 CONCLUSION

Sulfonamide antibiotics can be readily removed by free chlorination in drinking water treatment plants. Reactions were simulated in under-chlorinated and over-chlorinated conditions. Results showed that DBPs were formed from SMX, SDM, and STZ in reaction with FAC. In SMX-FAC, SDM-FAC, and STZ-FAC reactions, 8, 9, and 8 DBP peaks were observed on HPLC-UV-VIS and 16, 18, and 16 candidate DBP masses were detected by HPLC-MS, respectively. Most peaks observed on UV-VIS can be matched with masses obtained by MS according to RTs and trends of peak area over FAC concentrations. The MS data were used to propose structures of the DBPs. Each structure was proposed according to the integrated intensity of each sample, XIC, the MS spectra, reported oxidation reaction mechanisms of sulfonamide antibiotics and chlorination reaction mechanisms. Pathways of chlorination reaction for each of the studied sulfonamide antibiotics (SMX, SDM, and STZ) were proposed according to the proposed structures of products, Sieve integrated intensity data, and previously published reaction mechanisms. A total of 7, 6, 8 pathways were proposed to explain the formation of products in SMX-FAC, SDM-FAC, and STZ-FAC reactions, respectively. Among them, 5 pathways were common to all three reactions. The mechanisms responsible for those 5 pathways were considered as mechanisms of how the three sulfonamide antibiotics react with FAC: when in reaction with FAC, chlorine substitution reaction, hydrolysis reaction initiated by S-N bond cleavage, hydrolysis reaction started with S-C bond cleavage, hydroxylation reaction, and SO₂ extrusion reaction are likely to take place. This result is

important in predicting how sulfonamide antibiotics, as a group of micropollutants, react upon free chlorination.

Limitations of this study mainly include three aspects: first, some masses/frames that are possible DBPs were not assigned with structures. Among the 35, 31, 28 candidate DBP masses in positive ionization mode and the 4, 3, 11 candidate DBP masses in negative ionization mode in SMX-FAC, SDM-FAC, STZ-FAC reactions, only 16, 18, and 16 of them were assigned with structures, respectively. Those candidate DBP masses still have the potential to be proposed with structures given more time, more knowledge in oxidation reactions of sulfonamide antibiotics, and more knowledge of chlorination reactions. Second, proposed structures of DBPs are not confirmed. With no MS/MS data, structures of DBPs are considered only tentatively assigned. The confirmation of pathways and mechanisms rely on confirmation of structures of DBPs. Third, toxicity of most proposed DBPs remains unstudied. Though some DBPs were reported with toxicity, others were considered toxic because they preserved certain functional group. If they preserve toxicity, and if they do, would the toxicity worth our attention remain undiscussed in this thesis.

Six questions remain to be answered in future research. First, although toxicity of every DBP formed in the sulfonamide antibiotics-FAC reactions was not fully investigated in this study, it is worth studying in the future since it can be a concern to public health. DBPs formed that still preserve the sulfonamide functional groups may still preserve antibacterial activity, but the antibacterial activity for each DBP needs to be confirmed.

Also, the DBPs that have neither the sulfonamide functional group nor the halogen group could still be toxic, and their toxicity is worth future investigation. Second, the structures assigned for each DBP in this study were based on the available data and should be considered as proposals at this stage. The structures can be further validated by acquiring MS/MS data and confirmed by purchasing or synthesizing an authentic standard. Also, complementary analytical techniques (such as NMR) can be employed to confirm proposed structures. After validating assigned structures, proposed pathways and putative mechanisms need to be consolidated accordingly. Third, for some putatively identified DBPs, pathways leading to the formation of them are still unclear. Future research should investigate the mechanisms of these reaction pathways further for a comprehensive understanding of the reactions. Fourth, to examine if the putative mechanisms are applicable to all sulfonamide antibiotics, more experiments regarding sulfonamide antibiotics and FAC reactions could be done with other kinds of sulfonamide antibiotics. Fifth, the experiments were conducted with initial concentrations of sulfonamide antibiotics which were much higher than their concentrations in drinking water resources. Since previous studies reported that kinetics of chlorination reactions of certain sulfonamide antibiotics were influenced by the concentration of sulfonamide antibiotics, would the DBPs formed in environmental relevant concentrations of sulfonamide antibiotics and FAC within the time of drinking water treatment processes the same as what we determined here is a question worth exploring. Sixth, mechanisms of how sulfonamide antibiotics react with FAC may be applicable to other micropollutants with similar structures in reactions with FAC. Combining chlorination products of other

micropollutant included in Appendix A, future research studying if the mechanisms behind sulfonamide antibiotics-FAC reactions are behind reactions of other micropollutants upon chlorination is of broader significance. This is important in enhancing our understanding of DBPs in drinking water treatment and is worth being studied in the future.

In the process of doing research and writing this thesis, I have gained skills in analytical chemistry, data analysis, and academic writing. I particularly enjoyed the process of proposing pathways for those reactions. Studying the chlorination reaction mechanisms and previously reported oxidation reaction mechanisms of sulfonamide antibiotics and other chemicals became so interesting and motivating when the gained knowledge can be applied directly. The world of how micropollutants react with FAC is fascinating. I have gained a lot of valuable experience from doing this thesis, yet the one thing I benefit from this study that is maybe of most importance to me, is my developed interests in the mysterious world of chemical reactions: there are so many chemicals, so many micropollutants exist, and their structures differ and their reactions upon FAC differ. But there are similarities in their reaction mechanisms. That diversity and that integrity, to me, are more of art than science. And the beauty behind those structures of chemicals and reaction mechanisms is enchanting, and I will never stop pursuing the beauty from now on. For me, that is the meaning of attending graduate school. And I have my eternal gratitude to my advisor, for leading me along the way.

REFERENCES

1. Burkhardt-Holm, P., Endocrine Disruptors and Water Quality: A State-of-the-Art Review. *International Journal of Water Resources Development* **2010**, *26*, (3), 477-493.
2. Diamanti-Kandarakis, E.; Bourguignon, J.-P.; Giudice, L. C.; Hauser, R.; Prins, G. S.; Soto, A. M.; Zoeller, R. T.; Gore, A. C., Endocrine-Disrupting Chemicals: An Endocrine Society Scientific Statement. *Endocrine Reviews* **2009**, *30*, (4), 293-342.
3. de Jesus Gaffney, V.; Almeida, C. M. M.; Rodrigues, A.; Ferreira, E.; Benoliel, M. J.; Cardoso, V. V., Occurrence of pharmaceuticals in a water supply system and related human health risk assessment. *Water Research* **2015**, *72*, (0), 199-208.
4. Benner, J.; Helbling, D. E.; Kohler, H. P.; Wittebol, J.; Kaiser, E.; Prasse, C.; Ternes, T. A.; Albers, C. N.; Aamand, J.; Horemans, B.; Springael, D.; Walravens, E.; Boon, N., Is biological treatment a viable alternative for micropollutant removal in drinking water treatment processes? *Water Res* **2013**, *47*, (16), 5955-76.
5. Kor-Bicakci, G.; Pala-Ozkok, I.; Rehman, A.; Jonas, D.; Ubay-Cokgor, E.; Orhon, D., Chronic impact of sulfamethoxazole on acetate utilization kinetics and population dynamics of fast growing microbial culture. *Bioresource Technology* **2014**, *166*, 219-228.
6. Baquero, F.; Martinez, J. L.; Canton, R., Antibiotics and antibiotic resistance in water environments. *Current Opinion in Biotechnology* **2008**, *19*, (3), 260-265.
7. Lacaze, E.; Pedelucq, J.; Fortier, M.; Brousseau, P.; Auffret, M.; Budzinski, H.; Fournier, M., Genotoxic and immunotoxic potential effects of selected psychotropic drugs and antibiotics on blue mussel (*Mytilus edulis*) hemocytes. *Environmental pollution (Barking, Essex : 1987)* **2015**, *202*, 177-86.
8. Wang, Z.; Hop, C.; Kim, M. S.; Huskey, S. E. W.; Baillie, T. A.; Guan, Z. Q., The unanticipated loss of SO₂ from sulfonamides in collision-induced dissociation. *Rapid Communications in Mass Spectrometry* **2003**, *17*, (1), 81-86.
9. Gibbons, J.; Laha, S., Water purification systems: a comparative analysis based on the occurrence of disinfection by-products. *Environmental Pollution* **1999**, *106*, (3), 425-428.
10. Hrudey, S. E., Chlorination disinfection by-products, public health risk tradeoffs and me. *Water Research* **2009**, *43*, (8), 2057-2092.

11. Calabrese, E. J., *Safe Drinking Water Act*. CRC Press: 1989.
12. Majewsky, M.; Wagner, D.; Delay, M.; Brase, S.; Yargeau, V.; Horn, H., Antibacterial Activity of Sulfamethoxazole Transformation Products (TPs): General Relevance for Sulfonamide TPs Modified at the para Position. *Chem. Res. Toxicol.* **2014**, *27*, (10), 1821-1828.
13. Bell, K. Y.; Wells, M. J. M.; Traexler, K. A.; Pellegrin, M. L.; Morse, A.; Bandy, J., Emerging Pollutants. *Water Environ. Res.* **2011**, *83*, (10), 1906-1984.
14. Helbling, D. E.; Johnson, D. R.; Lee, T. K.; Scheidegger, A.; Fenner, K., A framework for establishing predictive relationships between specific bacterial 16S rRNA sequence abundances and biotransformation rates. *Water Research* **2015**, *70*, 471-484.
15. Helbling, D. E., Bioremediation of pesticide-contaminated water resources: the challenge of low concentrations. *Current Opinion in Biotechnology* **2015**, *33*, (0), 142-148.
16. Houtman, C. J.; Kroesbergen, J.; Lekkerkerker-Teunissen, K.; van der Hoek, J. P., Human health risk assessment of the mixture of pharmaceuticals in Dutch drinking water and its sources based on frequent monitoring data. *Science of The Total Environment* **2014**, *496*, (0), 54-62.
17. de Jesus Gaffney, V.; Almeida, C. M.; Rodrigues, A.; Ferreira, E.; Benoliel, M. J.; Cardoso, V. V., Occurrence of pharmaceuticals in a water supply system and related human health risk assessment. *Water Res* **2015**, *72*, 199-208.
18. Benotti, M. J.; Trenholm, R. A.; Vanderford, B. J.; Holady, J. C.; Stanford, B. D.; Snyder, S. A., Pharmaceuticals and Endocrine Disrupting Compounds in U.S. Drinking Water. *Environ. Sci. Technol.* **2009**, *43*, (3), 597-603.
19. Backe, W. J.; Day, T. C.; Field, J. A., Zwitterionic, Cationic, and Anionic Fluorinated Chemicals in Aqueous Film Forming Foam Formulations and Groundwater from US Military Bases by Nonaqueous Large-Volume Injection HPLC-MS/MS. *Environ. Sci. Technol.* **2013**, *47*, (10), 5226-5234.
20. Mawhinney, D. B.; Young, R. B.; Vanderford, B. J.; Borch, T.; Snyder, S. A., Artificial sweetener sucralose in U.S. drinking water systems. *Environ Sci Technol* **2011**, *45*, (20), 8716-22.
21. Yan, S.; Subramanian, S. B.; Tyagi, R. D.; Surampalli, R. Y.; Zhang, T. C., Emerging contaminants of environmental concern: source, transport, fate, and treatment. *Practice Periodical of Hazardous, Toxic and Radioactive Waste Management* **2010**, *14*, (1), 2-20.

22. Helbling, D. E.; Johnson, D. R.; Honti, M.; Fenner, K., Micropollutant biotransformation kinetics associate with WWTP process parameters and microbial community characteristics. *Environ Sci Technol* **2012**, *46*, (19), 10579-88.
23. Martin, J. W.; Asher, B. J.; Beesoon, S.; Benskin, J. P.; Ross, M. S., PFOS or PreFOS? Are perfluorooctane sulfonate precursors (PreFOS) important determinants of human and environmental perfluorooctane sulfonate (PFOS) exposure? *Journal of Environmental Monitoring* **2010**, *12*, (11), 1979-2004.
24. Steen, P. O.; Grandbois, M.; McNeill, K.; Arnold, W. A., Photochemical Formation of Halogenated Dioxins from Hydroxylated Polybrominated Diphenyl Ethers (OH-PBDEs) and Chlorinated Derivatives (OH-PBCDEs). *Environ. Sci. Technol.* **2009**, *43*, (12), 4405-4411.
25. Richardson, S. D.; Ternes, T. A., Water analysis: emerging contaminants and current issues. *Anal Chem* **2011**, *83*, (12), 4614-48.
26. Sorensen, J. P. R.; Lapworth, D. J.; Nkhuwa, D. C. W.; Stuart, M. E.; Gooddy, D. C.; Bell, R. A.; Chirwa, M.; Kabika, J.; Liemisa, M.; Chibesa, M.; Pedley, S., Emerging contaminants in urban groundwater sources in Africa. *Water Research* **2015**, *72*, (0), 51-63.
27. Kim, S. D.; Cho, J.; Kim, I. S.; Vanderford, B. J.; Snyder, S. A., Occurrence and removal of pharmaceuticals and endocrine disruptors in South Korean surface, drinking, and waste waters. *Water Res* **2007**, *41*, (5), 1013-21.
28. Le-Minh, N.; Khan, S. J.; Drewes, J. E.; Stuetz, R. M., Fate of antibiotics during municipal water recycling treatment processes. *Water Research* **2010**, *44*, (15), 4295-4323.
29. Petrie, B.; Barden, R.; Kasprzyk-Hordern, B., A review on emerging contaminants in wastewaters and the environment: Current knowledge, understudied areas and recommendations for future monitoring. *Water Research* **2015**, *72*, (0), 3-27.
30. Metcalfe, C.; Miao, X. S.; Hua, W.; Letcher, R.; Servos, M., Pharmaceuticals in the Canadian Environment. In *Pharmaceuticals in the Environment*, Kümmerer, K., Ed. Springer Berlin Heidelberg: 2004; pp 67-90.
31. Stackelberg, P. E.; Gibs, J.; Furlong, E. T.; Meyer, M. T.; Zaugg, S. D.; Lippincott, R. L., Efficiency of conventional drinking-water-treatment processes in removal of pharmaceuticals and other organic compounds. *Sci Total Environ* **2007**, *377*, (2-3), 255-72.

32. Adams, C.; Wang, Y.; Loftin, K.; Meyer, M., Removal of antibiotics from surface and distilled water in conventional water treatment processes. *Journal of Environmental Engineering-Asce* **2002**, *128*, (3), 253-260.
33. Ternes, T. A.; Meisenheimer, M.; McDowell, D.; Sacher, F.; Brauch, H. J.; Gulde, B. H.; Preuss, G.; Wilme, U.; Seibert, N. Z., Removal of pharmaceuticals during drinking water treatment. *Environ. Sci. Technol.* **2002**, *36*, (17), 3855-3863.
34. Westerhoff, P.; Yoon, Y.; Snyder, S.; Wert, E., Fate of endocrine-disruptor, pharmaceutical, and personal care product chemicals during simulated drinking water treatment processes. *Environ. Sci. Technol.* **2005**, *39*, (17), 6649-6663.
35. Meffe, R.; Kohfahl, C.; Holzbecher, E.; Massmann, G.; Richter, D.; Dunnbier, U.; Pekdeger, A., Modelling the removal of p-TSA (para-toluenesulfonamide) during rapid sand filtration used for drinking water treatment. *Water Research* **2010**, *44*, (1), 205-213.
36. Richter, D.; Massmann, G.; Dunnbier, U., Behaviour and biodegradation of sulfonamides (p-TSA, o-TSA, BSA) during drinking water treatment. *Chemosphere* **2008**, *71*, (8), 1574-1581.
37. Zearley, T. L.; Summers, R. S., Removal of Trace Organic Micropollutants by Drinking Water Biological Filters. *Environ. Sci. Technol.* **2012**, *46*, (17), 9412-9419.
38. Zuehlke, S.; Duennbier, U.; Heberer, T., Investigation of the behavior and metabolism of pharmaceutical residues during purification of contaminated ground water used for drinking water supply. *Chemosphere* **2007**, *69*, (11), 1673-1680.
39. <Sulfamethoxazole kinetics and pathways.pdf>.
40. Padhye, L. P.; Yao, H.; Kung'u, F. T.; Huang, C. H., Year-long evaluation on the occurrence and fate of pharmaceuticals, personal care products, and endocrine disrupting chemicals in an urban drinking water treatment plant. *Water Res* **2014**, *51*, 266-76.
41. Ivančev-Tumbas, I., The fate and importance of organics in drinking water treatment: a review. *Environ Sci Pollut Res* **2014**, *21*, (20), 11794-11810.
42. Murray, K. E.; Thomas, S. M.; Bodour, A. A., Prioritizing research for trace pollutants and emerging contaminants in the freshwater environment. *Environmental Pollution* **2010**, *158*, (12), 3462-3471.
43. Daughton, C. G.; Ternes, T. A., Pharmaceuticals and personal care products in the environment: Agents of subtle change? *Environ. Health Perspect.* **1999**, *107*, 907-938.
44. McKinlay, R.; Plant, J. A.; Bell, J. N. B.; Voulvoulis, N., Endocrine disrupting pesticides: implications for risk assessment. *Environment International* **2008**, *34*, (2), 168-183.

45. Boyd, G. R.; Reemtsma, H.; Grimm, D. A.; Mitra, S., Pharmaceuticals and personal care products (PPCPs) in surface and treated waters of Louisiana, USA and Ontario, Canada. *Science of The Total Environment* **2003**, *311*, (1-3), 135-149.
46. Rosi-Marshall, E. J.; Kelly, J. J., Antibiotic Stewardship Should Consider Environmental Fate of Antibiotics. *Environ. Sci. Technol.* **2015**, *49*, (9), 5257-5258.
47. Fent, K.; Weston, A. A.; Caminada, D., Ecotoxicology of human pharmaceuticals. *Aquatic Toxicology* **2006**, *76*, (2), 122-159.
48. Bulloch, D. N.; Lavado, R.; Forsgren, K. L.; Beni, S.; Schlenk, D.; Larive, C. K., Analytical and biological characterization of halogenated gemfibrozil produced through chlorination of wastewater. *Environ Sci Technol* **2012**, *46*, (10), 5583-9.
49. Carbajo, J. B.; Perdigon-Melon, J. A.; Petre, A. L.; Rosal, R.; Leton, P.; Garcia-Calvo, E., Personal care product preservatives: Risk assessment and mixture toxicities with an industrial wastewater. *Water Research* **2015**, *72*, 174-185.
50. Zarrelli, A.; Dellagreca, M.; Iesce, M. R.; Lavorgna, M.; Temussi, F.; Schiavone, L.; Criscuolo, E.; Parrella, A.; Previtera, L.; Isidori, M., Ecotoxicological evaluation of caffeine and its derivatives from a simulated chlorination step. *Sci Total Environ* **2014**, *470-471*, 453-8.
51. Maier, D.; Blaha, L.; Giesy, J. P.; Henneberg, A.; Kohler, H. R.; Kuch, B.; Osterauer, R.; Peschke, K.; Richter, D.; Scheurer, M.; Tribskorn, R., Biological plausibility as a tool to associate analytical data for micropollutants and effect potentials in wastewater, surface water, and sediments with effects in fishes. *Water Research* **2015**, *72*, 127-144.
52. Virto, R.; Sanz, D.; Alvarez, I.; Condon, S.; Raso, J., Relationship between inactivation kinetics of a *Listeria monocytogenes* suspension by chlorine and its chlorine demand. *J. Appl. Microbiol.* **2004**, *97*, (6), 1281-1288.
53. Virto, R.; Manas, P.; Alvarez, I.; Condon, S.; Raso, J., Membrane damage and microbial inactivation by chlorine in the absence and presence of a chlorine-demanding substrate. *Applied and Environmental Microbiology* **2005**, *71*, (9), 5022-5028.
54. Bersillon, J. L., Water purification and disinfection processes. *Acta Hydrochimica Et Hydrobiologica* **1999**, *27*, (2), 98-100.
55. Helbling, D. E.; VanBriesen, J. M., Free chlorine demand and cell survival of microbial suspensions. *Water Research* **2007**, *41*, (19), 4424-4434.

56. Gopal, K.; Tripathy, S. S.; Bersillon, J. L.; Dubey, S. P., Chlorination byproducts, their toxicodynamics and removal from drinking water. *J. Hazard. Mater.* **2007**, *140*, (1-2), 1-6.
57. White, D. M.; Garland, D. S.; Narr, J.; Woolard, C. R., Natural organic matter and DBP formation potential in Alaskan water supplies. *Water Research* **2003**, *37*, (4), 939-947.
58. Richardson, S. D.; Plewa, M. J.; Wagner, E. D.; Schoeny, R.; DeMarini, D. M., Occurrence, genotoxicity, and carcinogenicity of regulated and emerging disinfection by-products in drinking water: A review and roadmap for research. *Mutation Research/Reviews in Mutation Research* **2007**, *636*, (1-3), 178-242.
59. Chisholm, K.; Cook, A.; Bower, C.; Weinstein, P., Risk of birth defects in Australian communities with high levels of brominated disinfection by-products. *Environ. Health Perspect.* **2008**, *116*, (9), 1267-1273.
60. Pan, S. L.; An, W.; Li, H. Y.; Su, M.; Zhang, J. L.; Yang, M., Cancer risk assessment on trihalomethanes and haloacetic acids in drinking water of China using disability-adjusted life years. *J. Hazard. Mater.* **2014**, *280*, 288-294.
61. Porter, C. K.; Putnam, S. D.; Hunting, K. L.; Riddle, M. R., The effect of trihalomethane and haloacetic acid exposure on fetal growth in a Maryland county. *Am. J. Epidemiol.* **2005**, *162*, (4), 334-344.
62. Bove, F.; Shim, Y.; Zeitz, P., Drinking water contaminants and adverse pregnancy outcomes: A review. *Environ. Health Perspect.* **2002**, *110*, 61-74.
63. Nieuwenhuijsen, M. J.; Toledano, M. B.; Eaton, N. E.; Fawell, J.; Elliott, P., Chlorination disinfection byproducts in water and their association with adverse reproductive outcomes: a review. *Occup. Environ. Med.* **2000**, *57*, (2), 73-85.
64. Waller, K.; Swan, S. H.; DeLorenze, G.; Hopkins, B., Trihalomethanes in drinking water and spontaneous abortion. *Epidemiology* **1998**, *9*, (2), 134-140.
65. Quintana, J. B.; Rodil, R.; Lopez-Mahia, P.; Muniategui-Lorenzo, S.; Prada-Rodriguez, D., Investigating the chlorination of acidic pharmaceuticals and by-product formation aided by an experimental design methodology. *Water Res* **2010**, *44*, (1), 243-55.
66. Bedner, M.; Maccrehan, W. A., Transformation of acetaminophen by chlorination produces the toxicants 1,4-benzoquinone and N-acetyl-p-benzoquinone imine. *Environ. Sci. Technol.* **2006**, *40*, (2), 516-522.

67. Dodd, M. C., Transformation of the Antibacterial Agent Sulfamethoxazole in Reactions with Chlorine: Kinetics, Mechanisms, and Pathways. *Environ Sci Technol* **2004**.
68. Minguet, F.; Van Den Boogerd, L.; Salgado, T. M.; Correr, C. J.; Fernandez-Llimos, F., Characterization of the Medical Subject Headings thesaurus for pharmacy. *American Journal of Health-System Pharmacy* **2014**, *71*, (22), 1965-1972.
69. Heuer, H.; Solehati, Q.; Zimmerling, U.; Kleineidam, K.; Schlöter, M.; Müller, T.; Focks, A.; Thiele-Bruhn, S.; Smalla, K., Accumulation of Sulfonamide Resistance Genes in Arable Soils Due to Repeated Application of Manure Containing Sulfadiazine. *Applied and Environmental Microbiology* **2011**, *77*, (7), 2527-2530.
70. Managaki, S.; Murata, A.; Takada, H.; Tuyen, B. C.; Chiem, N. H., Distribution of macrolides, sulfonamides, and trimethoprim in tropical waters: Ubiquitous occurrence of veterinary antibiotics in the Mekong Delta. *Environ. Sci. Technol.* **2007**, *41*, (23), 8004-8010.
71. Gobel, A.; Thomsen, A.; McArdell, C. S.; Joss, A.; Giger, W., Occurrence and sorption behavior of sulfonamides, macrolides, and trimethoprim in activated sludge treatment. *Environ. Sci. Technol.* **2005**, *39*, (11), 3981-3989.
72. Garcia-Galan, M. J.; Diaz-Cruz, M. S.; Barcelo, D., Occurrence of sulfonamide residues along the Ebro river basin Removal in wastewater treatment plants and environmental impact assessment. *Environment International* **2011**, *37*, (2), 462-473.
73. Bolong, N.; Ismail, A. F.; Salim, M. R.; Matsuura, T., A review of the effects of emerging contaminants in wastewater and options for their removal. *Desalination* **2009**, *239*, (1-3), 229-246.
74. Onesios, K. M.; Yu, J. T.; Bouwer, E. J., Biodegradation and removal of pharmaceuticals and personal care products in treatment systems: a review. *Biodegradation* **2009**, *20*, (4), 441-466.
75. Mompelat, S.; Le Bot, B.; Thomas, O., Occurrence and fate of pharmaceutical products and by-products, from resource to drinking water. *Environment International* **2009**, *35*, (5), 803-814.
76. Postigo, C.; Richardson, S. D., Transformation of pharmaceuticals during oxidation/disinfection processes in drinking water treatment. *J. Hazard. Mater.* **2014**, *279*, 461-475.
77. Chen, H.; Gao, B.; Li, H.; Ma, L. Q., Effects of pH and ionic strength on sulfamethoxazole and ciprofloxacin transport in saturated porous media. *Journal of Contaminant Hydrology* **2011**, *126*, (1-2), 29-36.

78. Boreen, A. L.; Arnold, W. A.; McNeill, K., Photochemical fate of sulfa drugs in the aquatic environment: Sulfa drugs containing five-membered heterocyclic groups. *Environ. Sci. Technol.* **2004**, 38, (14), 3933-3940.
79. Zhong, Z. X.; Xu, J.; Zhang, Y.; Li, L.; Guo, C. S.; He, Y.; Fan, W. H.; Zhang, B. P., Adsorption of sulfonamides on lake sediments. *Front. Env. Sci. Eng.* **2013**, 7, (4), 518-525.
80. Chamberlain, E.; Adams, C., Oxidation of sulfonamides, macrolides, and carbadox with free chlorine and monochloramine. *Water Research* **2006**, 40, (13), 2517-2526.
81. J.P., G., Kinetics and products of caffeine chlorination. *Water Res* **1984**.
82. Rule, V., Formation of Chloroform and Chlorinated Organics by Free-Chlorine-Mediated Oxidation of Triclosan.
83. Gao, S.; Zhao, Z.; Xu, Y.; Tian, J.; Qi, H.; Lin, W.; Cui, F., Oxidation of sulfamethoxazole (SMX) by chlorine, ozone and permanganate--a comparative study. *J Hazard Mater* **2014**, 274, 258-69.
84. Helbling, D. E.; Hollender, J.; Kohler, H. P. E.; Fenner, K., Structure-Based Interpretation of Biotransformation Pathways of Amide-Containing Compounds in Sludge-Seeded Bioreactors. *Environ. Sci. Technol.* **2010**, 44, (17), 6628-6635.
85. Helbling, D. E.; Hollender, J.; Kohler, H. P. E.; Singer, H.; Fenner, K., High-Throughput Identification of Microbial Transformation Products of Organic Micropollutants. *Environ. Sci. Technol.* **2010**, 44, (17), 6621-6627.
86. Helbling, D. E.; Hammes, F.; Egli, T.; Kohler, H. P., Kinetics and yields of pesticide biodegradation at low substrate concentrations and under conditions restricting assimilable organic carbon. *Appl Environ Microbiol* **2014**, 80, (4), 1306-13.
87. Prasse, C.; Zech, W.; Itanna, F.; Glaser, B., Contamination and source assessment of metals, polychlorinated biphenyls, and polycyclic aromatic hydrocarbons in urban soils from Addis Ababa, Ethiopia. *Toxicological and Environmental Chemistry* **2012**, 94, (10), 1954-1979.
88. Gassman, P. G.; Campbell, G. A., CHEMISTRY OF NITRENIUM IONS .22. THERMAL REARRANGEMENT OF N-CHLOROANILINES - EVIDENCE FOR INTERMEDIACY OF NITRENIUM IONS. *Journal of the American Chemical Society* **1972**, 94, (11), 3891-&.
89. Dodd, M. C.; Huang, C. H., Aqueous chlorination of the antibacterial agent trimethoprim: reaction kinetics and pathways. *Water Res* **2007**, 41, (3), 647-55.

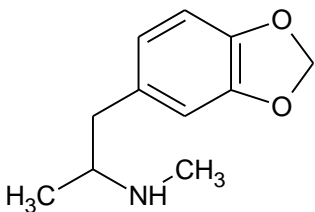
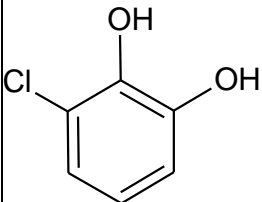
90. Uetrecht, J. P.; Shear, N. H.; Zahid, N., N-CHLORINATION OF SULFAMETHOXAZOLE AND DAPSONE BY THE MYELOPEROXIDASE SYSTEM. *Drug Metab. Dispos.* **1993**, *21*, (5), 830-834.
91. Gassman, P. G.; Frederic, R.; Campbell, G. A., CHEMISTRY OF NITRENIUM IONS. 21. NUCLEOPHILIC AROMATIC SUBSTITUTION OF ANILINES VIA ARYL NITRENIUM IONS (ANILENIUM IONS). *Journal of the American Chemical Society* **1972**, *94*, (11), 3884-&.
92. Haberfield, P.; Paul, D., The Chlorination of Anilines. Proof of the Existence of an N-Chloro Intermediate. *Journal of the American Chemical Society* **1965**, *87*, (23), 5502-5502.
93. Manzo, R. H.; Martinez de Bertorello, M., Isoxazoles. 4. Hydrolysis of sulfonamide isoxazole derivatives in concentrated sulfuric acid solutions. A new treatment of the medium effects on protonation equilibria and reaction rates. *The Journal of Organic Chemistry* **1978**, *43*, (6), 1173-1177.
94. Gao, J.; Hedman, C.; Liu, C.; Guo, T.; Pedersen, J. A., Transformation of sulfamethazine by manganese oxide in aqueous solution. *Environ Sci Technol* **2012**, *46*, (5), 2642-51.
95. Bonvin, F.; Omlin, J.; Rutler, R.; Schweizer, W. B.; Alaimo, P. J.; Strathmann, T. J.; McNeill, K.; Kohn, T., Direct photolysis of human metabolites of the antibiotic sulfamethoxazole: evidence for abiotic back-transformation. *Environ Sci Technol* **2013**, *47*, (13), 6746-55.
96. Garcia-Galan, M. J.; Diaz-Cruz, M. S.; Barcelo, D., Kinetic studies and characterization of photolytic products of sulfamethazine, sulfapyridine and their acetylated metabolites in water under simulated solar irradiation. *Water Res* **2012**, *46*, (3), 711-22.
97. Hu, L. H.; Flanders, P. M.; Miller, P. L.; Strathmann, T. J., Oxidation of sulfamethoxazole and related antimicrobial agents by TiO₂ photocatalysis. *Water Research* **2007**, *41*, (12), 2612-2626.
98. Trovo, A. G.; Nogueira, R. F. P.; Agüera, A.; Fernandez-Alba, A. R.; Sirtori, C.; Malato, S., Degradation of sulfamethoxazole in water by solar photo-Fenton. Chemical and toxicological evaluation. *Water Research* **2009**, *43*, (16), 3922-3931.
99. Kwart, H.; Body, R. W., Further Studies of Mechanisms of Chlorinolysis of Sulfur-Carbon Bonds. The Mechanism of Abnormal Chlorinolysis and Desulfonylation of Sulfonyl Chlorides. III. *The Journal of Organic Chemistry* **1965**, *30*, (4), 1188-1195.

100. Zhao, Z.; Koeplinger, K. A.; Peterson, T.; Conradi, R. A.; Burton, P. S.; Suarato, A.; Heinrikson, R. L.; Tomasselli, A. G., Mechanism, Structure-Activity Studies, and Potential Applications of Glutathione S-Transferase-Catalyzed Cleavage of Sulfonamides. *Drug Metab. Dispos.* **1999**, 27, (9), 992-998.
101. Timbrell, J., *Principles of biochemical toxicology*. CRC Press: 1999.
102. Sternson, L. A.; Hes, J., Electrochemical method for the determination of aniline hydroxylation in liver. *Analytical Biochemistry* **1975**, 67, (1), 74-80.
103. Tomoda, A.; Yubisui, T.; Ida, M.; Kawachi, N.; Yoneyama, Y., Aniline hydroxylation in the human red cells. *Experientia* **1977**, 33, (10), 1276-1277.
104. Zhao, J.-S.; Singh, A.; Huang, X.-D.; Ward, O. P., Biotransformation of Hydroxylaminobenzene and Aminophenol by *Pseudomonas putida* 2NP8 Cells Grown in the Presence of 3-Nitrophenol. *Applied and Environmental Microbiology* **2000**, 66, (6), 2336-2342.
105. Ricken, B.; Fellmann, O.; Kohler, H.-P. E.; Schäffer, A.; Corvini, P. F.-X.; Kolvenbach, B. A., Degradation of sulfonamide antibiotics by *Microbacterium* sp. strain BR1 – elucidating the downstream pathway. *New Biotechnology* **2015**, (0).
106. Avdeenko, A. P.; Marchenko, I. L., Chlorination of N-acyl Derivatives of p-Aminophenols (Naphthols) and p-Phenylenediamines. *Russian Journal of Organic Chemistry* **2001**, 37, (6), 822-829.
107. Schwarz, J.; Aust, M.-O.; Thiele-Bruhn, S., Metabolites from fungal laccase-catalysed transformation of sulfonamides. *Chemosphere* **2010**, 81, (11), 1469-1476.
108. Gassman, P. G.; Campbell, G. A.; Frederick, R. C., Chemistry of nitrenium ions. XXI. Nucleophilic aromatic substitution of anilines via aryl nitrenium ions (anilenium ions). *Journal of the American Chemical Society* **1972**, 94, (11), 3884-3891.
109. Perisa, M.; Babic, S.; Skoric, I.; Fromel, T.; Knepper, T. P., Photodegradation of sulfonamides and their N (4)-acetylated metabolites in water by simulated sunlight irradiation: kinetics and identification of photoproducts. *Environ Sci Pollut Res* **2013**, 20, (12), 8934-8946.
110. Deborde, M.; von Gunten, U., Reactions of chlorine with inorganic and organic compounds during water treatment-Kinetics and mechanisms: a critical review. *Water Res* **2008**, 42, (1-2), 13-51.
111. Morris, J. C., *THE CHEMISTRY OF AQUEOUS CHLORINE IN RELATION TO WATER CHLORINATION*. 1978; p 21-35.

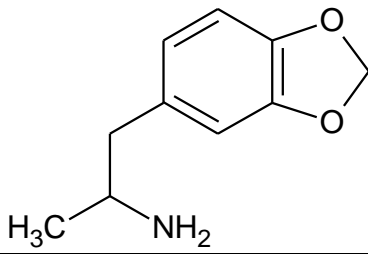
112. Larson, R. A.; Weber, E. J., *Reaction mechanisms in environmental organic chemistry*. CRC press: 1994.
113. Goldschmidt, S.; Strohmenger, L., Aromatic chloramine(II). *Berichte Der Deutschen Chemischen Gesellschaft* **1922**, *55*, 2450-2470.
114. Noller, C. R., *Chemistry of organic compounds*. Saunders: Philadelphia, 1951; p ix, 885 p.
115. Fox, T. C.; Keefe, D. J.; Scully, F. E.; Laikhter, A., Chloramines VII: Chlorination of Alanine/phenylalanine in Model Solutions and in a Wastewater. *Environ. Sci. Technol.* **1997**, *31*, (7), 1979-1984.
116. Conyers, B.; Scully, F. E., Chloramines V: Products and Implications of the Chlorination of Lysine in Municipal Wastewaters. *Environ. Sci. Technol.* **1997**, *31*, (6), 1680-1685.
117. Nweke, A.; Scully, F. E., Stable N-chloroaldehydes and other products of the chlorination of isoleucine in model solutions and in a wastewater. *Environ. Sci. Technol.* **1989**, *23*, (8), 989-994.
118. Benjamin, M. M.; Lawler, D. F., *Water quality engineering: physical/chemical treatment processes*. John Wiley & Sons: 2013.
119. Bulloch, D. N.; Nelson, E. D.; Carr, S. A.; Wissman, C. R.; Armstrong, J. L.; Schlenk, D.; Larive, C. K., Occurrence of halogenated transformation products of selected pharmaceuticals and personal care products in secondary and tertiary treated wastewaters from southern California. *Environ Sci Technol* **2015**, *49*, (4), 2044-51.
120. Cai, M.-Q.; Zhang, L.-Q.; Feng, L., Influencing factors and degradation behavior of propyphenazone and aminopyrine by free chlorine oxidation. *Chemical Engineering Journal* **2014**, *244*, (0), 188-194.
121. Huang, D.-J.; Hou, J.-H.; Kuo, T.-F.; Lai, H.-T., Toxicity of the veterinary sulfonamide antibiotic sulfamonomethoxine to five aquatic organisms. *Environmental Toxicology and Pharmacology* **2014**, *38*, (3), 874-880.
122. Siekierski, S.; Burgess, J., 13 - Group 17. The halogens. In *Concise Chemistry of the Elements*, Burgess, S. S., Ed. Woodhead Publishing: 2002; pp 121-126.
123. Dodd, M. C.; Rentsch, D.; Singer, H. P.; Kohler, H.-P. E.; Gunten, U. v., Transformation of β -Lactam Antibacterial Agents during Aqueous Ozonation: Reaction Pathways and Quantitative Bioassay of Biologically-Active Oxidation Products. *Environ. Sci. Technol.* **2010**, *44*, (15), 5940-5948.

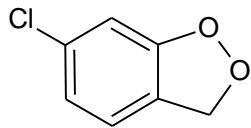
APPENDIX A – DATABASE OF PREVIOUSLY REPORTED PRODUCTS OF REACTIONS BETWEEN ORGANIC CHEMICALS AND FREE CHLORINE

3,4-Methylenedioxymethamphetamine(MDMA)

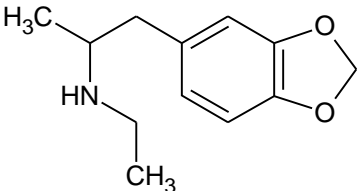
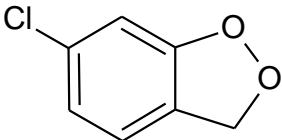
3,4-Methylenedioxymethamphetamine(MDMA)				
Smile				
CC(CC1=CC2=C(C=C1)OCO2)NC				
Potential Harm				
potent psychoactive properties and unknown effects to the aquatic environment				
Author	Year Published	Journal	Paper Link	
Huerta-Fontela	2012	Water Research	http://www.sciencedirect.com/science/article/pii/S0043135412001923	
Contaminant Concentration (ng/L)		Chlorine Concentration (mg/L)	Reaction Time	pH
2.3 - 78		1 – 1000	NA	7
Product	Name	Smile	Structure	
1	3-chlorocatechol 1	C1=CC(=C(C(=C1)Cl)O)O		

3,4-Methylenedioxyamphetamine(MDA)

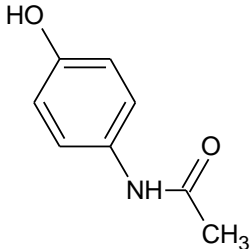
3,4-Methylenedioxyamphetamine(MDA)			
Smile			
CC(CC1=CC2=C(C=C1)OCO2)N			
Potential Harm			
potent psychoactive properties and unknown effects to the aquatic environment			
Author	Year Published	Journal	Paper Link
Huerta-Fontela	2012	Water Research	http://www.sciencedirect.com/science/article/pii/S0043135412001923

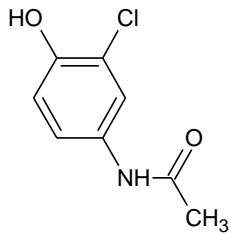
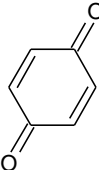
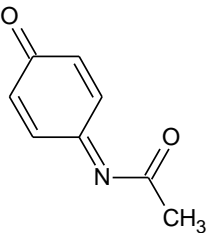
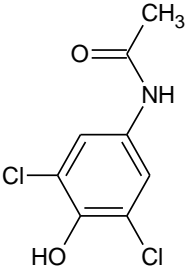
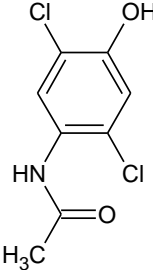
Contaminant Concentration (ng/L)		Chlorine Concentration (mg/L)	Reaction Time	pH
2.3 - 78		1 – 1000	NA	7
	Name	Smile	Structure	
Product	(3-chlorobenzo)-1,3-dioxole	Clc1ccc2COOc2c1		

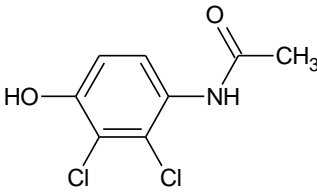
3,4-methylenedioxyethylamphetamine(MDEA)

3,4-methylenedioxyethylamphetamine(MDEA)				
Smile				
CC(NCC)Cc1ccc2COOc2c1				
Potential Harm				
potent psychoactive properties and unknown effects to the aquatic environment				
Author	Year Published	Journal	Paper Link	
Huerta-Fontela	2012	Water Research	http://www.sciencedirect.com/science/article/pii/S0043135412001923	
Contaminant Concentration (ng/L)		Chlorine Concentration (mg/L)	Reaction Time	pH
2.3 - 78		1 – 1000	NA	7
	Name	Smile	Structure	
Product	(3-chlorobenzo)-1,3-dioxole	Clc1ccc2COOc2c1		

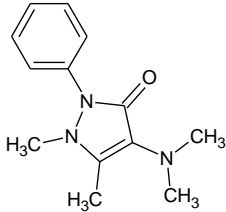
Acetaminophen

Acetaminophen	
Smile	
CC(=O)NC1=CC=C(C=C1)O	
Potential Harm	
N-acetyl-p-benzoquinone imine is the toxicant associated with lethality in acetaminophen overdoses	

Author	Year Published	Journal	Paper Link	
Bedner	2006	Environmental Science and Technology	http://pubs.acs.org/doi/pdf/10.1021/es0509073	
Contaminant Concentration (mg/L)		Chlorine Concentration (μmole/L)	Reaction Time	pH
1.5		57	1 – 2 h	7.0
Product	Name	Smile	Structure	
1	Chloro-4-acetamidophenol	<chem>CC(=O)NC1=CC(=C(C=C1)O)Cl</chem>		
2	1,4-benzoquinone	<chem>C1=CC(=O)C=CC1=O</chem>		
3	N-acetyl-p-benzoquinone imine	<chem>CC(=O)N=C1C=CC(=O)C=C1</chem>		
4	Dichloro-4-acetamidophenol	<chem>Clc1cc(cc(Cl)c1O)NC(C)=O</chem>		
5	N-(2,5-dichloro-4-hydroxyphenyl)acetamide	<chem>Clc1cc(O)c(Cl)cc1NC(C)=O</chem>		

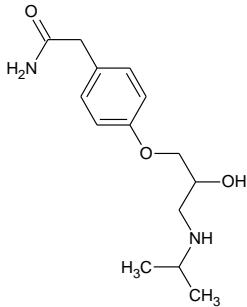
6	N-(2,3-dichloro-4-hydroxyphenyl)acetamide	<chem>Clc1c(NC(C)=O)ccc(O)c1Cl</chem>	
---	---	---------------------------------------	---

Aminopyrine (AMP)

Aminopyrine(AMP)				
Smile				
<chem>Cc1c(c(=O)n(n1C)c2ccccc2)N(C)C</chem>				
Potential Harm				
Author	Year Published	Journal	Paper Link	
Cai	2014	Chemical Engineering Journal	http://www.sciencedirect.com/science/article/pii/S1385894714000746	
Contaminant Concentration (μM)		Chlorine Concentration (μM)	Reaction Time	pH
0.1 – 1.25		14.08 – 28.17	24 h	3.0 – 9.0
They explored the reaction mechanism, but did not detect products.				

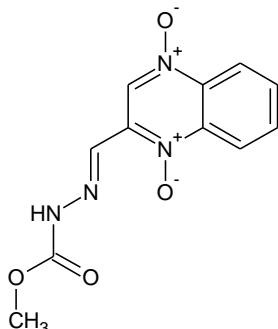
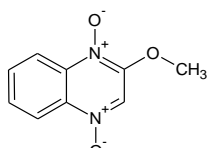
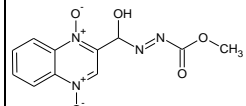
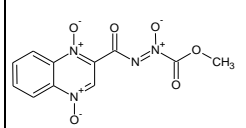
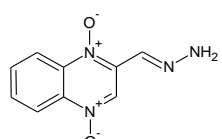
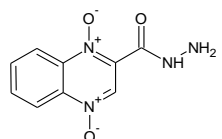
*kinetics studied

Atenolol (At)

Atenolol				
Smile				
<chem>CC(C)NCC(COc1ccc(cc1)CC(=O)N)O</chem>				
Potential Harm				
Author	Year Published	Journal	Paper Link	
Quintana	2012	Analytical and Bioanalytical Chemistry	http://link.springer.com/article/10.1007%2Fs00216-011-5707-7	
Contaminant Concentration (µg/mL)		Chlorine Concentration (mg/L)	Reaction Time	pH
1		10 (as Cl ₂)	NA	7.1

	Name	Smile	Structure
1	2-[4-(3-amino-2-hydroxypropoxy)phenyl]acetamide	<chem>NC(=O)Cc1ccc(OCC(O)CN)cc1</chem>	
2	(4-{2-hydroxy-3-[(propan-2-yl)amino]propoxy}phenyl)acetic acid	<chem>CC(C)NCC(O)COc1ccc(cc1)CC(=O)O</chem>	
3	4-{2-hydroxy-3-[(propan-2-yl)amino]propoxy}benzaldehyde	<chem>CC(C)NCC(O)COc1ccc(cc1)C=O</chem>	
4	NA	NA	

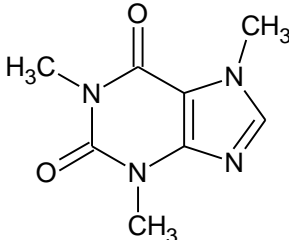
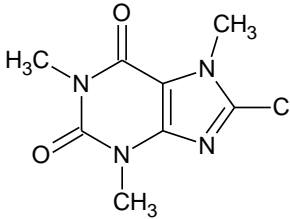
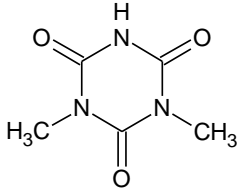
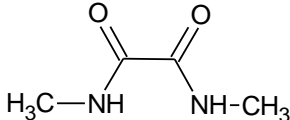
Carbadox

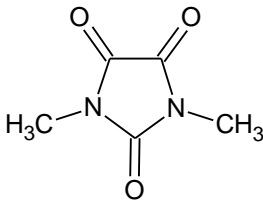
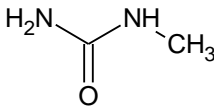
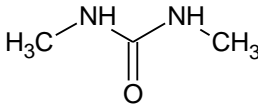
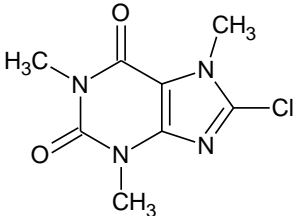
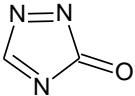
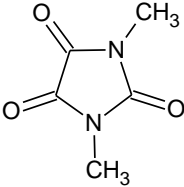
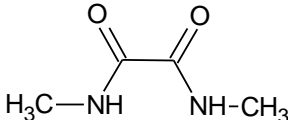
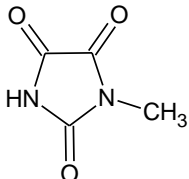
Carbadox				
Smile				
<chem>COC(=O)N/N=C/C1=[N+](C2=CC=CC=C2[N+](=C1)[O-])[O-]</chem>				
Potential Harm				
In recent years, carbadox and one of its major metabolites desoxycarbadox (DCDX) have been shown to harbor carcinogenic and genotoxic effects				
Author	Year Published	Journal	Paper Link	
Shah	2006	Environmental Science and Technology	http://pubs.acs.org/doi/pdf/10.1021/es060404c	
Contaminant Concentration (mg/L)		Chlorine Concentration (mg/L)	Reaction Time	pH
10× 10 ⁻⁶		10× 10 ⁻⁶	6.8 min	4 - 11
	Name	Smile	Structure	
1	2-methoxy-1,4-dioxo-1□ ⁵ ,4□ ⁵ -quinoxaline	<chem>[O-][n+]2c1cccc1[n+](c2)cc2OC</chem>		
2	methyl (<i>E</i>)-[(1,4-dioxo-1□ ⁵ ,4□ ⁵ -quinoxalin-2-yl)(hydroxy)methyl]diazene-1-carboxylate	<chem>O=C(OC)/N=N/C(O)c2c[n+](c2)cc1cccc1[n+](c1)[O-]</chem>		
3	2-{[(<i>Z</i>)-(methoxycarbonyl)- <i>ONN</i> -azoxy]carbonyl}-1,4-dioxo-1□ ⁵ ,4□ ⁵ -quinoxaline	<chem>O=C(OC)[N+](c2c[n+](c2)cc1cccc1[n+](c1)[O-])=N/C(=O)c2c[n+](c2)cc1cccc1[n+](c1)[O-]</chem>		
4	2-[(<i>E</i>)-hydrazinylidenemethyl]-1,4-dioxo-1□ ⁵ ,4□ ⁵ -quinoxaline	<chem>[O-][n+]2c1cccc1[n+](c2)cc2C=N\N</chem>		
5	1,4-dioxo-1□ ⁵ ,4□ ⁵ -quinoxaline-2-carbohydrazide	<chem>NNC(=O)c2c[n+](c2)cc1cccc1[n+](c1)[O-]</chem>		

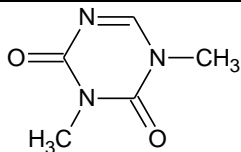
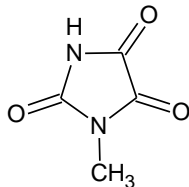
6	1,4-dioxo-1 ⁵ ,4 ⁵ -quinoxaline-2-carboxylic acid	<chem>O=C(O)c2c[n+](c1ccccc1[n+]2[O-])c1ccccc1[n+]2[O-]</chem>	
---	---	--	--

*kinetics studied

Caffeine

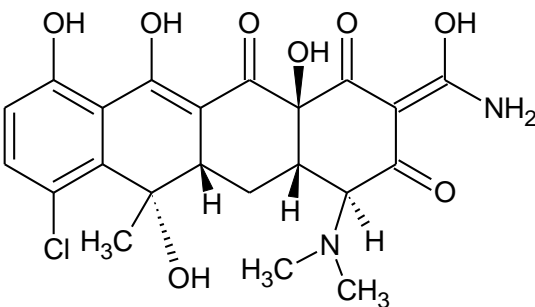
Caffeine				
Smile				
<chem>Cn1cnc2c1c(=O)n(c(=O)n2C)C</chem>				
Potential Harm				
Its product, N,N'-dimethylurea is toxic to algae. Another product, 8-chlorocaffeine, the most toxic compound in the long term on rotifers				
Author	Year Published	Journal	Paper Link	
Zarrelli	2014	Science of the Total Environment	http://www.sciencedirect.com/science/article/pii/S0048969713011492	
Contaminant Concentration (mg/L)		Chlorine Concentration (mg/L)	Reaction Time	pH
1000		100000	30 min	7
	Name	Smile	Structure	
1	8-chlorocaffeine	<chem>O=C2c1n(C)c(Cl)nc1N(C)C(=O)N2C</chem>		
2	1,3-dimethylparabanic acid	<chem>CN1C(=O)NC(=O)N(C)C1=O</chem>		
3	N,N'-dimethyloxalamide	<chem>CNC(=O)C(=O)NC</chem>		

4	N,N'-dimethylparabanic acid	<chem>O=C1C(=O)N(C)C(=O)N1C</chem>	
5	N-methylurea	<chem>NC(=O)NC</chem>	
6	N,N'-dimethylurea	<chem>CNC(=O)NC</chem>	
Author	Year Published	Journal	Paper Link
Gould	1984	Water Research	http://www.sciencedirect.com/science/article/pii/0043135484902513
Contaminant Concentration (mg/L)	Chlorine Concentration (mg/L)	Reaction Time	pH
97	136	3 h	7
	Name	Smile	Structure
1	8-chlorocaffeine	<chem>O=C2c1n(C)c(Cl)nc1N(C)C(=O)N2C</chem>	
2	1,2,4 - triazol - 3 - one	<chem>O=C1N=CN=N1</chem>	
3	N,N'-dimethylparabanic acid	<chem>O=C1C(=O)N(C)C(=O)N1C</chem>	
4	N,N'-dimethyloxalamide	<chem>CNC(=O)C(=O)NC</chem>	
5	1 - methylimidazolidine - 2,4,5 - trione	<chem>O=C1C(=O)NC(=O)N1C</chem>	

6	1,3-Dimethyl-5-azauracil	<chem>CN1C=NC(=O)N(C)C1=O</chem>	
5	N-methylparabanic acid	<chem>O=C1C(=O)NC(=O)N1C</chem>	

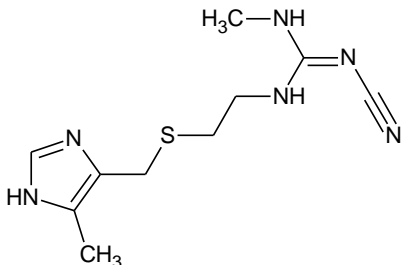
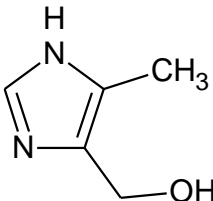
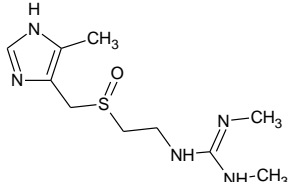
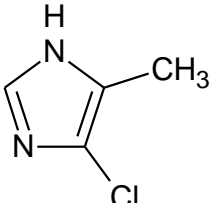
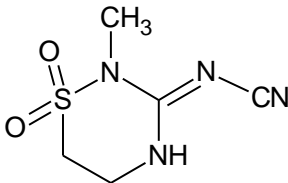
*kinetics studied

Chlorotetracycline(CTC)

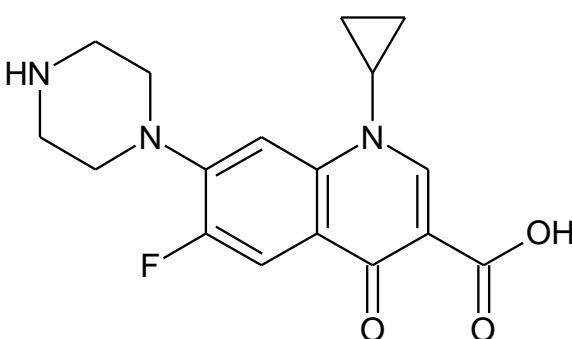
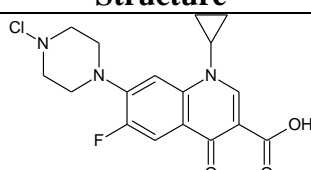
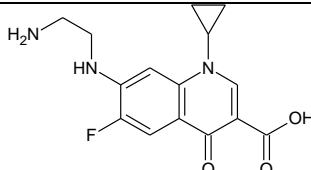
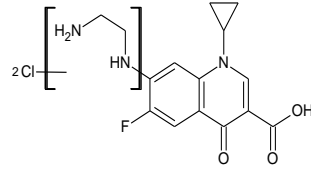
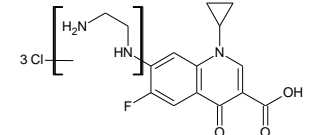
Chlorotetracycline(CTC)									
Smile									
<chem>N\C(O)=C1/C(=O)[C@@H](N(C)C)[C@@H]2C[C@H]4C(C(=O)[C@]2(O)C1=O)=C(O)c3c(O)ccc(Cl)c3[C@@]4(C)O</chem>									
Potential Harm									
The residues cause formation of TC resistance genes have been found in waste lagoons and groundwater									
Author	Year Published	Journal	Paper Link						
Wang	2011	Water Research	http://www.sciencedirect.com/science/article/pii/S0043135410008171						
Contaminant Concentration (μM)		Chlorine Concentration (mg/L)		Reaction Time	pH				
400		400 (ClO2)			7.5				
They detected signals for potential products on LC-MS. But they did not identify them.									
Table S2 - LC-ESI-MS fragments of TTC and its oxidation products by ClO₂.									
		TTC (M)		M+32		M-2		M-166	
Abundance		—		33%		26%		41%	
RT (min)		19.206		16.945		24.932		28.362	
		<i>m/z</i>	int.	<i>m/z</i>	int.	<i>m/z</i>	int.	<i>m/z</i>	int.
[MH] ⁺	0	445	100	477	100	443	100	279	100
[M+Na] ⁺	22	-	-	-	-	-	-	301	22

*kinetics studied

Cimetidine

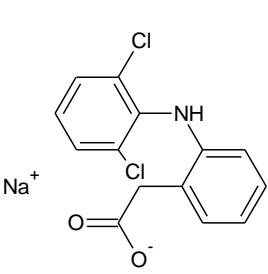
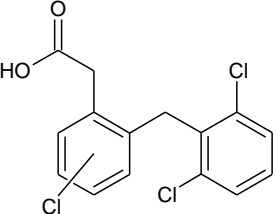
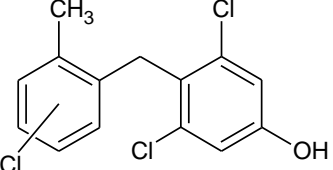
Cimetidine				
Smile				
<chem>Cc1ncnc1CSCCNC(=N\C#N)/NC</chem>				
Potential Harm				
Author	Year Published	Journal	Paper Link	
Buth	2007	Environmental Science and Technology	http://pubs.acs.org/doi/abs/10.1021/es070606o	
Contaminant Concentration (μM)		Chlorine Concentration (μM)	Reaction Time	pH
100		10-fold molar excess of NaOCl	8 min	4, 7, 10
	Name	Smile	Structure	
1	(5-methyl-1 <i>H</i> -imidazol-4-yl)methanol	<chem>Cc1ncnc1CO</chem>		
2	<i>N,N'</i> -dimethyl- <i>N'</i> -{2-[(5-methyl-1 <i>H</i> -imidazol-4-yl)methanesulfinyl]ethyl}guanine	<chem>Cc1ncnc1CS(=O)CCNC(=N\C)\NC</chem>		
3	4-chloro-5-methyl-1 <i>H</i> -imidazole	<chem>Cc1ncnc1Cl</chem>		
4	(2-methyl-1,1-dioxo-1,2,4-thiadiazinan-3-ylidene)cyanamide	<chem>CN1C(\NCCS1(=O)=O)=N\C#N</chem>		

Ciprofloxacin

Ciprofloxacin				
Smile				
CC(N)Cc1ccc2OCOc2c1				
Potential Harm				
Continuous exposure of bacterial communities to growth-inhibitory concentrations of antibacterial agents can promote induction or dissemination of resistant bacterial phenotypes. Induction of fluoroquinolone resistance can also bring about cross-resistance to various other classes of antibacterial agents.				
Author	Year Published	Journal	Paper Link	
Dodd	2005	Environmental Science and Technology	http://pubs.acs.org/doi/abs/10.1021/es050054e	
Contaminant Concentration (mg/L)		Chlorine Concentration (mg/L)	Reaction Time	pH
270× 10 ⁻⁶		0.6-1.2× 10 ⁻⁶	30 min	7
Product	Name	Smile	Structure	
1	7-(4-chloropiperazin-1-yl)-1-cyclopropyl-6-fluoro-4-oxo-1,4-dihydroquinoline-3-carboxylic acid	O=C(O)C2=CN(c1cc(c(F)cc1C2=O)N3CCNCC3)C4CC4		
2	7-[(2-aminoethyl)amino]-1-cyclopropyl-6-fluoro-4-oxo-1,4-dihydroquinoline-3-carboxylic acid	O=C(O)C2=CN(c1cc(c(NCCN)c(F)cc1C2=O)C3CC3		
3	CF-Ia2			
4	CF-Ia3			

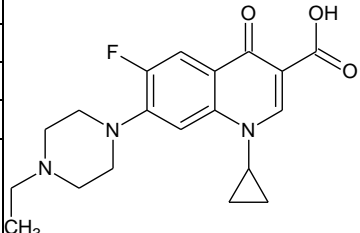
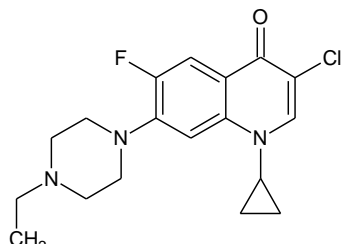
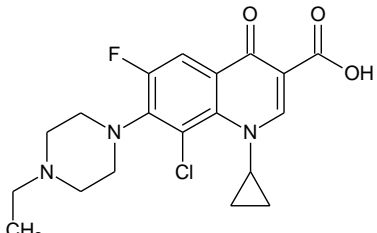
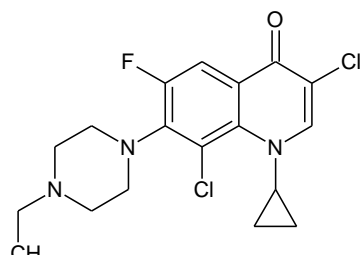
5	7-amino-1-cyclopropyl-6-fluoro-4-oxo-1,4-dihydroquinoline-3-carboxylic acid	<chem>O=C(O)C2=CN(c1cc(N)c(F)cc1C2=O)C3CC3</chem>	
6	7-amino-8-chloro-1-cyclopropyl-6-fluoro-4-oxo-1,4-dihydroquinoline-3-carboxylic acid	<chem>O=C(O)C2=CN(c1cc(Cl)c(N)c(F)cc1C2=O)C3CC3</chem>	

Diclofenac sodium

Diclofenac sodium				
Smile				
[Na+].Clc1cccc(Cl)c2Nc1ccccc1CC([O-])=O				
Potential Harm				
Author	Year Published	Journal		Paper Link
Quintana	2010	Water Research		http://www.ncbi.nlm.nih.gov/pubmed/19800649
Contaminant Concentration (ng/L)		Chlorine Concentration (mg/L)	Reaction Time	pH
		10 (Cl ₂)		
Product	Name	Smile	Structure	
1	Cl-diclo	NA		
2	Cl-diclo-CO	NA		

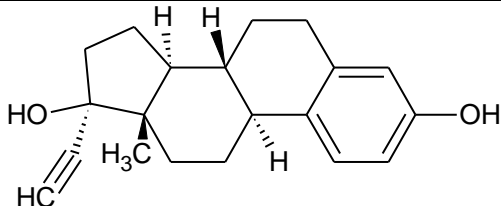
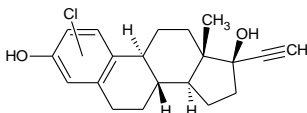
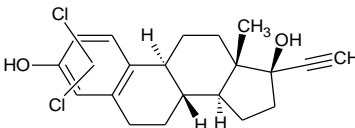
*kinetics studied

Enrofloxacin

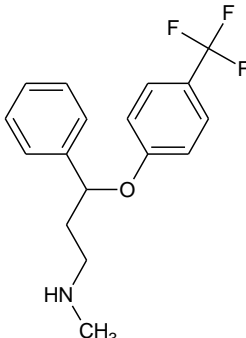
Enrofloxacin				
Smile				
<chem>CCN1CCN(CC1)c2cc3c(cc2F)c(=O)c(c3C4CC4)C(=O)O</chem>				
Potential Harm				
Author	Year Published	Journal	Paper Link	
Dodd	2005	Environmental Science and Technology	http://pubs.acs.org/doi/abs/10.1021/es050054e	
Contaminant Concentration (mg/L)		Chlorine Concentration (mg/L)	Reaction Time	pH
280×10^{-6}		$140\text{-}560\times 10^{-6}$	30 min	7
Product	Name	Smile	Structure	
1	3-chloro-1-cyclopropyl-7-(4-ethylpiperazin-1-yl)-6-fluoroquinolin-4(1 <i>H</i>)-one	<chem>CCN1CCN(CC1)c2cc3N(C=C(Cl)C(=O)c3cc2F)C4CC4</chem>		
2	8-chloro-1-cyclopropyl-7-(4-ethylpiperazin-1-yl)-6-fluoro-4-oxo-1,4-dihydroquinoline-3-carboxylic acid	<chem>CCN1CCN(CC1)c4c(F)cc3C(=O)C(=CN(C2CC2)c3c4Cl)C(=O)O</chem>		
3	3,8-dichloro-1-cyclopropyl-7-(4-ethylpiperazin-1-yl)-6-fluoroquinolin-4(1 <i>H</i>)-one	<chem>CCN1CCN(CC1)c2cc3N(C=C(Cl)C(=O)c3cc2F)C4CC4</chem>		

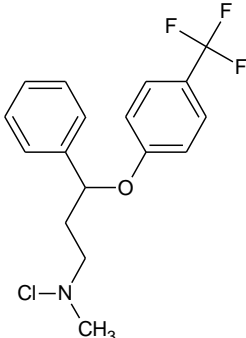
*kinetics studied

Ethinylestradiol (EE2)

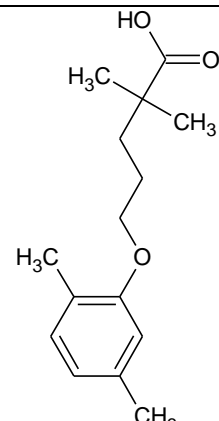
Ethinylestradiol					
Smile					
<chem>Oc3cc4CC[C@H]2[C@H](CC[C@@]1(C)[C@H]2CC[C@@]1(O)C#C)c4cc3</chem>					
Potential Harm					
The results suggest that products of estrogen bromination are potentially biologically active, and that their formation, as well as the presence of reactive bromine species in municipal drinking water, could perturb ecotoxicity studies with waterborne contaminants.					
Author	Year Published	Journal	Paper Link		
Pereira	2011	Chemosphere	http://www.sciencedirect.com/science/article/pii/S0045653508009119		
Contaminant Concentration (ng/L)		Chlorine Concentration (mg/L)	Reaction Time	pH	
Product	Name	Smile	Structure		
1	4-chloro-EE2				
2	2, 4-dichloro-EE2				

Fluoxetine

Fluoxetine	
Smile	
<chem>FC(F)(F)c2ccc(OC(CCNC)c1ccccc1)cc2</chem>	
Potential Harm	

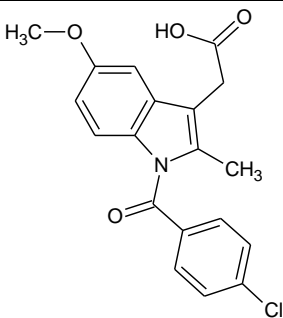
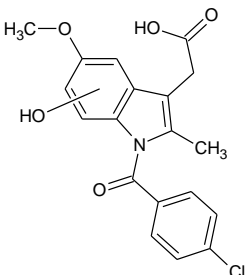
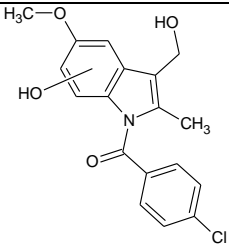
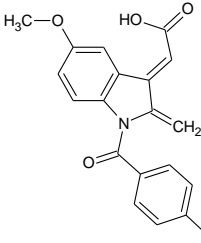
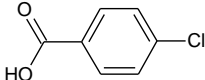
Author	Year Published	Journal	Paper Link
Bedner	2006	Chemosphere	http://www.sciencedirect.com/science/article/pii/S0045653506007545
Contaminant Concentration (ng/L)	Chlorine Concentration (mg/L)	Reaction Time	pH
10 µM	57 µM	<2min	7.0
	Name	Smile	Structure
1	N-chlorofluoxetine	<chem>FC(F)(F)c2ccc(OC(CCNC(Cl)C)cc2</chem>	

Gemfibrozil

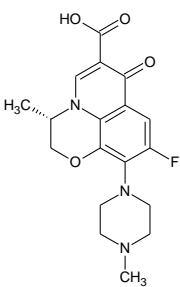
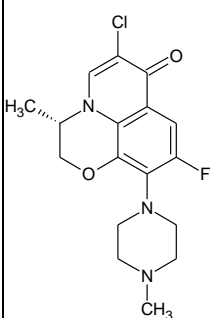
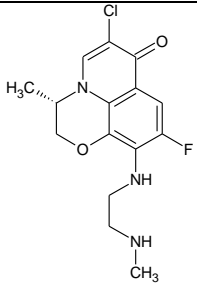
Gemfibrozil				
Smile				
O=C(O)C(C)(C)CCCOc1cc(C)ccc1C				
Potential Harm				
Gemfibrozil has the potential of enhanced bioavailability due to halogenation.				
Author	Year Published	Journal	Paper Link	
Bulloch	2012	Environmental Science and Technology	http://pubs.acs.org/doi/abs/10.1021/es3006173	
Contaminant Concentration (ng/L)		Chlorine Concentration (mg/L)	Reaction Time	pH
100 µg/L		13% active chlorine solution	60min	

	Name	Smile	Structure
1	4'-chloro-gemfibrozil	<chem>Cc1cc(OCCCC(C)(C)C(=O)O)c(C)cc1Cl</chem>	
2	4',6'-dichlorogemfibrozil	<chem>Cc1cc(OCCCC(C)(C)C(=O)O)c(cc1Cl)CCl</chem>	
3	3',4',6'-trichlorogemfibrozil	<chem>ClCc1cc(OCCCC(C)(C)C(=O)O)c(cc1Cl)CCl</chem>	
4	6'-chlorogemfibrozil	<chem>Cc1cc(OCCCC(C)(C)C(=O)O)c(C)cc1Cl</chem>	

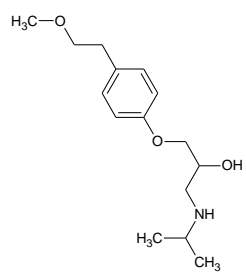
Indomethacine

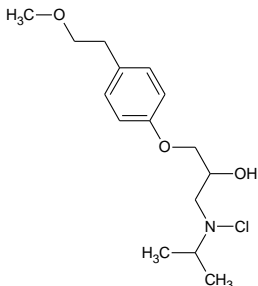
Indomethacine					
Smile					
Cc1c(c2cc(ccc2n1C(=O)c3ccc(cc3)Cl)OC)CC(=O)O					
Potential Harm					
Author	Year Published	Journal	Paper Link		
Quintana	2010	Analytical and Bioanalytical Chemistry	http://link.springer.com/article/10.1007%2Fs00216-011-5707-7		
Contaminant Concentration (µg/L)		Chlorine Concentration (mg/L)		Reaction Time	pH
1		10 (as Cl ₂)		24 h	
Product	Name	Smile		Structure	
1	OH-indo				
2	OH-indo-CO2				
3	Indo-H2	Clc1ccc(cc1)C(=O)N3c2ccc(cc2\C(=C/C(=O)O)C3=C)OC			
4	4-chlorobenzoic acid	OC(=O)c1ccc(Cl)cc1			

Levofloxacin

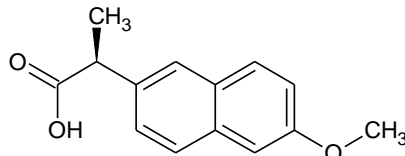
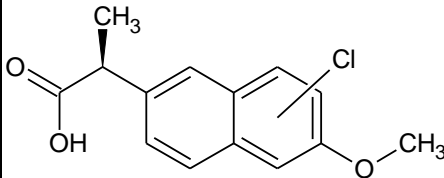
Levofloxacin				
Smile				
C[C@H]1COc2c3n1cc(c(=O)c3cc(c2N4CCN(CC4)C)F)C(=O)O				
Potential Harm				
Author	Year Published	Journal	Paper Link	
Naijar	2013	Chemosphere	http://www.ncbi.nlm.nih.gov/pubmed/23850240	
Contaminant Concentration (ng/L)		Chlorine Concentration (mg/L)	Reaction Time	pH
0.36		≥2.13	< 1min	7.2
Product	Name	Smile	Structure	
1	(3S)-6-chloro-9-fluoro-3-methyl-10-(4-methylpiperazin-1-yl)-2,3-dihydro-7H-[1,4]oxazino[2,3,4-ij]quinolin-7-one	CN1CCN(CC1)c4c(F)cc2c3N(C=C(Cl)C2=O)[C@@H](C)COc34		
2	(3S)-6-chloro-9-fluoro-3-methyl-10-{[2-(methylamino)ethyl]amino}-2,3-dihydro-7H-[1,4]oxazino[2,3,4-ij]quinolin-7-one	Fc3cc1c2N(C=C(Cl)C1=O)[C@@H](C)COc2c3NCCNC		

Metoprolol

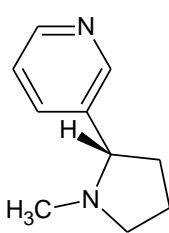
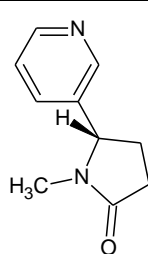
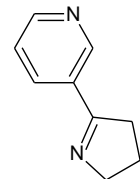
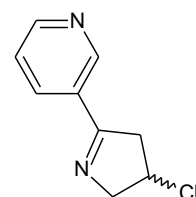
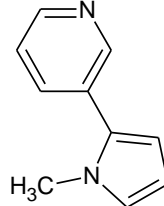
Metoprolol	
Smile	
CC(C)NCC(COc1ccc(cc1)CCOC)O	
Potential Harm	
Several studies focusing on the toxicological potential of propranolol signify an environmental relevance. Huggett et al. showed an effect on the reproduction and steroid levels in medaka (<i>Oryzias latipes</i>) at propranolol concentrations as	

low as 0.5 µg/L for a 4-week exposure experiment. For mixtures of beta blockers toxicological effects were also found at lower concentrations.				
Author	Year Published	Journal	Paper Link	
Bedner	2006	Environmental Science and Technology	http://pubs.acs.org/doi/full/10.1021/es900282c	
Contaminant Concentration (ng/L)		Chlorine Concentration (mg/L)	Reaction Time	pH
10µM		57 µM	<2min	7.0
Product	Name	Smile	Structure	
1	N-chlorometoprolol	<chem>CC(C)N(Cl)CC(O)COc1ccc(cc1)CCOC</chem>		

Naproxen

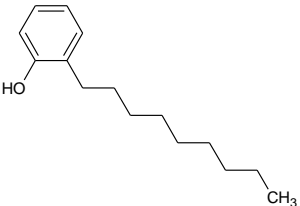
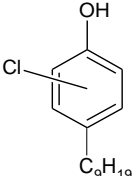
Naproxen				
Smile				
C[C@@H](c1ccc2cc(ccc2c1)OC)C(=O)O				
Potential Harm				
Author	Year Published	Journal	Paper Link	
Quintana	2010	Water Research	http://www.sciencedirect.com/science/article/pii/S0043135409005983	
Contaminant Concentration (ng/L)		Chlorine Concentration (mg/L)	Reaction Time	pH
		10 (Cl ₂)	24h	
Product	Name	Smile	Structure	
1	Cl-Naproxen			

Nicotine

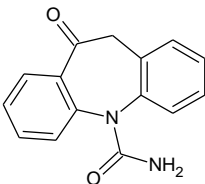
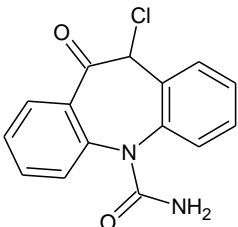
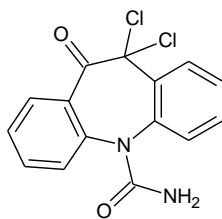
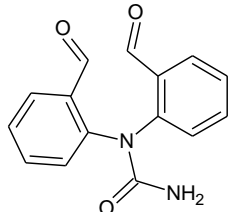
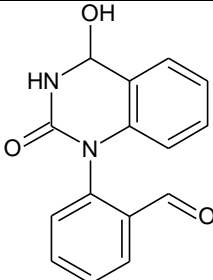
Nicotine				
Smile				
CN2CCCC[C@H]2c1cnccc1				
Potential Harm				
Genotoxic evaluation of main degradation products of nicotine				
Author	Year Published	Journal	Paper Link	
Zarrelli	2012	Science of the Total Environment	http://www.sciencedirect.com/science/article/pii/S0048969712004081	
Contaminant Concentration (g/L)		Chlorine Concentration (mg/L)	Reaction Time	pH
1		10% HOCl	30 min	8.5 – 9.5
	Name	Smile	Structure	
1	(5 <i>S</i>)-1-methyl-5-(pyridin-3-yl)pyrrolidin-2-one	CN2C(=O)CC[C@H]2c1cnccc1		
2	3-(3,4-dihydro-2 <i>H</i> -pyrrol-5-yl)pyridine	c1ncc(cc1)C=2CCCN=2		
3	3-(3-chloro-3,4-dihydro-2 <i>H</i> -pyrrol-5-yl)pyridine	ClC1CC(=NC1)c2cnccc2		
4	3-(1-methyl-1 <i>H</i> -pyrrol-2-yl)pyridine	Cn2cccc2c1cnccc1		

5	3-(5-chloro-1-methyl-1 <i>H</i> -pyrrol-2-yl)pyridine	<chem>Clc2ccc(c1cnccc1)n2C</chem>	
6	pyridine-3-carboxylic acid	<chem>O=C(O)c1ccncc1</chem>	
7	3-(methylamino)propionic acid	<chem>CNCCC(=O)O</chem>	
8	3-[(2 <i>S</i>)-pyrrolidin-2-yl]pyridine	<chem>c1ncc(cc1)[C@@H]2CCCN2</chem>	

Nonylphenol

Nonylphenol				
Smile				
CCCCCCCCCc1ccccc1O				
Potential Harm				
Products may be able to disturb the hormone imbalance of exposed organisms.				
Author	Year Published	Journal	Paper Link	
Petrovic	2003	Environmental Science and Technology	http://pubs.acs.org/doi/pdf/10.1021/es034139w	
Contaminant Concentration (ng/L)		Chlorine Concentration (mg/L)	Reaction Time	pH
8.3 to 22		1.4–2.05		
Product	Name	Smile	Structure	
1	Chlorinated nonylphenol			

Oxcarbazepine (OXC)

Oxcarbazepine					
Smile					
c1ccc2c(c1)CC(=O)c3ccccc3N2C(=O)N					
Potential Harm					
Author	Year Published	Journal	Paper Link		
Li	2011	Water Research	http://www.sciencedirect.com/science/article/pii/S004313541000816X		
Contaminant Concentration (ng/L)		Chlorine Concentration (mg/L)		Reaction Time	pH
	Name		Smile	Structure	
1	10-chloro-11-oxo-10,11-dihydro-5H-dibenzo[b,f]azepine-5-carboxamide		NC(=O)N3c1ccccc1C(=O)C(Cl)c2ccccc23		
2	10,10-dichloro-11-oxo-10,11-dihydro-5H-dibenzo[b,f]azepine-5-carboxamide		NC(=O)N3c1ccccc1C(=O)C(Cl)(Cl)c2ccccc23		
3	N,N-bis(2-formylphenyl)urea		O=C(N)N(c1ccccc1C=O)c2ccccc2C=O		
4	2-(4-hydroxy-2-oxo-3,4-dihydroquinazolin-1(2H)-yl)benzaldehyde		O=Cc1ccccc1N3c2ccccc2C(O)NC3=O		

Oxytetracycline

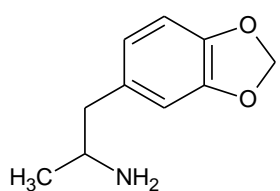
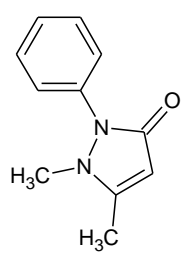
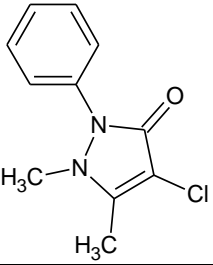
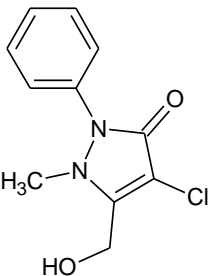
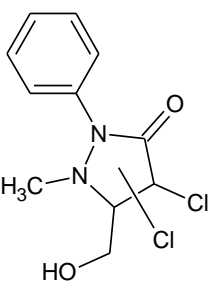
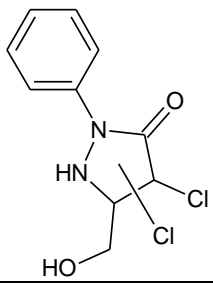
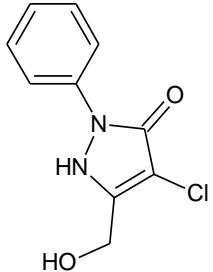
Oxytetracycline					
Smile					
CC(N)Cc1ccc2OCOC2c1					
Potential Harm					
Author	Year Published	Journal	Paper Link		
Wang	2011	Water Research	http://www.sciencedirect.com/science/article/pii/S043135410008171		
Contaminant Concentration (μM)		Chlorine Concentration (μM)		Reaction Time	pH
400 μM		800 μM			7
	Name		Smile		Structure
Byproduct	They detected signals of potential products. But they did not identify them.				

Table S6 - LC-ESI-MS fragments of OTC and its oxidation products by free chlorine.									
		OTC (M)		M+16		M+34		M+42	
Abundance		—		22%		37%		41%	
RT (min)		19.011		20.112		22.934		24.576	
		m/z	int.	m/z	int.	m/z	int.	m/z	int.
[MH] ⁺	0	461	100	477	100	495	100	503	100
[M-NH ₃] ⁺	-17	444	56	-	-	478	23	-	-
[M-H ₂ O] ⁺	-18	-	-	459	32	-	-	-	-
[M-NH ₃ -H ₂ O] ⁺	-35	426	22	-	-	-	-		

*kinetics studied

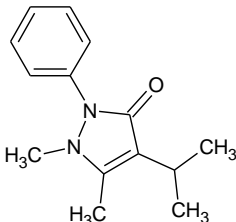
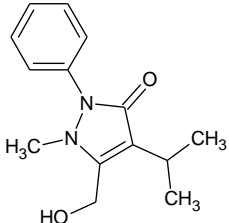
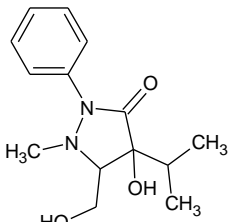
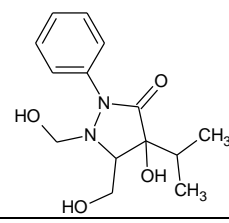
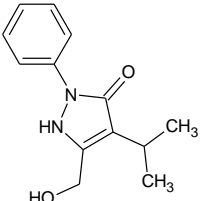
Phenazone

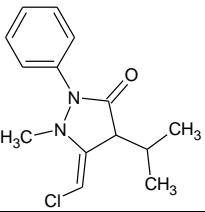
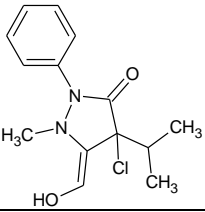
Phenazone				
Smile				
Cc1cc(=O)n(n1C)c2ccccc2				
Potential Harm				
The ecotoxicity of phenazone-type drugs is still largely unknown. Their expected EC50 values estimated from QSAR calculations are in the 0.8–6.7 mg/L level (Sanderson et al., 2003).				
Author	Year Published	Journal	Paper Link	
Rodil	2012	Water Research	http://www.sciencedirect.com/science/article/pii/S0043135412001212	

Contaminant Concentration (ng/L)		Chlorine Concentration (mg/L)	Reaction Time	pH
50		1 – 10	346 s	5.7 – 8.3
	Name	Smile	Structure	
1	4-chloro-1,5-dimethyl-2-phenyl-1,2-dihydro-3H-pyrazol-3-one (Cl – Phe)	<chem>O=C2C(Cl)=C(C)N(C)N2c1ccccc1</chem>		
2	4-chloro-5-(hydroxymethyl)-1-methyl-2-phenyl-1,2-dihydro-3H-pyrazol-3-one (Cl, OH – Phe)	<chem>O=C2C(Cl)=C(CO)N(C)N2c1ccccc1</chem>		
3	(Cl ₂ , OH – Phe)	<chem>O=C2C(Cl)=C(CO)N(C)N2c1ccccc1</chem>		
4	Cl ₂ , OH – Phe - Me	<chem>O=C2C(Cl)=C(CO)N(C)N2c1ccccc1</chem>		
5	4-chloro-5-(hydroxymethyl)-2-phenyl-1,2-dihydro-3H-pyrazol-3-one (Cl, OH – Phe - Me)	<chem>OCC=2NN(c1ccccc1)C(=O)C=2Cl</chem>		

*kinetics studied

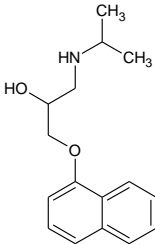
Propyphenazone

Propyphenazone					
Smile					
<chem>Cc1c(c(=O)n(n1C)c2ccccc2)C(C)C</chem>					
Potential Harm					
The ecotoxicity of phenazone-type drugs is still largely unknown. Their expected EC50 values estimated from QSAR calculations are in the 0.8–6.7 mg/L level (Sanderson et al., 2003).					
Author	Year Published	Journal	Paper Link		
Rodil	2012	Water Research	http://www.sciencedirect.com/science/article/pii/S0043135412001212		
Contaminant Concentration (ng/L)		Chlorine Concentration (mg/L)		Reaction Time	pH
50		1 – 10		346 s	5.7 – 8.3
Product	Name	Smile	Structure		
1	OH - Prophe	<chem>CC(C)C=2C(=O)N(c1ccccc1)N(C)C=2CO</chem>			
2	(OH) ₂ - Prophe	<chem>CN2C(CO)C(O)(C(=O)N2c1ccccc1)C(C)C</chem>			
3	(OH) ₃ - Prophe	<chem>OCN2C(CO)C(O)(C(=O)N2c1ccccc1)C(C)C</chem>			
4	OH – Prophe - Me	<chem>CC(C)C2=C(CO)NN(c1ccccc1)C2=O</chem>			

5	Cl - Prophe	<chem>CC(C)C/2C(=O)N(c1ccccc1)N(C)C\2=C\Cl</chem>	
6	Cl, OH- Prophe	<chem>CC(C)C2(Cl)C(=O)N(c1ccccc1)N(C)/C2=C\O</chem>	

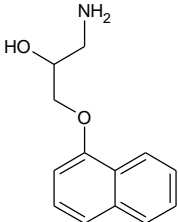
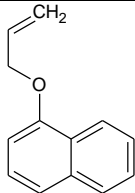
*kinetics studied

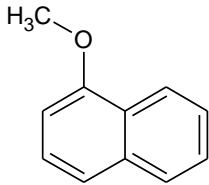
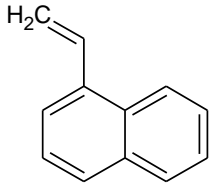
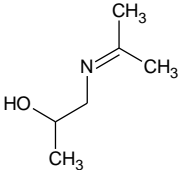
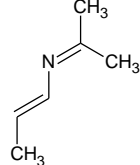
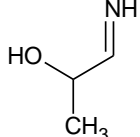
Propranolol

Propranolol			
Smile			
CC(C)NCC(COc1cccc2c1cccc2)O			
Potential Harm			

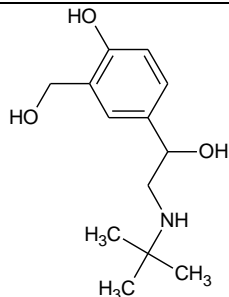
Author	Year Published	Journal	Paper Link
Benner	2009	Environmental Science and Technology	http://pubs.acs.org/doi/pdf/10.1021/es900282c

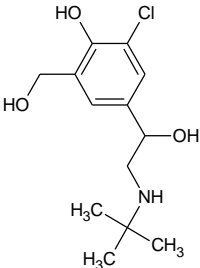
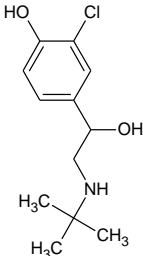
Contaminant Concentration (ng/L)		Chlorine Concentration (mg/L)	Reaction Time	pH

	Name	Smile	Structure
1	1-amino-3-[(naphthalen-1-yl)oxy]propan-2-ol	NCC(O)COc2cccc1ccccc12	
2	1-[(prop-2-en-1-yl)oxy]naphthalene	C=CCOc2cccc1ccccc12	

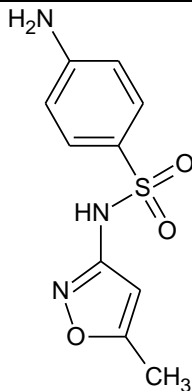
3	1-methoxynaphthalene	<chem>COc2cccc1ccccc12</chem>	
4	1-ethenynaphthalene	<chem>C=Cc2cccc1ccccc12</chem>	
5	1-[(propan-2-ylidene)amino]propan-2-ol	<chem>C/C(C)=N\CC(C)O</chem>	
6	<i>N</i> -[(1 <i>E</i>)-prop-1-en-1-yl]propan-2-imine	<chem>C/C(C)=N\C=C\C</chem>	
7	1-iminopropan-2-ol	<chem>N=CC(C)O</chem>	

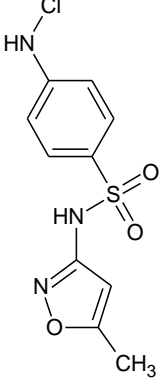
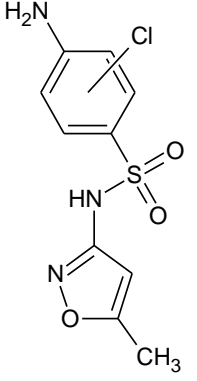
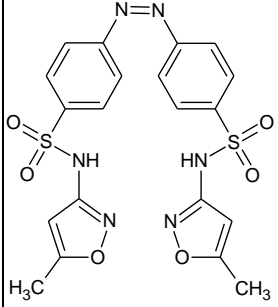
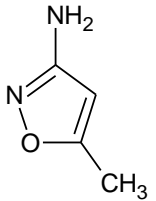
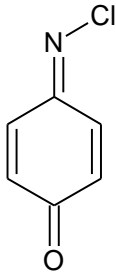
Salbutamol

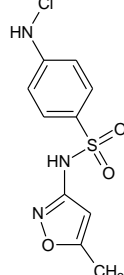
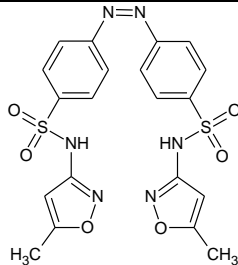
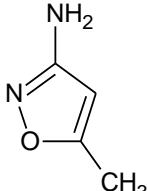
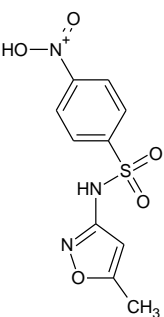
Salbutamol				
Smile				
<chem>CC(C)(C)NCC(c1ccc(c(c1)CO)O)O</chem>				
Potential Harm				
Author	Year Published	Journal	Paper Link	
Quintana	2012	Analytical and Bioanalytical Chemistry	http://link.springer.com/article/10.1007%2Fs00216-011-5707-7	
Contaminant Concentration (µg/mL)		Chlorine Concentration (mg/L)	Reaction Time	pH
1		10 mg/L Cl ₂	72h	7.1

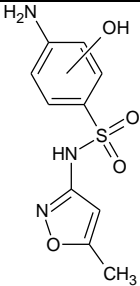
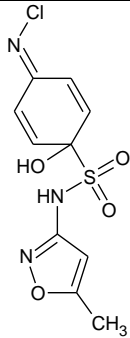
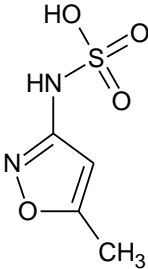
	Name	Smile	Structure
1	4-[2-(<i>tert</i> -butylamino)-1-hydroxyethyl]-2-chloro-6-(hydroxymethyl)phenol	<chem>Oc1c(CO)cc(cc1Cl)C(O)CNC(C)(C)C</chem>	
2	4-[2-(<i>tert</i> -butylamino)-1-hydroxyethyl]-2-chlorophenol	<chem>Oc1ccc(cc1Cl)C(O)CNC(C)(C)C</chem>	

Sulfamethoxazole

Sulfamethoxazole					
Smile					
<chem>Cc1cc(no1)NS(=O)(=O)c2ccc(cc2)N</chem>					
Potential Harm					
Author	Year Publi shed	Journal	Paper Link		
Dodd	2011	Environmental Science and Technology	http://pubs.acs.org/doi/abs/10.1021/es035225z		
Contaminant Concentration (ng/L)		Chlorine Concentration (mg/L)		Reaction Time	pH
4-10		100		30min	6.5
Product	Name	Smile			Structure

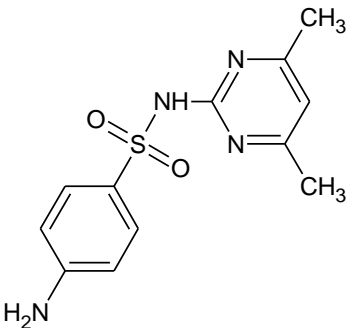
1	N – chlorinated SMX	<chem>Cc2cc(NS(=O)(=O)c1ccc(NCl)cc1)no2</chem>	
2	Ring-chlorinated SMX	<chem>Cc2cc(NS(=O)(=O)c1ccc(NCl)cc1)no2</chem>	
3	Azosulfamethoxazole	<chem>Cc2cc(NS(=O)(=O)c1ccc(NCl)cc1)no2</chem> <chem>Cc4cc(NS(=O)(=O)c3ccc(\N=N/c1ccc(cc1)S(=O)(=O)Nc2cc(C)on2)cc3)no4</chem>	
4	5-methyl-1,2-oxazol-3-amine (AMI)	<chem>Cc1cc(N)no1</chem>	
5	N-(4-oxocyclohexa-2,5-dien-1-ylidene)hypochlorous amide (NCBQ)	<chem>Cl\N=C1/C=CC(=O)C=C1</chem>	

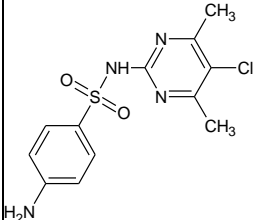
Author	Year Published	Journal	Paper Link		
Gao	2014	Journal of Hazardous Materials	http://www.ncbi.nlm.nih.gov/pubmed/24793298		
Contaminant Concentration (ng/L)		Chlorine Concentration (mg/L)	Reaction Time	pH	
4-10		100	30min	6.5	
Product	Name	Smile	Structure		
1	N – chlorinated SMX	<chem>Cc2cc(NS(=O)(=O)c1ccc(NCl)cc1)no2</chem>			
2	Azosulfame thoxazole	<chem>Cc2cc(NS(=O)(=O)c1ccc(NCl)cc1)no2</chem> <chem>Cc4cc(NS(=O)(=O)c3ccc(\N=N/c1cc c(cc1)S(=O)(=O)Nc2cc(C)on2)cc3)no4</chem>			
3	5-methyl-1,2-oxazol-3-amine (AMI)	<chem>Cc1cc(N)no1</chem>			
4	hydroxy{ 4-[(5-methyl-1,2-oxazol-3-yl)sulfamoyl]phenyl}oxoammonium	<chem>Cc2cc(NS(=O)(=O)c1ccc(cc1)[N+](=O)O)no2</chem>			

5	OH-SMX		
6	4-(chloroimino)-1-hydroxy-N-(5-methyl-1,2-oxazol-3-yl)cyclohexa-2,5-diene-1-sulfonamide	<chem>Cc2cc(NS(=O)(=O)C1(O)C=C/C(=N\Cl)C=C1)no2</chem>	
7	(5-methyl-1,2-oxazol-3-yl)sulfamic acid	<chem>Cc1cc(NS(O)(=O)=O)no1</chem>	

*Kinetics studied

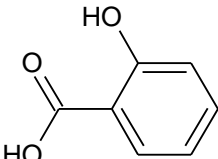
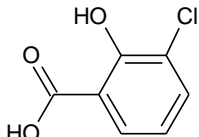
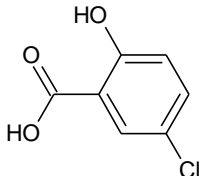
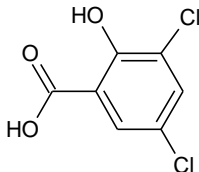
Sulfamethazine

Sulfamethazine				
Smile				
<chem>Cc1cc(nc(n1)NS(=O)(=O)c2ccc(cc2)N)C</chem>				
Potential Harm				
Author	Year Published	Journal	Paper Link	
Melton	2012	International Journal of Medicinal Chemistry	http://www.hindawi.com/journals/ijmc/2012/693903/	
Contaminant		Chlorine	Reaction Time	pH

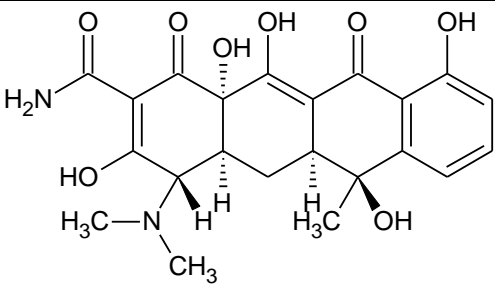
Concentration (µg/mL)		Concentration (µg/mL)		
10		380	2 h	NA
	Name	Smile	Structure	
1	4-amino-(5-chloro-4,6-dimethyl-2-pyrimidinyl)-benzenesulfonamide	<chem>Oc1c(cccc1Cl)C(=O)O</chem>		

* Kinetics studied

Salicylic acid (aspirin)

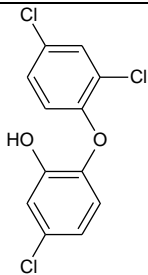
Salicylic acid (aspirin)				
Smile				
OC(=O)c1ccccc1O				
Potential Harm				
Author	Year Published	Journal	Paper Link	
Quintana	2010	Water Research	http://www.sciencedirect.com/science/article/pii/S0043135409005983	
Contaminant Concentration (ng/L)		Chlorine Concentration (mg/L)	Reaction Time	pH
		10 (Cl ₂)	24 h	
	Name	Smile	Structure	
1	3-chloro-salicylic acid	Oc1c(cccc1Cl)C(=O)O		
2	5-chloro-salicylic acid	Oc1ccc(Cl)cc1C(=O)O		
3	3,5-dichlorosalicylic acid	Oc1c(cc(Cl)cc1Cl)C(=O)O		

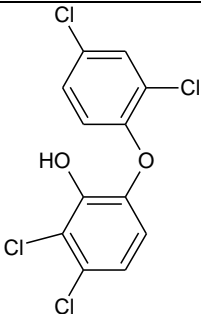
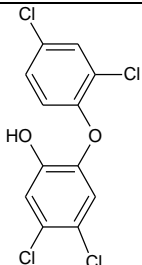
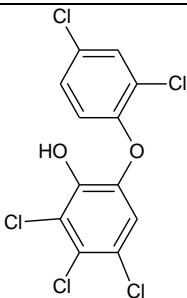
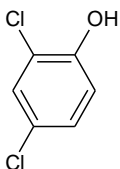
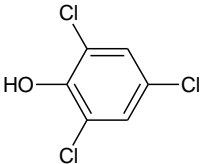
Tetracycline

Tetracycline										
Smile										
<chem>C[C@]1(c2cccc(c2C(=O)C3=C([C@]4([C@@H](C[C@@H]31)[C@@H](C(=C(C4=O)C(=O)N)O)N(C)C)O)O)O</chem>										
Potential Harm										
Author	Year Published	Journal	Paper Link							
Wang	2011	Water Research	http://www.sciencedirect.com/science/article/pii/S0043135410008171							
Contaminant Concentration (ng/L)		Chlorine Concentration (mg/L)				Reaction Time				pH
		100								7
They only detected signals of potential products. They did not identify the products.										
Table S5 - LC-ESI-MS fragments of TTC and its oxidation products by free chlorine.										
		TTC (M)		M+52		M+25		M+42		
Abundance		—		47%		24%		29%		
RT (min)		19.218		18.304		21.311		24.150		
		<i>m/z</i>	int.	<i>m/z</i>	int.	<i>m/z</i>	int.	<i>m/z</i>	int.	
[MH] ⁺	0	445	100	497	100	470	100	487	100	
[M-NH ₃] ⁺	-17	428	29	-	-	453	36	-	-	
[M-H ₂ O] ⁺	-18	-	-	479	45	-	-	-	-	
[M-NH ₃ -H ₂ O] ⁺	-35	410	42	-	-	-	-	-	-	

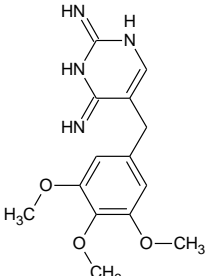
*kinetics studied

Triclosan (5-chloro-2-(2,4-dichlorophenoxy)phenol)

Triclosan				
Smile				
c1cc(c(cc1Cl)O)Oc2ccc(cc2Cl)Cl				
Potential Harm				
Author	Year Published	Journal	Paper Link	
Rule	2005	Environmental Science and Technology	http://pubs.acs.org/doi/abs/10.1021/es048943+	

Contaminant Concentration (ng/L)		Chlorine Concentration (mg/L)	Reaction Time	pH
0.72-8.0		0.192-1.77		4-11.5
	Name	Smile	Structure	
1	5,6-dichloro-2-(2,4-dichlorophenoy)phenol	<chem>Oc1c(ccc(Cl)c1Cl)Oc2ccc(Cl)cc2Cl</chem>		
2	5,6-dichloro-2-(2,4-dichlorophenoy)phenol	<chem>Oc2cc(Cl)c(Cl)cc2Oc1ccc(Cl)cc1Cl</chem>		
3	4,5,6-trichloro-(2,4-dichlorophenoxy)phenol	<chem>Clc2cc(Oc1ccc(Cl)cc1Cl)c(O)c(Cl)c2Cl</chem>		
4	2,4-dichlorophenol	<chem>Clc1cc(Cl)c(O)cc1</chem>		
5	2,4,6-trichlorophenol	<chem>Clc1cc(Cl)cc(Cl)c1O</chem>		

Trimethoprim

Trimethoprim																																																																										
Smile																																																																										
<chem>COc1cc(cc(c1OC)OC)Cc2c[nH]c(=N)[nH]c2=N</chem>																																																																										
Potential Harm																																																																										
Author	Year Published	Journal	Paper Link																																																																							
Dodd	2006	Water Research	http://www.sciencedirect.com/science/article/pii/S0043135406005756																																																																							
Contaminant Concentration (ng/L)		Chlorine Concentration (mg/L)	Reaction Time	pH																																																																						
3.4×10 ⁻⁴		6.9×10 ⁻⁴ of FAC		4, 7																																																																						
<p>Table S1 - Reaction products of TMP with FAC at pH 4.0 detected by LC/MS in unquenched reaction solutions ([TMP]₀ = 3.4 × 10⁻⁴ M, [FAC]₀ = 6.8 × 10⁻⁴ M).</p> <table><tr><th>Order of abund.</th><th>R. T. (min)</th><th>Compd</th><th>m/z of molecular and fragment ions</th><th># Cl atoms</th></tr><tr><td></td><td>12.02</td><td>TMP</td><td>291</td><td>-</td></tr><tr><td></td><td>14.40</td><td></td><td>377 (379, 381), 215 (18%, 217)</td><td>2</td></tr><tr><td>1</td><td>15.74</td><td>P1-A</td><td>325 (327)</td><td>1</td></tr><tr><td>2</td><td>17.07</td><td>P2-A</td><td>359 (361, 363), 325 (17%, 327)</td><td>2</td></tr><tr><td></td><td>22.08</td><td></td><td>411 (413, 415, 417), 325 (12%), 215 (29%, 217)</td><td>3</td></tr><tr><td>3</td><td>24.33</td><td>P3-A</td><td>445 (447, 449, 451), 249 (22%, 251), 215 (38%, 13)</td><td>4</td></tr><tr><td></td><td>27.88</td><td></td><td>459 (461, 463, 465), 249 (21%, 251), 215 (66%, 19)</td><td>4</td></tr><tr><td></td><td>28.59</td><td></td><td>445 (447, 449, 451), 375 (17%, 377), 344 (19%), 249 (43%, 251), 215 (47%, 217)</td><td>4</td></tr><tr><td></td><td>28.96</td><td></td><td>393 (395, 397, 399), 323 (7%, 325), 287 (8%)</td><td>3</td></tr></table> <ul style="list-style-type: none">• R. T. = LC retention time.• Most abundant products are shown in red and indicated with their order of abundance in the LC/MS chromatogram.• Base peaks are shown in bold, with fragment ion peaks in plain text. Relative fragment peak abundances are given in parentheses as percentage of base peak height. m/z values of Cl isotope peaks are also indicated in parentheses.• Number of Cl atoms deduced from observed Cl isotope peak signal ratios• The listed mass spectral information was obtained at 70 eV fragmentation voltage. Higher voltage (120 eV) resulted in similar fragmentation patterns with only difference in relative abundance.					Order of abund.	R. T. (min)	Compd	m/z of molecular and fragment ions	# Cl atoms		12.02	TMP	291	-		14.40		377 (379, 381), 215 (18%, 217)	2	1	15.74	P1-A	325 (327)	1	2	17.07	P2-A	359 (361, 363), 325 (17%, 327)	2		22.08		411 (413, 415, 417), 325 (12%), 215 (29%, 217)	3	3	24.33	P3-A	445 (447, 449, 451), 249 (22%, 251), 215 (38%, 13)	4		27.88		459 (461, 463, 465), 249 (21%, 251), 215 (66%, 19)	4		28.59		445 (447, 449, 451), 375 (17%, 377), 344 (19%), 249 (43%, 251), 215 (47%, 217)	4		28.96		393 (395, 397, 399), 323 (7%, 325), 287 (8%)	3																				
Order of abund.	R. T. (min)	Compd	m/z of molecular and fragment ions	# Cl atoms																																																																						
	12.02	TMP	291	-																																																																						
	14.40		377 (379, 381), 215 (18%, 217)	2																																																																						
1	15.74	P1-A	325 (327)	1																																																																						
2	17.07	P2-A	359 (361, 363), 325 (17%, 327)	2																																																																						
	22.08		411 (413, 415, 417), 325 (12%), 215 (29%, 217)	3																																																																						
3	24.33	P3-A	445 (447, 449, 451), 249 (22%, 251), 215 (38%, 13)	4																																																																						
	27.88		459 (461, 463, 465), 249 (21%, 251), 215 (66%, 19)	4																																																																						
	28.59		445 (447, 449, 451), 375 (17%, 377), 344 (19%), 249 (43%, 251), 215 (47%, 217)	4																																																																						
	28.96		393 (395, 397, 399), 323 (7%, 325), 287 (8%)	3																																																																						
<p>Table S2 - Reaction products of TMP with FAC at pH 7.0 detected by LC/MS in unquenched reaction solutions ([TMP]₀ = 3.4 × 10⁻⁴ M, [FAC]₀ = 6.8 × 10⁻⁴ M).</p> <table><tr><th>Order of abund.</th><th>R. T. (min)</th><th>Compd</th><th>m/z of molecular and fragment ions</th><th># Cl atoms</th></tr><tr><td></td><td>11.46</td><td></td><td>359 (361, 363), 181 (17%)</td><td>1</td></tr><tr><td></td><td>11.73</td><td>TMP</td><td>291</td><td>-</td></tr><tr><td></td><td>12.47</td><td></td><td>373 (76%, 375, 377), 291, 181 (36%)</td><td>1</td></tr><tr><td>4</td><td>13.29</td><td>P1-N</td><td>325 (327), 291 (9%)</td><td>1</td></tr><tr><td>2</td><td>14.37</td><td></td><td>377 (379, 381), 343 (5%), 181 (22%)</td><td>2</td></tr><tr><td>1</td><td>16.76</td><td>P2-N</td><td>377 (379, 381), 181 (51%)</td><td>2</td></tr><tr><td></td><td>17.50</td><td></td><td>391 (393, 395), 357 (5%, 359), 181 (19%)</td><td>2</td></tr><tr><td></td><td>18.12</td><td></td><td>393 (395, 397), 357 (5%, 359), 321 (8%), 215 (29%, 217), 181 (41%)</td><td>2</td></tr><tr><td>5</td><td>19.69</td><td>P3-N</td><td>377 (379, 381), 181 (32%)</td><td>2</td></tr><tr><td></td><td>20.60</td><td></td><td>407 (409, 411), 377 (9%, 379), 215 (48%, 217), 181 (30%)</td><td>2</td></tr><tr><td>3</td><td>21.92</td><td></td><td>411 (413, 415, 417), 375 (24%, 377, 379), 339 (16%, 341), 215 (11%, 217), 181 (29%)</td><td>3</td></tr><tr><td></td><td>24.33</td><td></td><td>445 (447, 449, 451, 453), 427 (15%, 429)</td><td>4</td></tr><tr><td></td><td>25.80</td><td></td><td>425 (427, 429, 431), 391 (20%, 393), 357 (15%, 359), 181 (56%)</td><td>3</td></tr></table> <ul style="list-style-type: none">• R. T. = LC retention time.• Most abundant products are shown in red and indicated with their order of abundance in the LC/MS chromatogram.• Base peaks are shown in bold, with fragment ion peaks in plain text. Relative fragment peak abundances are given as percentage of base peak height. Cl isotope peak masses are also indicated in parentheses.• Number of Cl atoms deduced from observed Cl isotope peak signal ratios• The listed mass spectral information was obtained at 70 eV fragmentation voltage. Higher voltage (120 eV) resulted in similar fragmentation patterns with only difference in relative abundance.					Order of abund.	R. T. (min)	Compd	m/z of molecular and fragment ions	# Cl atoms		11.46		359 (361, 363), 181 (17%)	1		11.73	TMP	291	-		12.47		373 (76%, 375, 377), 291 , 181 (36%)	1	4	13.29	P1-N	325 (327), 291 (9%)	1	2	14.37		377 (379, 381), 343 (5%), 181 (22%)	2	1	16.76	P2-N	377 (379, 381), 181 (51%)	2		17.50		391 (393, 395), 357 (5%, 359), 181 (19%)	2		18.12		393 (395, 397), 357 (5%, 359), 321 (8%), 215 (29%, 217), 181 (41%)	2	5	19.69	P3-N	377 (379, 381), 181 (32%)	2		20.60		407 (409, 411), 377 (9%, 379), 215 (48%, 217), 181 (30%)	2	3	21.92		411 (413, 415, 417), 375 (24%, 377, 379), 339 (16%, 341), 215 (11%, 217), 181 (29%)	3		24.33		445 (447, 449, 451, 453), 427 (15%, 429)	4		25.80		425 (427, 429, 431), 391 (20%, 393), 357 (15%, 359), 181 (56%)	3
Order of abund.	R. T. (min)	Compd	m/z of molecular and fragment ions	# Cl atoms																																																																						
	11.46		359 (361, 363), 181 (17%)	1																																																																						
	11.73	TMP	291	-																																																																						
	12.47		373 (76%, 375, 377), 291 , 181 (36%)	1																																																																						
4	13.29	P1-N	325 (327), 291 (9%)	1																																																																						
2	14.37		377 (379, 381), 343 (5%), 181 (22%)	2																																																																						
1	16.76	P2-N	377 (379, 381), 181 (51%)	2																																																																						
	17.50		391 (393, 395), 357 (5%, 359), 181 (19%)	2																																																																						
	18.12		393 (395, 397), 357 (5%, 359), 321 (8%), 215 (29%, 217), 181 (41%)	2																																																																						
5	19.69	P3-N	377 (379, 381), 181 (32%)	2																																																																						
	20.60		407 (409, 411), 377 (9%, 379), 215 (48%, 217), 181 (30%)	2																																																																						
3	21.92		411 (413, 415, 417), 375 (24%, 377, 379), 339 (16%, 341), 215 (11%, 217), 181 (29%)	3																																																																						
	24.33		445 (447, 449, 451, 453), 427 (15%, 429)	4																																																																						
	25.80		425 (427, 429, 431), 391 (20%, 393), 357 (15%, 359), 181 (56%)	3																																																																						

APPENDIX B – MOBILE PHASE FOR HPLC-UV AND HPLC-MS ANALYSIS

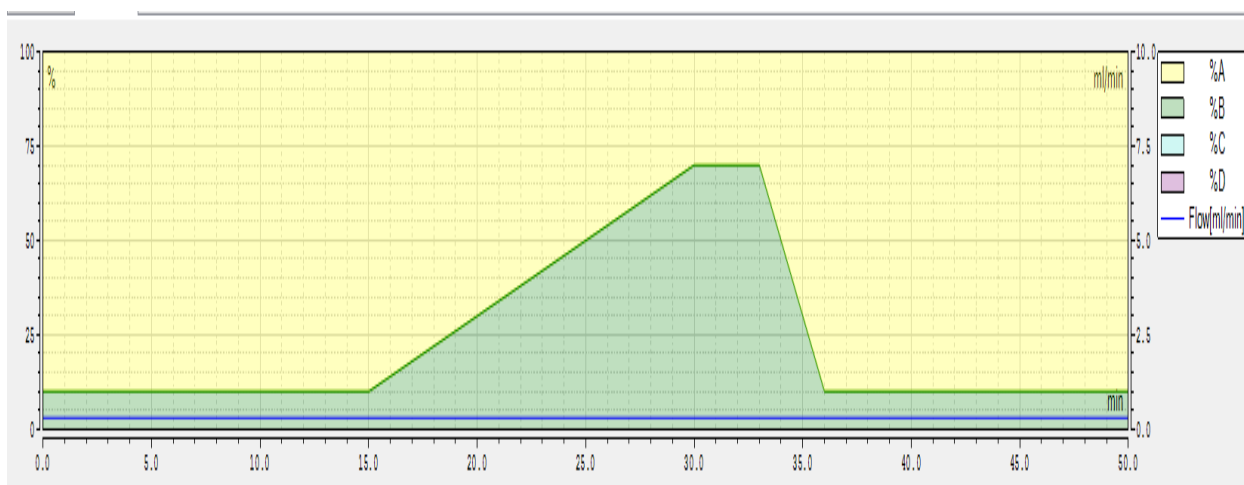


Figure B1: An eluent gradient mobile phase was applied to achieve separation of products. The mobile phase consists of nanopure water (A) and HPLC-grade methanol (B), each amended with 0.1% (volume) formic acid (98 to 100%). The percentage of (A) was changed linearly according to time: 0-15 min, 90%; 30 min, 30%; 33min, 30%; 36min, 90%. The flow rate was 0.3 mL/min.

APPENDIX C - PEAK AREAS OF SULFONAMIDES REACTING WITH FREE CHLORINE

Table C1: Peak Areas of SMX/SDM/STZ Reacting with Different Concentrations of FAC on HPLC-UV-Vis. Concentrations are provided in lieu of peak areas for SMX, SDM, and STZ along with the product NCBQ based on an external calibration.

SMX					SDM					STZ				
C _{0, FAC} ¹ [mg/L]	RT ² [min]	N ³	Avg PA ⁴ [mAU*min]	C ⁵ [mg/L]	C _{0, FAC} [mg/L]	RT [min]	N	Avg PA [mAU*min]	C [mg/L]	C _{0, FAC} [mg/L]	RT [min]	N	Avg PA [mAU*min]	C [mg/L]
0	30.4	2	72.9	9.97	0	33.3	2	92.6	9.35	0	25.2	3	94.0	10.03
2	30.4	3	49.7	6.80	2	33.3	3	23.1	2.37	2	25.2	3	58.0	6.18
2	18.6	3	8.2	-	2	32.8	3	4.6	-	2	3.8	3	1.3	-
2	35.5	3	0.4	-	2	34.5	3	45.5	-	2	6.3	3	2.3	-
4	30.4	3	29.2	4.01	2	35.8	3	0.7	-	2	32.5	3	1.8	-
4	18.6	3	12.1	-	2	37.7	3	0.8	-	4	25.2	3	32.0	3.41
4	33.3	3	6	0.12	4	32.8	3	18.7	-	4	3.8	3	1.6	-
4	35.5	3	0.6	-	4	34.5	3	38	-	4	6.3	3	3.6	-
8	30.4	3	2.4	0.37	4	35.8	3	9.1	-	4	32.5	3	2.4	-
8	18.6	3	0.6	-	4	37.7	3	3.1	-	4	27.8	3	0.3	-
8	33.3	3	26.9	0.98	4	6.2	3	1.7	-	4	33.3	3	0.8	-
8	35.5	3	2.4	-	4	29.4	3	0.3	-	8	25.2	3	5.4	0.56
8	38.8	2	0.5	-	4	35.0	3	1.3	-	8	3.8	3	1.1	-
8	36.7	2	1.2	-	4	36.9	3	0.9	-	8	6.3	3	3.6	-
16	30.4	3	0.5	0.11	8	33.2	3	4.5	-	8	32.5	1	1.7	-
16	33.3	3	22	0.77	8	32.8	3	4.2	-	8	27.8	1	0.6	-
16	38.8	3	0.7	-	8	34.5	3	4	-	8	33.3	3	2.6	-
16	27.3	1	1.3	-	8	35.8	3	37	-	8	32.1	3	0.4	-
16	30.9	3	8.7	-	8	37.7	3	0.8	-	8	13.3	2	0.3	-
16	36.9	3	20.5	-	8	6.2	3	1.3	-	8	30.6	1	0.5	-
48	30.4	3	0.4	0.09	8	29.4	2	0.4	-	16	6.3	3	1.6	-
48	38.8	3	0.7	-	8	35.0	3	1.5	-	16	27.8	3	0.6	-
48	27.3	1	3.4	-	8	36.9	3	4.5	-	16	33.3	3	7.1	-
48	30.9	3	1.3	-	16	33.2	3	2.8	-	16	32.1	2	1	-
					16	34.5	3	0.5	-	16	13.3	3	0.2	-
					16	35.8	3	43.1	-	48	33.3	3	10.6	-
					16	36.9	3	4.8	-	48	30.6	2	2.2	-
					48	33.2	3	1.2	-					
					48	35.8	3	37.5	-					
					48	36.9	3	3.7	-					

¹C_{0,FAC} is the final concentration of free chlorine in the experiments. Concentration was measured for SMX and assumed for SDM and STZ. ²RT is the retention time in the HPLC-UV-Vis. ³N is the number of samples in which a peak was observed. ⁴PA is the peak area in the HPLC-UV-Vis. ⁵C is the concentration calculated from calibration curve.

APPENDIX D – ANALYTICAL DATA TO SUPPORT STRUCTURE ASSIGNMENT OF TRANSFORMATION PRODUCTS

1.1 SMX288

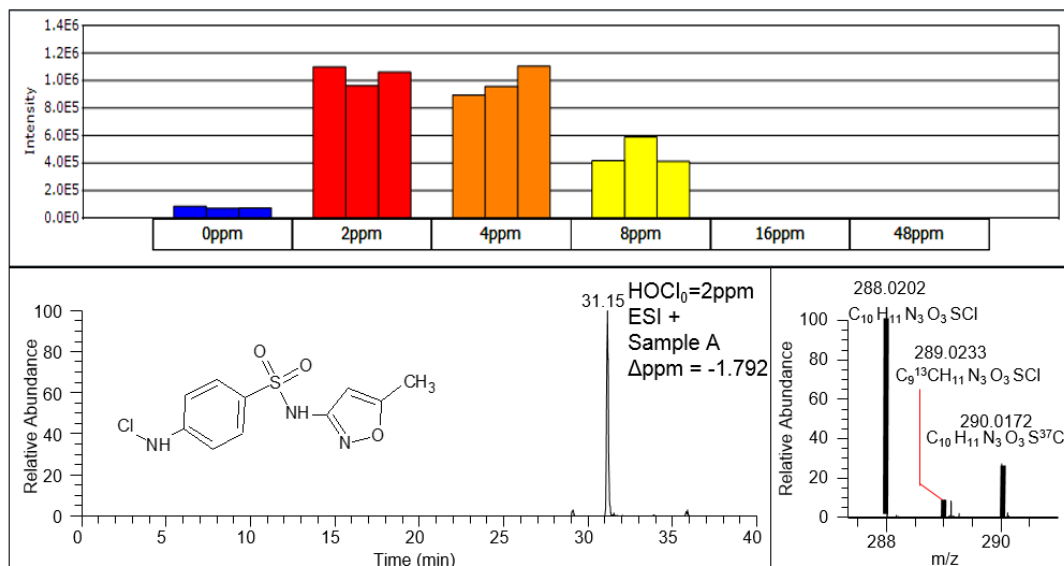


Figure D1: SMX288 had a RT of 31.15 min and MS spectra matched the exact mass of the proposed chemical ($m/z = 288.0202$ for MH^+ , $\Delta m = -1.792$ ppm) and the theoretical abundance (10%) of the ^{13}C monoisotopic mass and the theoretical abundance (35%) of the ^{37}Cl monoisotopic mass.

SMX288 was formed primarily in under-chlorinated reactions: abundance of SMX288 was much higher at initial FAC = 2 ppm and 4 ppm than at initial FAC = 8 ppm. This might suggest that SMX288 was one of the transformation products (TPs) that were directly formed from SMX-FAC reaction instead from TPs that were formed from other TPs. Abundance of ^{37}Cl monoisotopic mass suggested that SMX288 was a mono-chlorinated chemical. Combining previous studies reporting the formation of SMX288 in SMX-FAC reactions^{1,2} and theories on aniline chlorination patterns³⁻⁵, we propose SMX288 is the mono-chlorinated SMX. And the chlorination happened at the amino group of the aniline portion of SMX. Structure is shown in Figure D1.

1.2 SMX142

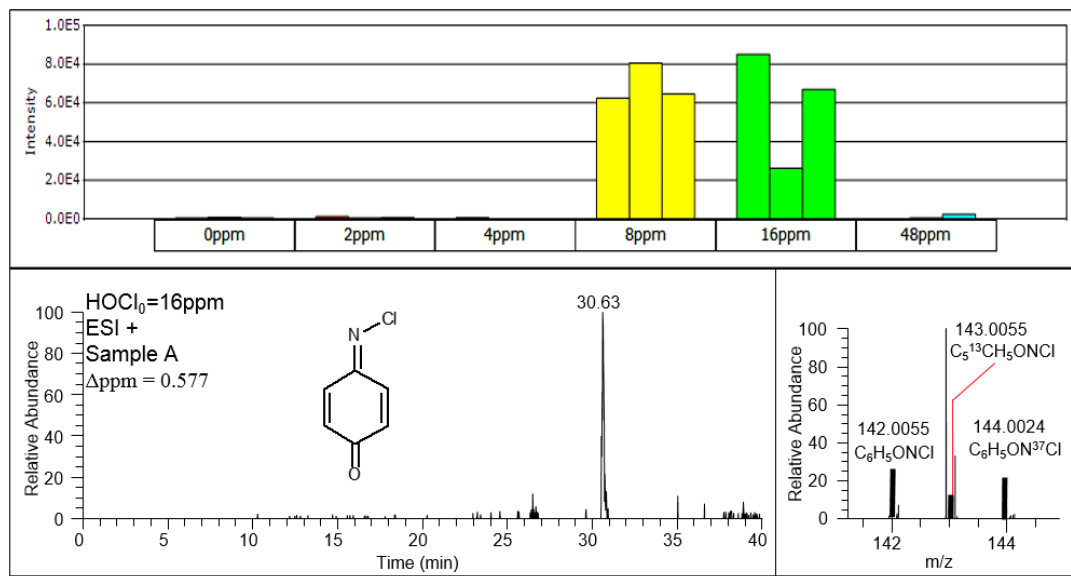


Figure D2: SMX142 had a RT of 30.63 min and MS spectra matched the exact mass of the proposed chemical ($m/z = 142.0055$ for MH^+ , $\Delta m = 0.577$ ppm) and the theoretical abundance (6%) of the ¹³C monoisotopic mass and the theoretical abundance (40%) of the ³⁷Cl monoisotopic mass.

SMX142 was formed in over-chlorinated reactions: mainly at initial FAC = 8 ppm and 16 ppm.

In over-chlorinated reactions, SMX288 underwent another chlorination substitution reaction and formed an intermediate, N, N-dichlorinated SMX, a heterolytic cleavage of N-X bond of which would lead to a phenylnitrenium ion (anilenium ion) represented by the resonance contributors 2, 3, 4 as shown in Figure D3.

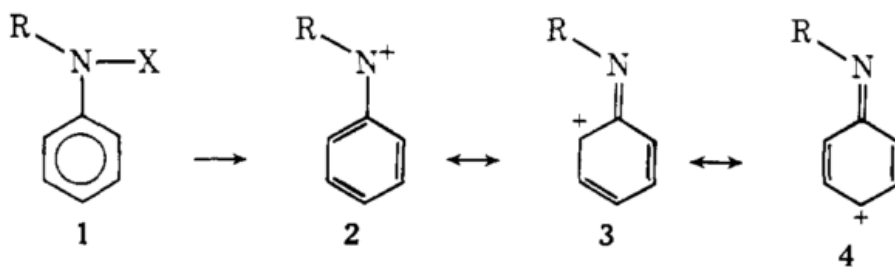


Figure D3: the presence of a suitable leaving group on the hetero atom could result in a positively charged species being generated, which, through charge delocalization, would render the aromatic nucleus vulnerable to nucleophilic attack. For instance, heterolytic cleavage of the N-X bond of 1, under solvolytic conditions, would lead to a phenylnitrenium ion (anilenium ion) represented by the resonance contributors 2, 3, and 4. Theory and picture from Gassman, et al. (1971)

Similarly, the N,N-dichlorinated SMX generated an aryl nitrenium cation, N-chlorinated SMX nitrenium ion, which can lead to distribution of strong electron-deficiency to the aromatic ring's *para* and *ortho* positions, resulting in the formation of SMX144. Similar structure rearrangement was found in biodegradation of SMX as illustrated in Figure D4. ⁶

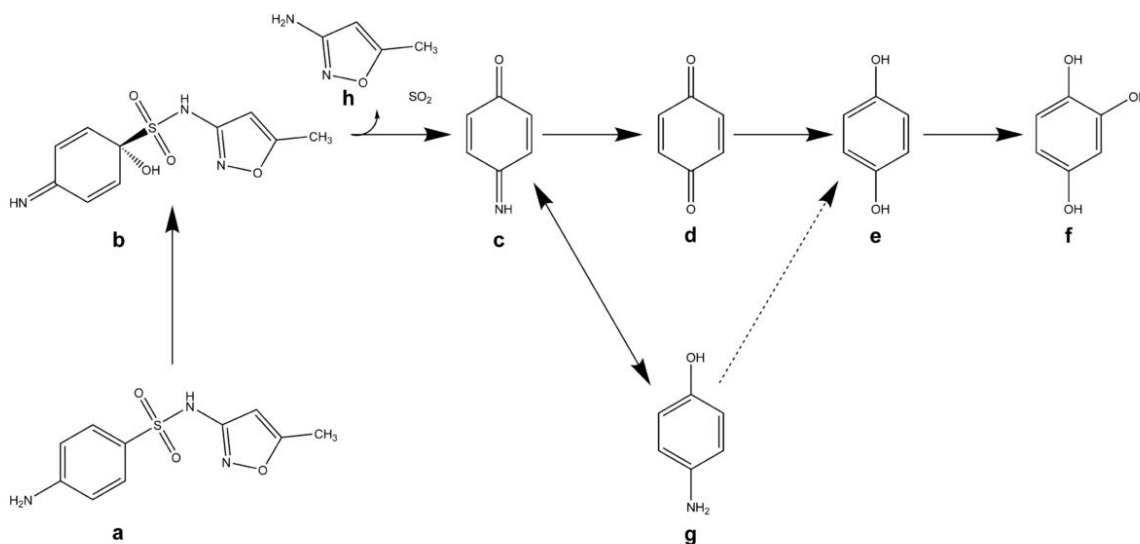


Figure D4: Ricken et al (2015) proposed degradation pathway of SMX by *Microbacterium* sp. strain BR1. The oxidation of SMX (a) at the ipso position leads to an instable intermediate (b) after electron rearrangement which subsequently fragments to 3A5MI (h), p-benzoquinone imine

(c), and SO₂ as previously postulated [5]. Upon hydrolysis to benzoquinone (d), the latter may be reduced to hydroquinone (e) which is then further transformed to 1,2,4-trihydroxybenzene (f). Alternatively, *p*-benzoquinone imine may be reduced to *p*-aminophenol (g), which could then be further transformed to hydroquinone by hydrolase activity.

1.3 SMX99

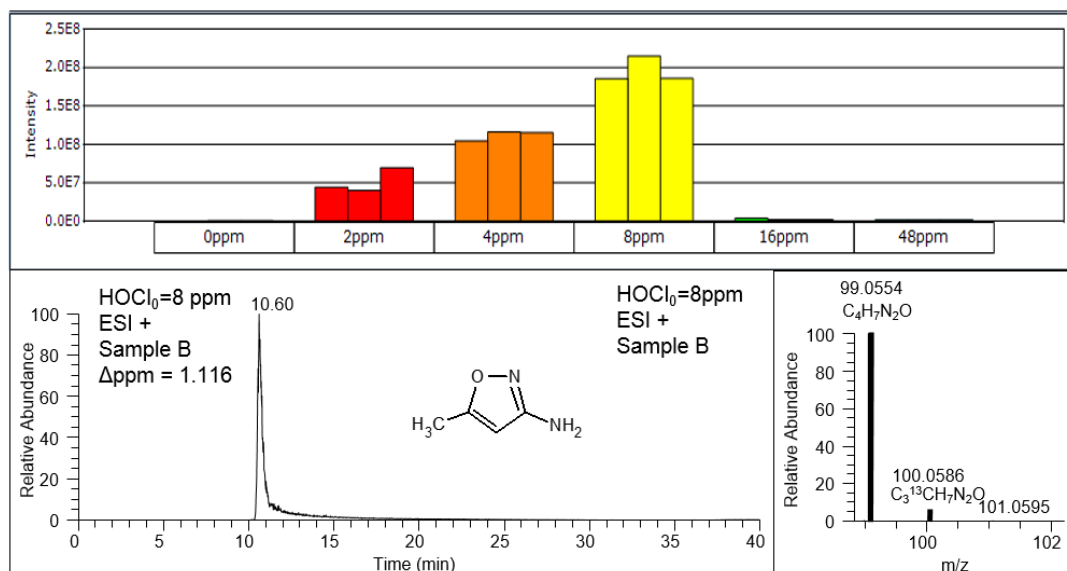


Figure D5: SMX99 had a RT of 10.60 min and MS spectra matched the exact mass of the proposed chemical ($m/z = 99.0554$ for MH^+ , $\Delta m = 1.116$ ppm) and the theoretical abundance (4%) of the ¹³C monoisotopic mass.

SMX99 was also detected and identified by Dodd and Huang¹, as well as by Gao et al.² as transformation product in chlorination of SMX. In addition, previous studies demonstrated that AMI could also be produced by SMX upon other oxidation treatment, such as ozone, permanganate, TiO₂ photocatalysis, Photo – Fenton, UV photolysis, etc.^{1, 2, 7-10} It was also proposed as a breakdown product in biotransformation reactions.¹¹ Its common occurrence found in oxidation reactions indicated that the S-N bond on the SMX was easily to be cleaved upon chemical oxidation and biodegradation. It could also be formed from intermediate a2 (see Figure 13 in Chapter 4.2.1) rearranged to a *p*-benzoquinoneimine structure, SMX144. The –NH₂ moiety

in AMI prepared it for further reaction: for example, though conjugation reactions, AMI could form a dimeric product, SDM193, as illustrated in the next following section.

1.4 SMX193

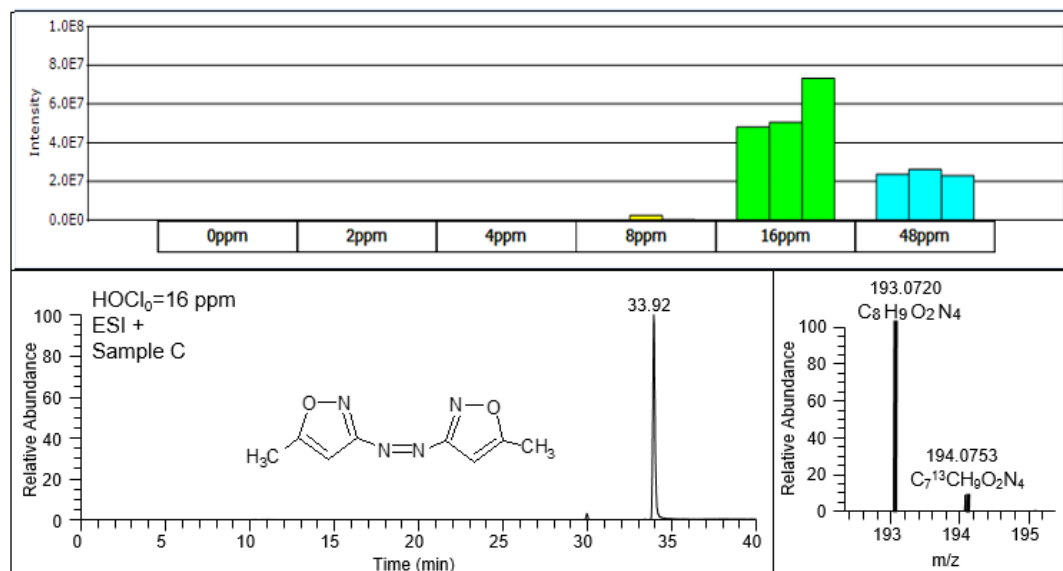


Figure D6: SMX193 had a RT of 33.92 min and MS spectra matched the exact mass of the proposed chemical ($m/z = 193.0720$ for MH^+ , $\Delta m = 0.507$ ppm) and the theoretical abundance (8%) of the ^{13}C monoisotopic mass.

SMX193 was the product formed from coupling reactions of SMX99. The Sieve integrated intensity pattern also suggest that SMX193 was possibly formed from SMX99.

1.5 SMX179

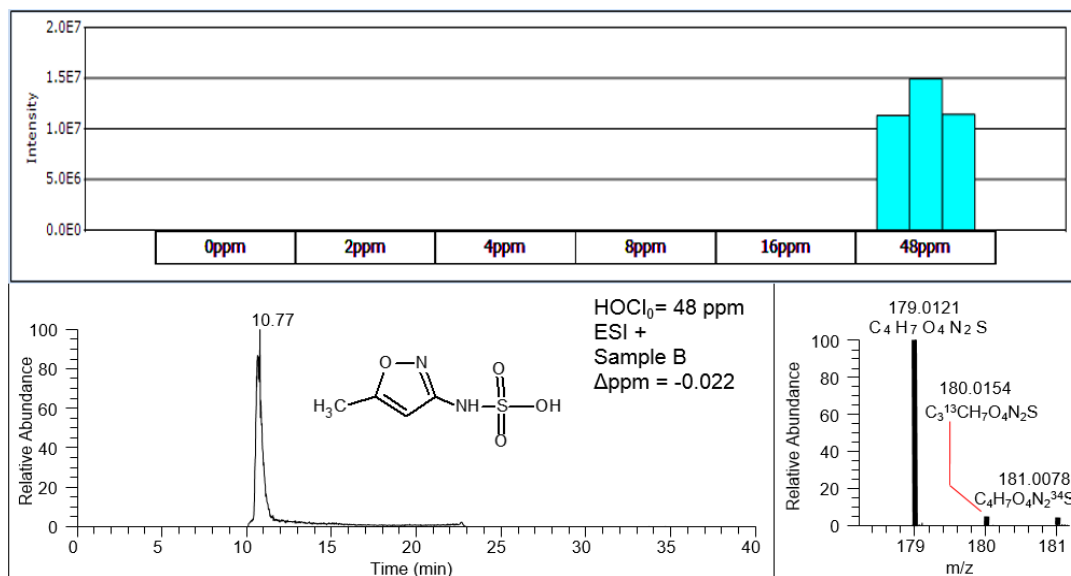


Figure D7: SMX179 had a RT of 10.77 min and MS spectra matched the exact mass of the proposed chemical ($m/z = 179.0121$ for MH^+ , $\Delta m = -0.022$ ppm) and the theoretical abundance (4%) of the ^{13}C monoisotopic mass and the theoretical abundance (2%) of the ^{34}S monoisotopic mass.

SMX179 indicated the occurrence of hydrolysis reaction of SMX when the S-C bond cleaved. It was only detected in highly over-chlorinated reactions: at initial FAC = 48 ppm.

1.6 SMX110

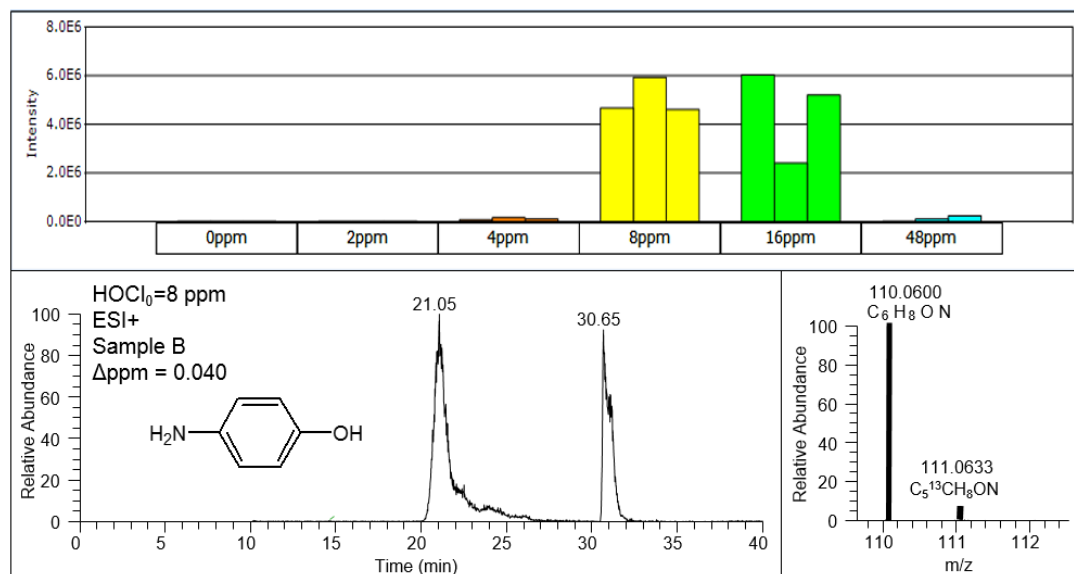


Figure D8: SMX110 had a RT of 30.65 min and MS spectra matched the exact mass of the proposed chemical ($m/z = 110.0600$ for MH^+ , $\Delta m = 0.040$ ppm) and the theoretical abundance (6%) of the ¹³C monoisotopic mass.

SMX110 was the hydroxylated product of an aniline, which was formed along with SMX179 through hydrolytic reaction. The hydroxylation could take place on both *ortho*- and *para*-positions of an aniline.¹² The substitution reaction was illustrated in Figure D9. Particularly, we are interested in the *para*-substituted SMX110, which could undergo further reactions and form other products that we identified.

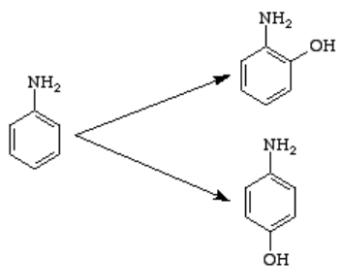


Figure D9: Hydroxylation happened on both *ortho*- and *para*- position of aniline.

1.7 SMX108

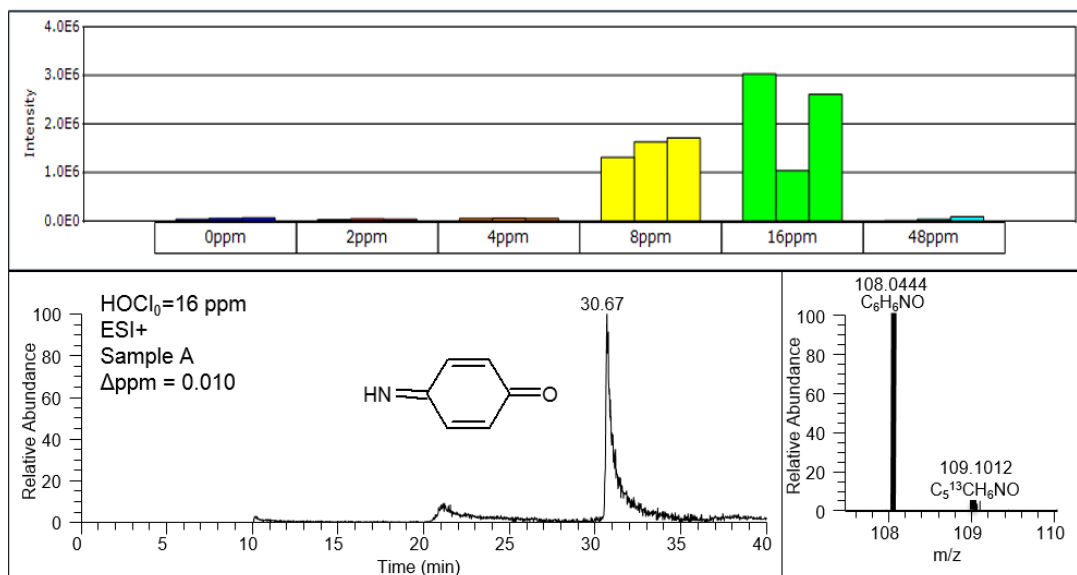


Figure D10: SMX108 had a RT of 30.67 min and MS spectra matched the exact mass of the proposed chemical ($m/z = 108.0444$ for MH^+ , $\Delta m = 0.010$ ppm) and the theoretical abundance (6%) of the ¹³C monoisotopic mass.

1.8 SMX144

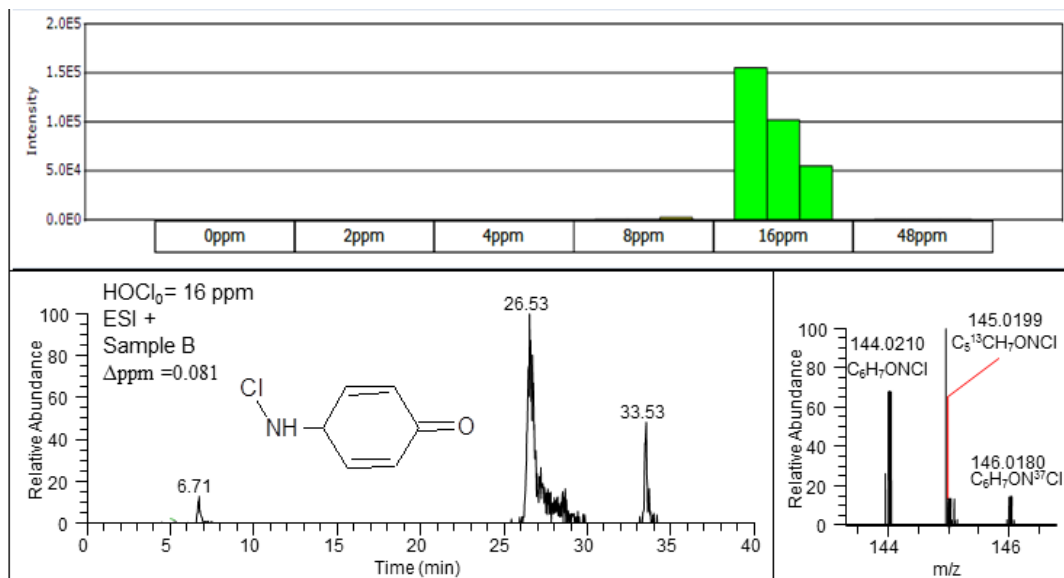


Figure D11: SMX144 had a RT of 26.53 min and MS spectra matched the exact mass of the proposed chemical ($m/z = 144.0210$ for MH^+ , $\Delta m = 0.081$ ppm) and the theoretical abundance (6%) of the ¹³C monoisotopic mass and the theoretical abundance (35%) of the ³⁷Cl monoisotopic mass.

1.9 SMX270

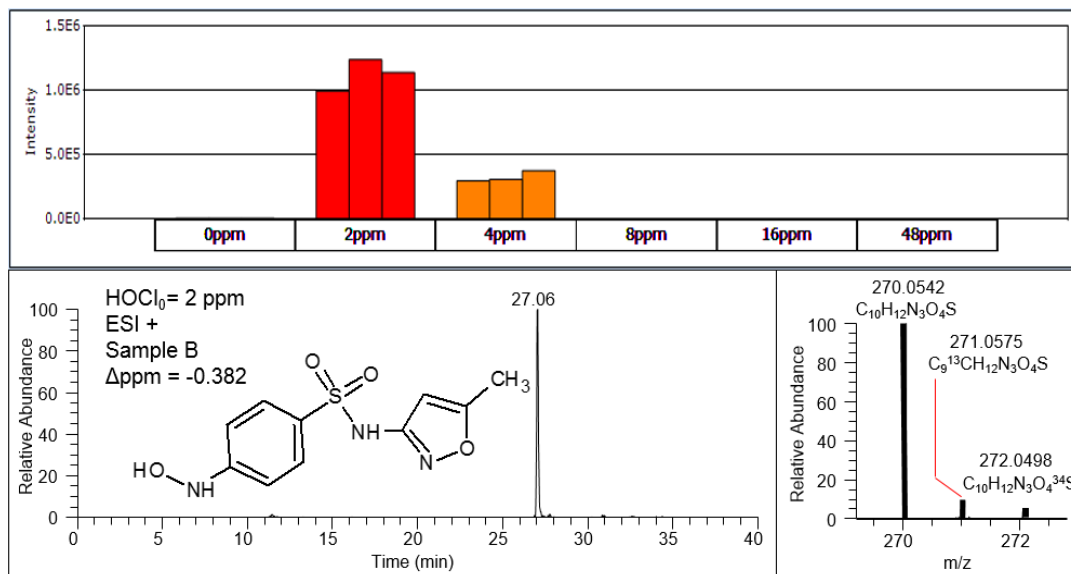


Figure D12: SMX270 had a RT of 27.06 min and MS spectra matched the exact mass of the proposed chemical ($m/z = 270.0542$ for MH^+ , $\Delta m = -0.382$ ppm) and the theoretical abundance (10%) of the ¹³C monoisotopic mass and the theoretical abundance (2%) of the ³⁴S monoisotopic mass.

Hydroxylation reactions lead to the formation of SMX270, which is the hydroxylated SMX. The –OH moiety took place at the N- ammonia on the aromatic amine portion of SMX for the same reason that SMX288 was N-chlorinated.

1.10 SMX284

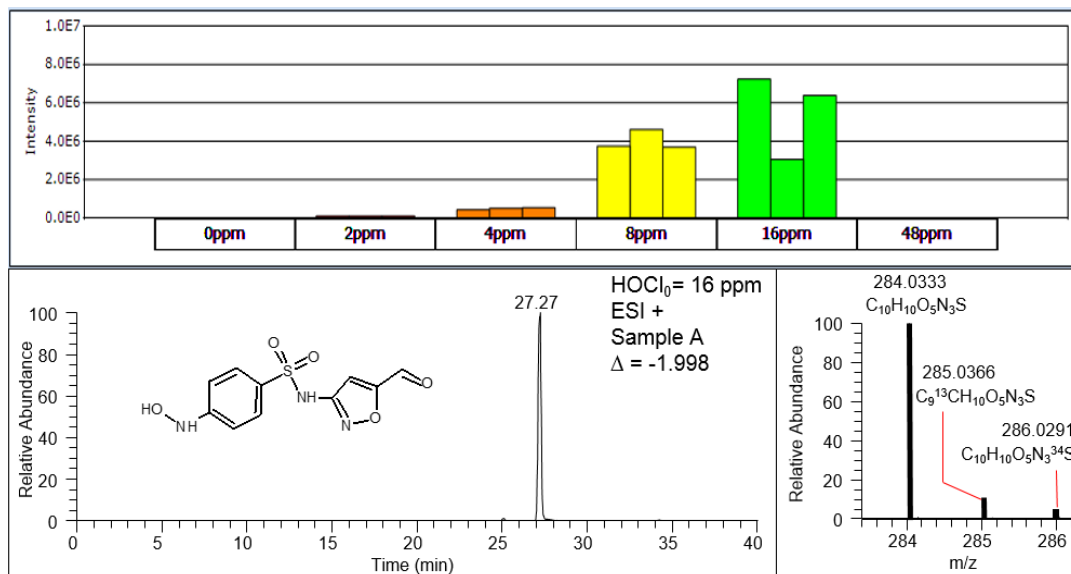


Figure D13: SMX284 had a RT of 27.27 min and MS spectra matched the exact mass of the proposed chemical ($m/z = 284.0333$ for MH^+ , $\Delta m = -1.998$ ppm) and the theoretical abundance (10%) of the ^{13}C monoisotopic mass and the theoretical abundance (2%) of the ^{34}S monoisotopic mass.

SMX284 is a product formed from SMX270 when further oxidized. Similar oxidation reaction also took place in biodegradation¹³, as illustrated in Figure D14.

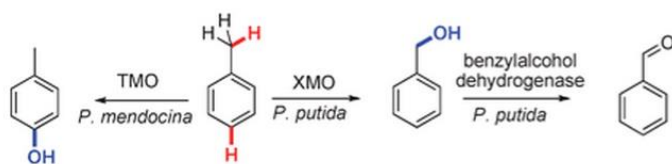


Figure D14: Toluene monooxygenase (aromatic oxidation) vs. xylene monooxygenase (benzylic oxidation) and subsequent dehydrogenation for the synthesis of phenols, alcohols, aldehydes. Theory and figure by Lewis et al. (2010).

1.11 SMX298

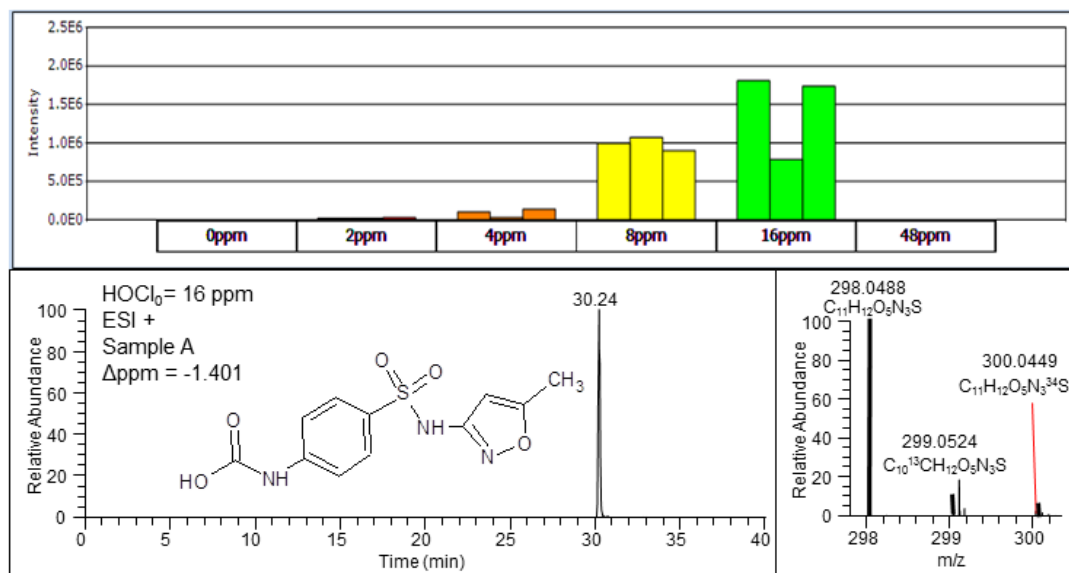


Figure D15: SMX298 had a RT of 30.24 min and MS spectra matched the exact mass of the proposed chemical ($m/z = 298.0488$ for MH^+ , $\Delta m = -1.401$ ppm) and the theoretical abundance (11%) of the ^{13}C monoisotopic mass and the theoretical abundance (2%) of the ^{34}S monoisotopic mass.

SMX298 was mostly formed in over-chlorinated reactions: at initial FAC = 8 ppm and 16 ppm.

The formation of SMX298 probably suggested the formation of an intermediate, Ac-SMX, which was commonly recognized as a metabolite of SMX.¹⁰ Mechanism of transformation from AC-SMX to SMX298 was previously reported as illustrated in Figure D16.¹⁴

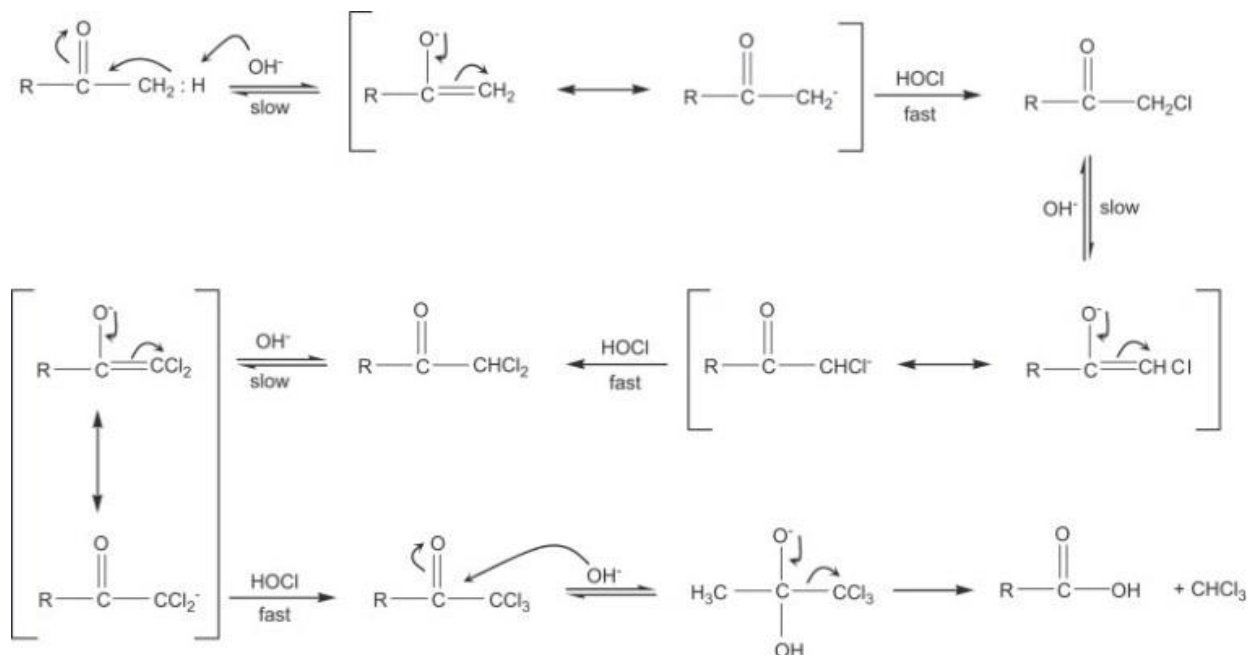


Figure D16: Base-catalyzed reaction pattern proposed for the reaction of chlorine with aldehydes and ketones. Adapted from Deborde and von Gunten (2007).

1.12 SMX503

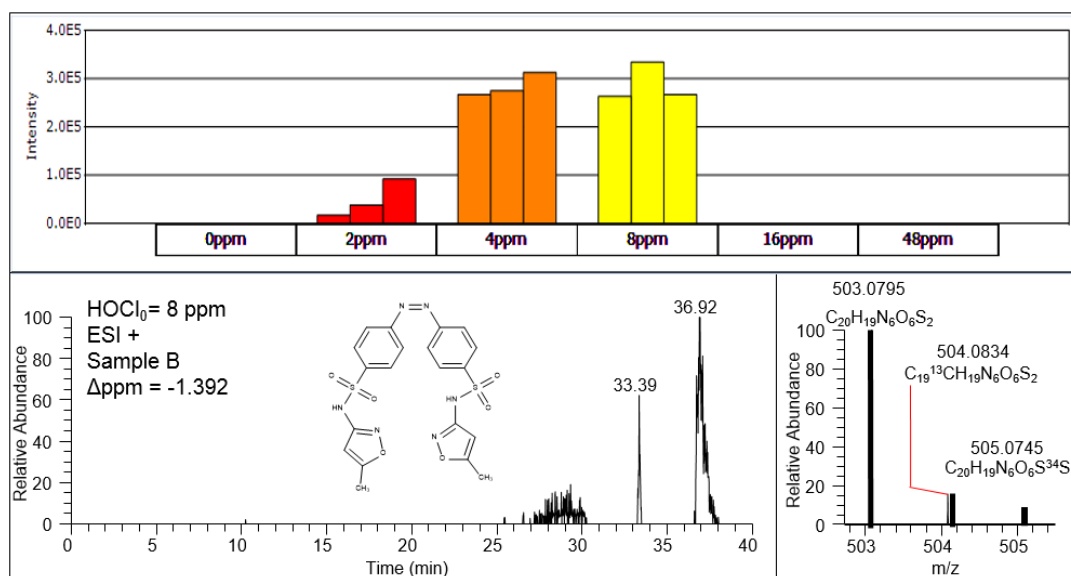


Figure D17: SMX503 had a RT of 36.92min and MS spectra matched the exact mass of the proposed chemical ($m/z = 503.0795$ for MH^+ , $\Delta m = -1.392$ ppm) and the theoretical abundance (20%) of the ¹³C monoisotopic mass and the theoretical abundance (4%) of the ³⁴S monoisotopic mass.

1.13 SMX190 (e1)

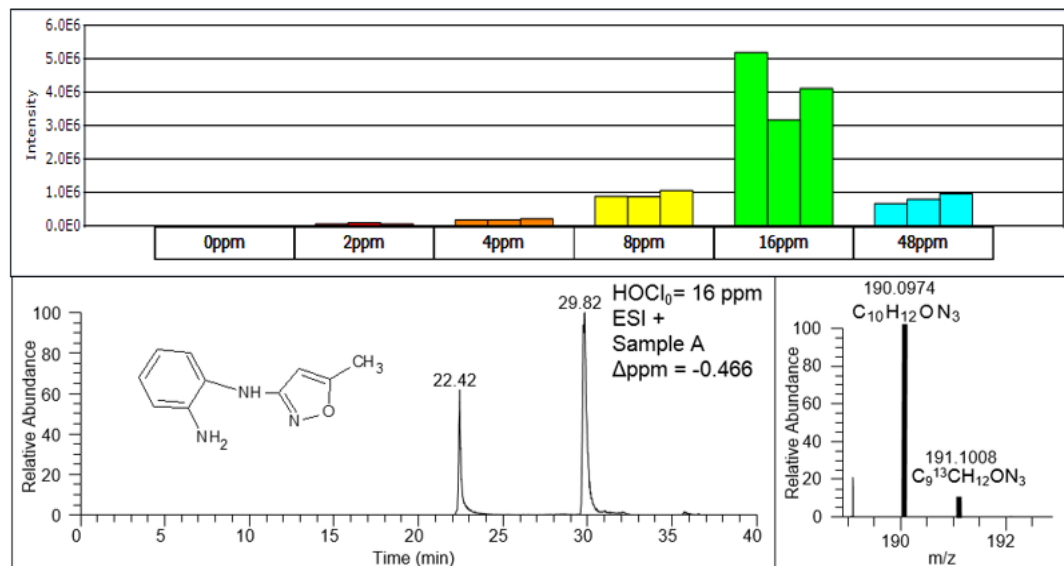


Figure D18: SMX190 e1 had a RT of 22.42 or 29.82 min and MS spectra matched the exact mass of the proposed chemical ($m/z = 190.0974$ for MH^+ , $\Delta m = -0.466$ ppm) and the theoretical abundance (10%) of the ^{13}C monoisotopic. Structure shown in this figure is e1 in Figure 13 of Chap 4.2.1 of the thesis.

The two different RTs suggested that two isomers were formed. SMX190 (e1) was proposed here as a substitution at the *ortho* position of aniline. SMX190 (e2) resulted from SO_2 extrusion reaction. Mechanisms of SO_2 extrusion reactions were studied with photolysis reactions of SMX^{15} and are illustrated in Figure 20.

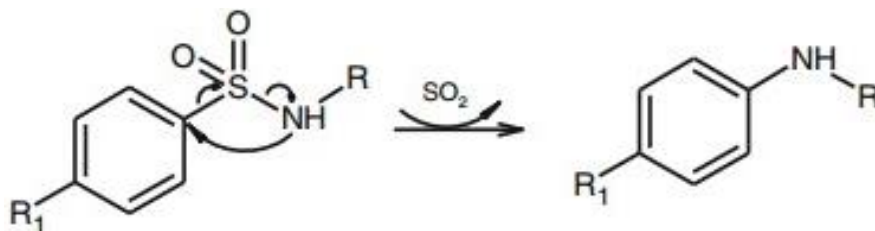


Figure D19: Proposed mechanisms of SO_2 extrusion reaction in sulfonamides by Perisa et al. (2013).

1.14 SMX190 (e2)

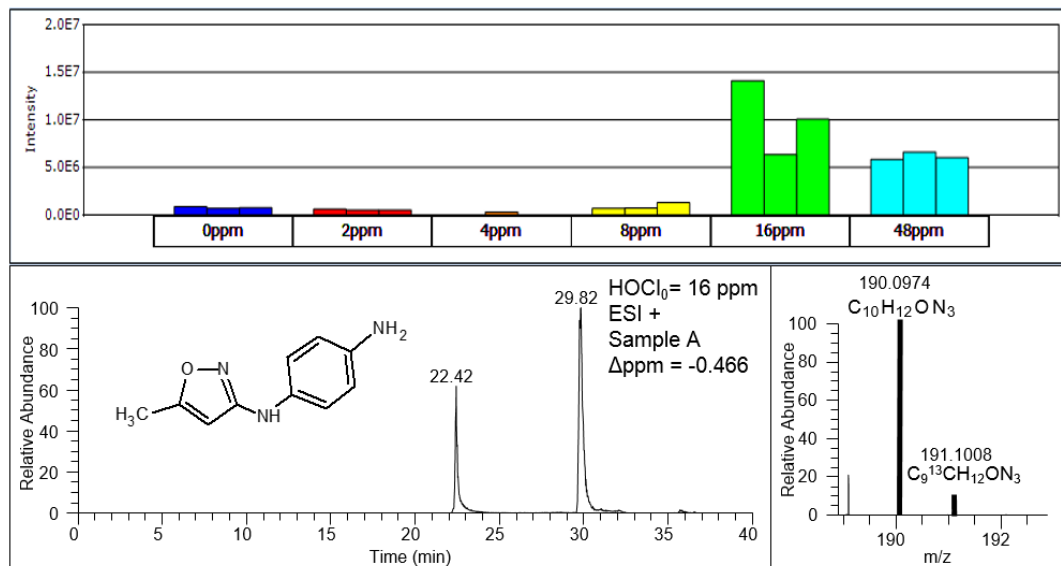


Figure D20: SMX190 e2 had a RT of 22.42 or 29.82 min and MS spectra matched the exact mass of the proposed chemical ($m/z = 190.0974$ for MH^+ , $\Delta m = -0.466$ ppm) and the theoretical abundance (10%) of the ^{13}C monoisotopic. Structure shown in this figure is e2 in Figure 13 of Chap 4.2.1 of the thesis.

1.15 SMX238

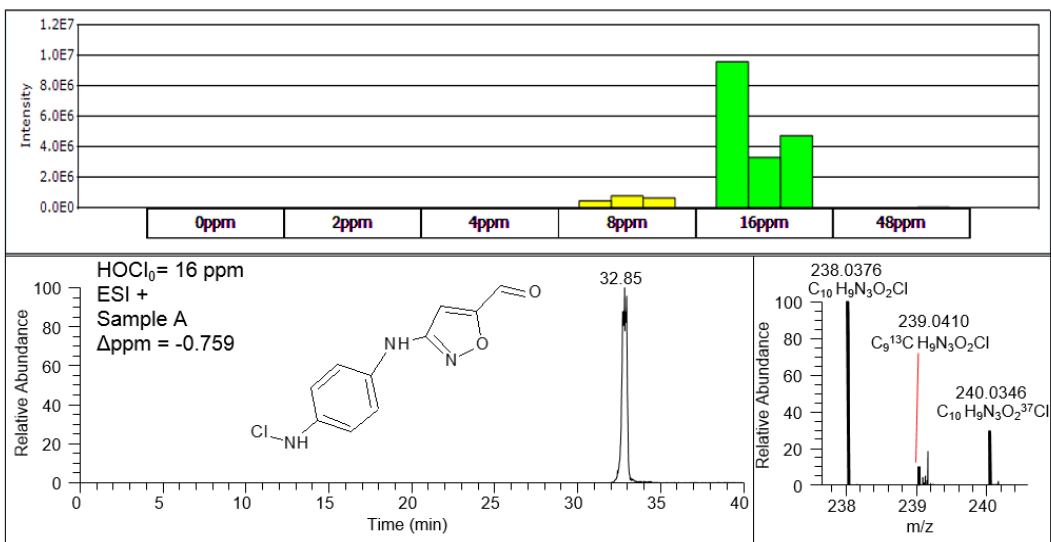


Figure D21: SMX238 had a RT of 32.85 min and MS spectra matched the exact mass of the proposed chemical ($m/z = 238.0376$ for MH^+ , $\Delta m = -0.759$ ppm) and the theoretical abundance (10%) of the ¹³C monoisotopic mass and the theoretical abundance (35%) of the ³⁷Cl monoisotopic mass.

SMX238 was mainly formed in over-chlorinated reactions: at initial FAC = 16 ppm, abundance of SMX238 reached its highest. The oxidation reaction from SMXf3 to SMX238 was very similar with that from SMX270 to SMX284.

1.16 SMX222

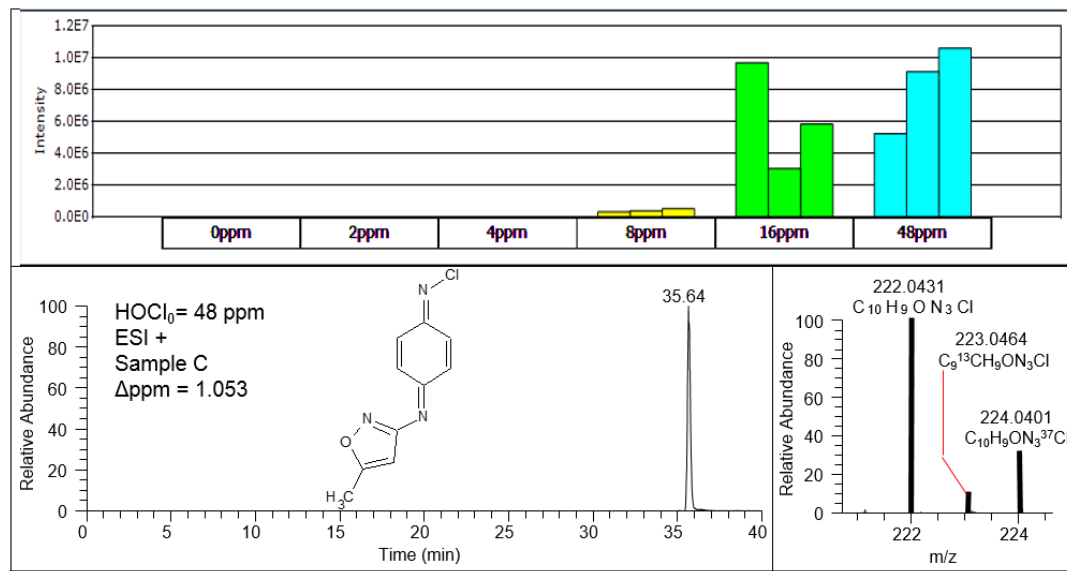


Figure D22: SMX222 had a RT of 35.64 min and MS spectra matched the exact mass of the proposed chemical ($m/z = 222.0431$ for MH^+ , $\Delta m = 1.053$ ppm) and the theoretical abundance (10%) of the ^{13}C monoisotopic mass and the theoretical abundance (35%) of the ^{37}Cl monoisotopic mass.

2.1 SDM345

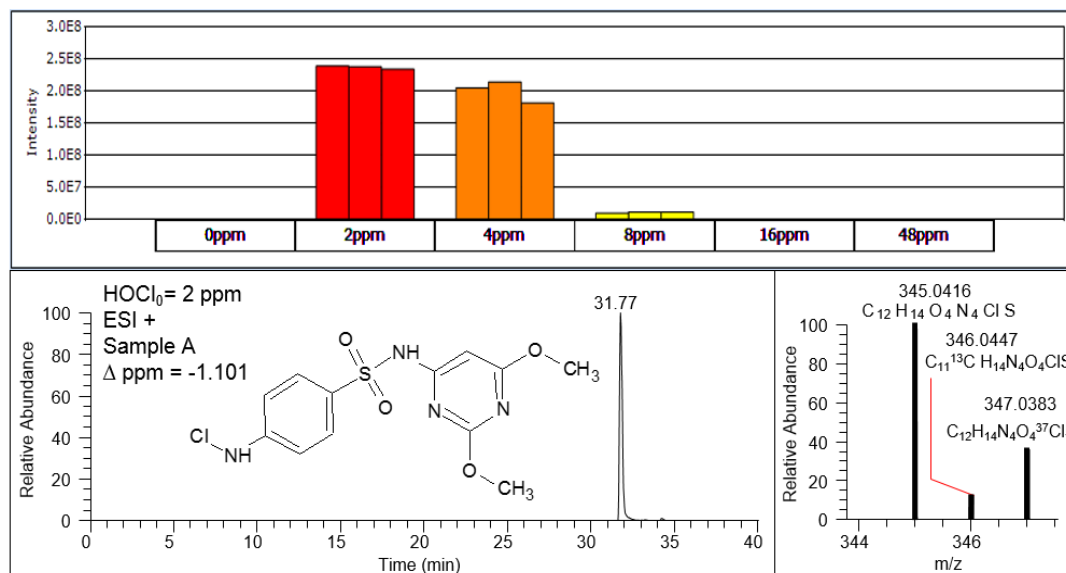


Figure D23: SDM345 had a RT of 31.77 min and MS spectra matched the exact mass of the proposed chemical ($m/z = 345.0416$ for MH^+ , $\Delta m = -1.101$ ppm) and the theoretical abundance (12%) of the ^{13}C monoisotopic mass and the theoretical abundance (40%) of the ^{37}Cl monoisotopic mass.

SDM345 was formed mainly in under-chlorinated reactions: at initial FAC = 2 ppm and 4 ppm.

The pattern of SDM345-FAC was very similar to that of SMX288-FAC, suggesting that

SDM345 could possibly be one of the TPs that were formed directly from SDM in reaction with

FAC. SDM345 was considered a N-chlorinated chemical for the same reason SMX288 was

considered N-chlorinated.

2.2 SDM361

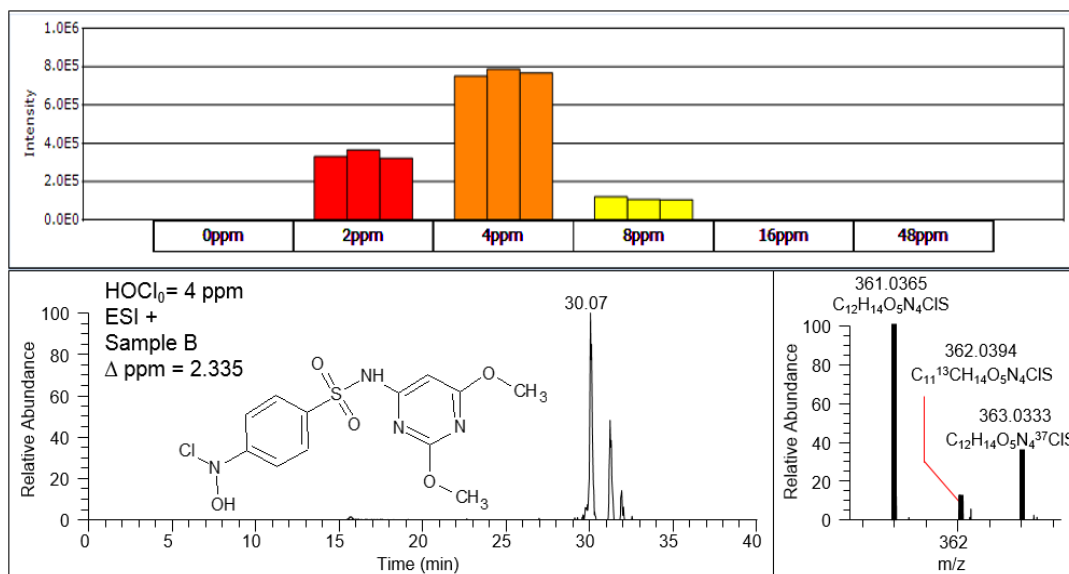


Figure D24: SDM361 had a RT of 30.07 min and MS spectra matched the exact mass of the proposed chemical ($m/z = 361.0365$ for MH^+ , $\Delta m = -1.101$ ppm) and the theoretical abundance (12%) of the ^{13}C monoisotopic mass and the theoretical abundance (40%) of the ^{37}Cl monoisotopic mass.

The Sieve integrated intensity patterns suggested that SDM361 was likely to be a TP of SDM345. Hydroxylation reaction mechanisms of SDM361 being formed was the same as previously explained for formation of hydroxylated SMX.

2.3 SDM379

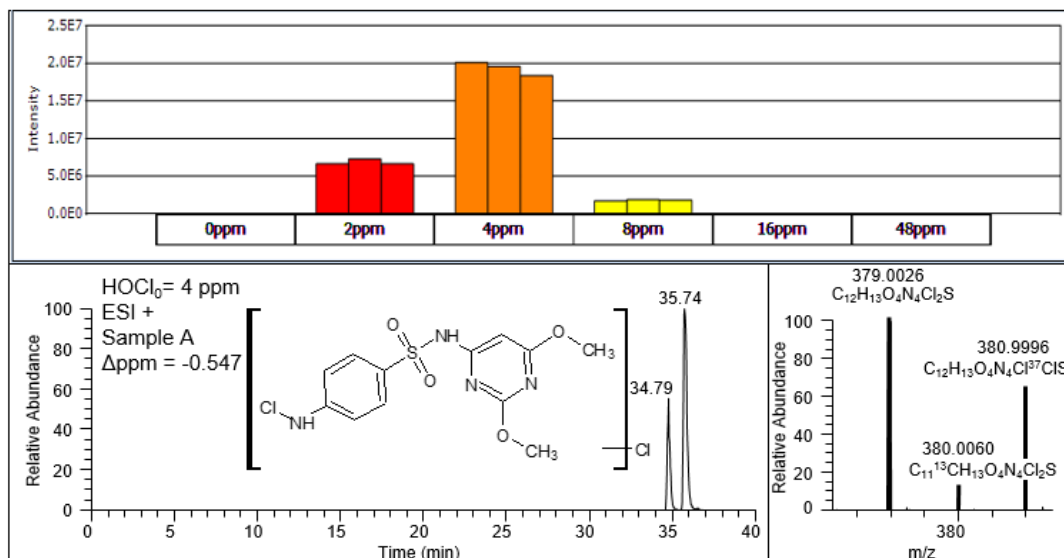


Figure D25: SDM379 had RTs of 34.79 and 35.74 min and MS spectra matched the exact mass of the proposed chemical ($m/z = 379.0026$ for MH^+ , $\Delta m = -0.547$ ppm) and the theoretical abundance (12%) of the ^{13}C monoisotopic mass and the theoretical abundance (70%) of the ^{37}Cl monoisotopic mass.

Sieve integrated intensity graphs suggested that SDM379 could also be a TP of SDM345. Being observed at two different RTs, SDM379 probably had two isomers. Given the first chlorine was substituted on the amino group of the aromatic amine portion of SDM as previously explained, the second chlorine substitution could take place at two different places. One possible isomer was N,N-dichlorinated SDM, given that previous researchers proposed that N,N-dichlorinated SMX could be formed in highly chlorinated solution.¹ Identification of structure of the other isomer was frustrated due to lack of MS-MS data.

2.4 SDM142

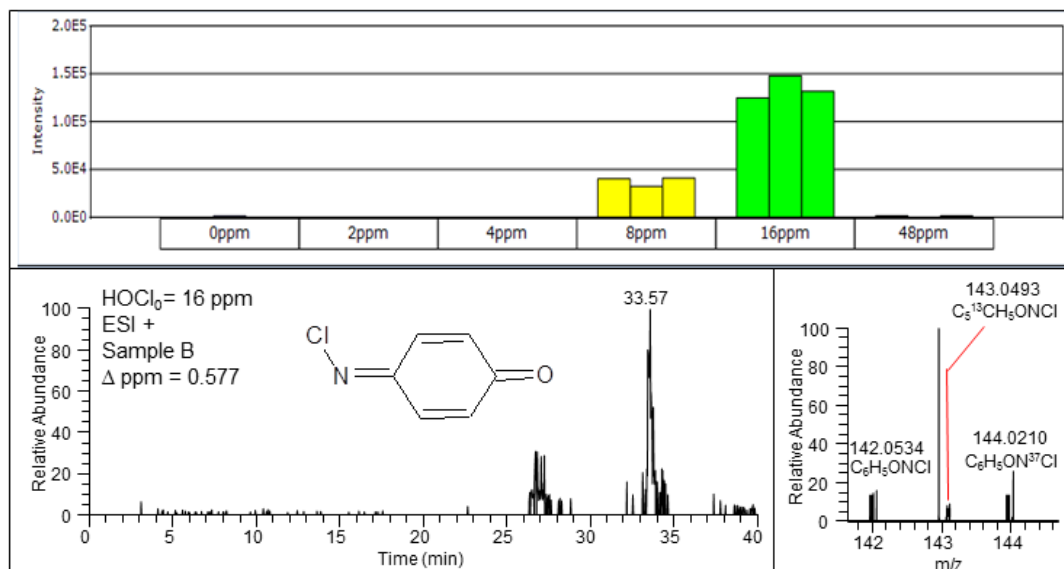


Figure D26: SDM142 had a RT of 33.57 min and MS spectra matched the exact mass of the proposed chemical ($m/z = 142.0055$ for MH^+ , $\Delta m = 0.577$ ppm) and the theoretical abundance (6%) of the ^{13}C monoisotopic mass and the theoretical abundance (40%) of the ^{37}Cl monoisotopic mass.

SDM142 was proposed to be exactly the same chemical as SMX142 that was formed in a similar reaction in SMX-FAC. Pathways and mechanisms of how SDM142 was formed was the same as those of how SMX142 was formed.

2.5 SDM174

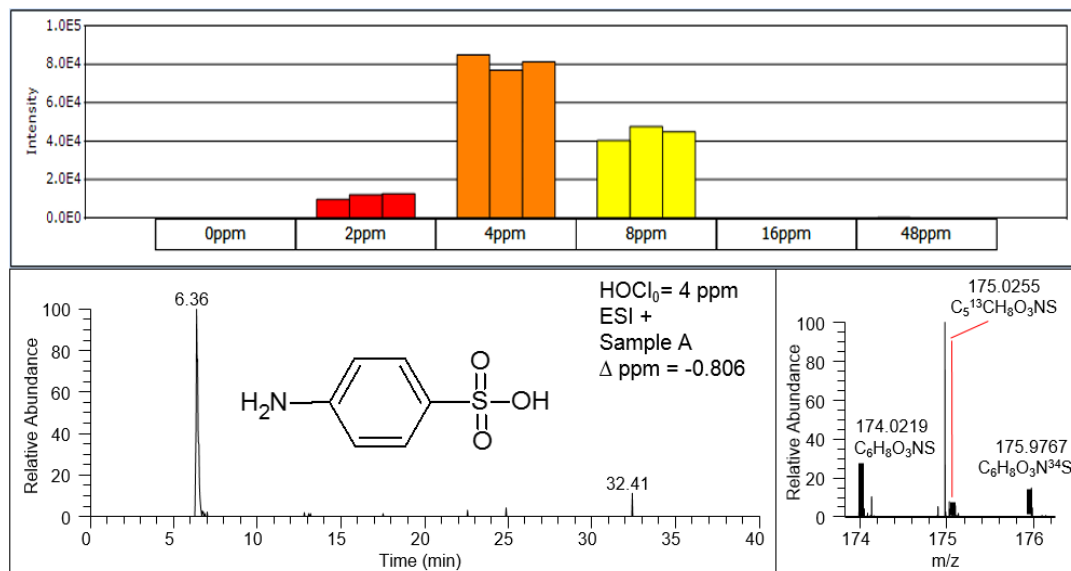


Figure D27: STZ174 had a RT of 6.36 min and MS spectra matched the exact mass of the proposed chemical ($m/z = 174.0219$ for MH^+ , $\Delta m = -0.806$ ppm) and the theoretical abundance (6%) of the ^{13}C monoisotopic mass.

SDM174 was proposed to be exactly the same chemical as STZ174. See description of STZ174 for details.

2.6 SDM156

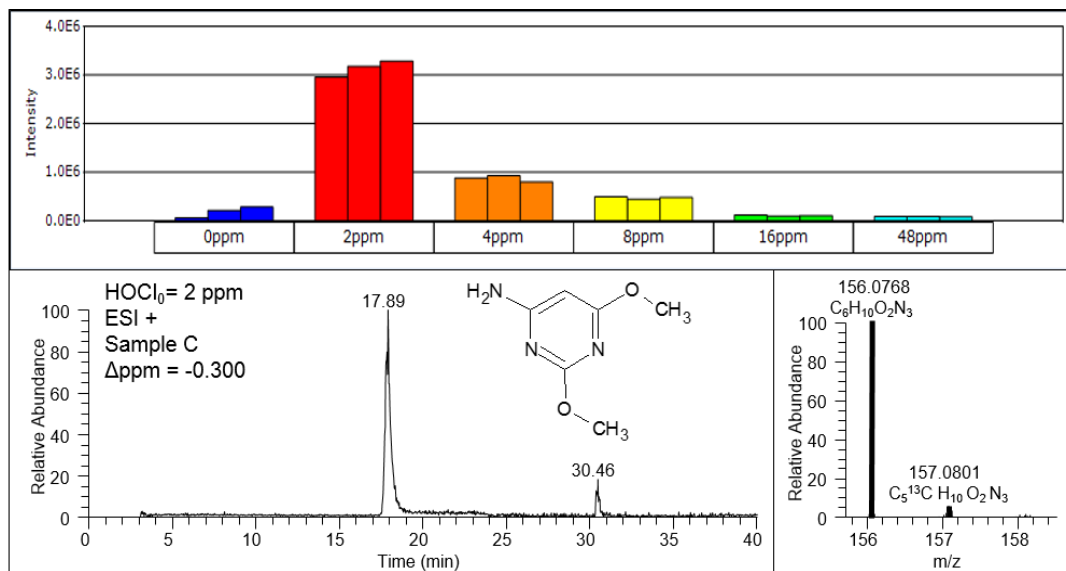


Figure D28: SDM156 had RTs of 17.89 and 31.66 min and MS spectra matched the exact mass of the proposed chemical ($m/z = 156.0768$ for MH^+ , $\Delta m = -0.300$ ppm) and the theoretical abundance (6%) of the ^{13}C monoisotopic mass.

SDM156 was detected at RT = 17.89 and 31.66, suggesting that there might be two isomers.

Only one structure was proposed according to our understanding of the reaction mechanisms at the time of writing this thesis. SDM156, shown in FigureD28, was formed upon hydrolysis of SDM when the S-N bond cleaved. The Sieve integrated intensity pattern was in compliance of our reasoning.

2.7 SDM190

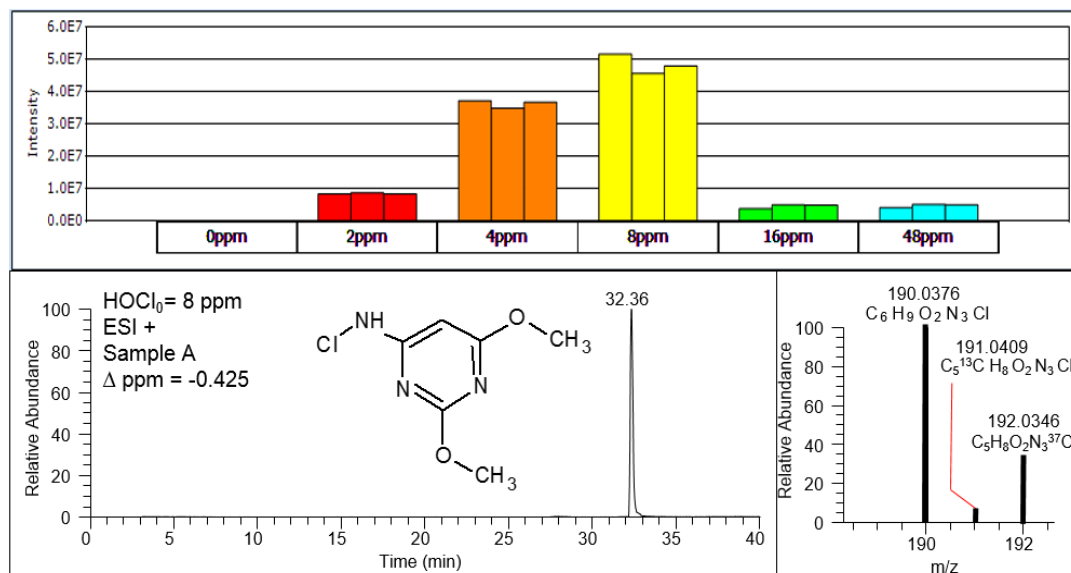


Figure D29: SDM190 had a RT of 32.36 min and MS spectra matched the exact mass of the proposed chemical ($m/z = 190.0376$ for MH^+ , $\Delta m = -0.425$ ppm) and the theoretical abundance (6%) of the ^{13}C monoisotopic mass and the theoretical abundance (35%) of the ^{37}Cl monoisotopic mass.

Sieve integrated intensity patterns indicated that SDM190 was possibly the TP of SDM156. The chlorination reaction possible happened at ammonia moiety, yet confirmation of the structure still needed MS-MS data.

2.8 SDM110

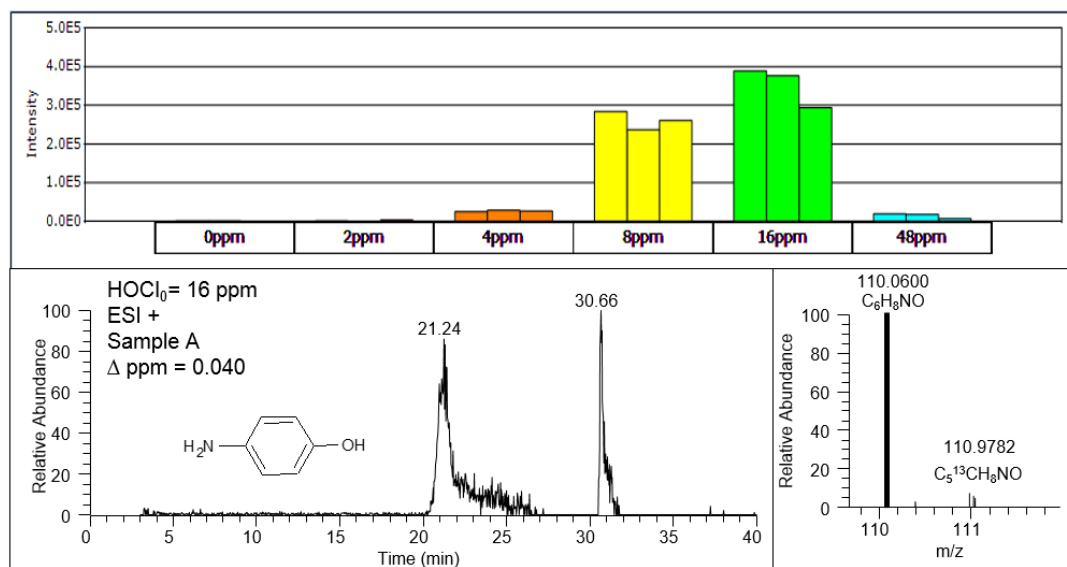


Figure D30: SDM110 had a RT of 30.66 min and MS spectra matched the exact mass of the proposed chemical ($m/z = 190.0376$ for MH^+ , $\Delta m = 0.040$ ppm) and the theoretical abundance (6%) of the ^{13}C monoisotopic mass.

2.9 SDM108

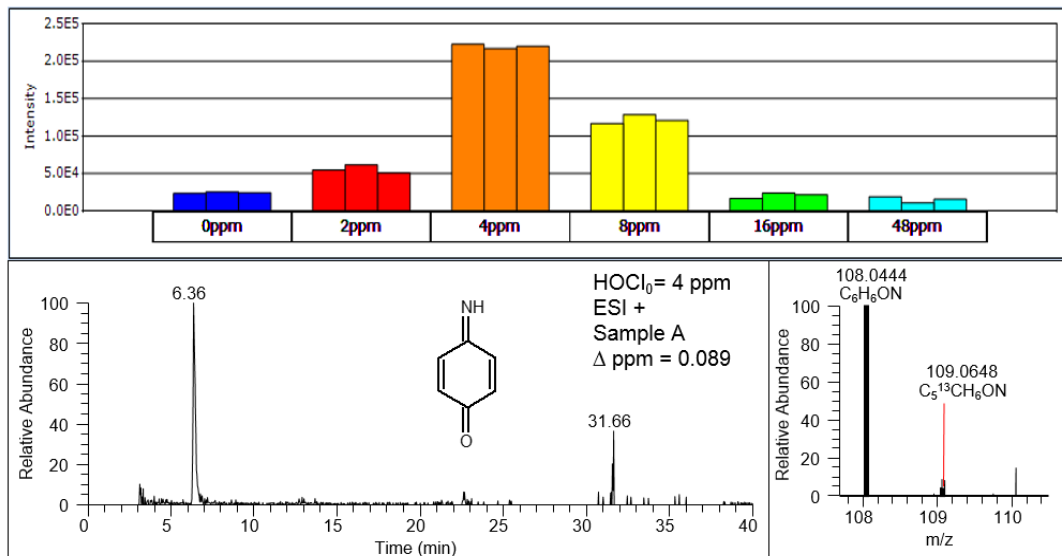


Figure D31: SDM108 had RTs of 6.36 and 31.66 min and MS spectra matched the exact mass of the proposed chemical ($m/z = 108.0444$ for MH^+ , $\Delta m = 0.089$ ppm) and the theoretical abundance (6%) of the ¹³C monoisotopic mass.

SDM108 was formed from SDM110. The reaction mechanism was the same as that when SMX110 formed SMX108. The sieve integrated intensity patterns were in compliance with the formation reasoning. Two peaks were observed on XIC. Only one structure was proposed at this time and it is shown in Figure D31.

2.10 SDM144

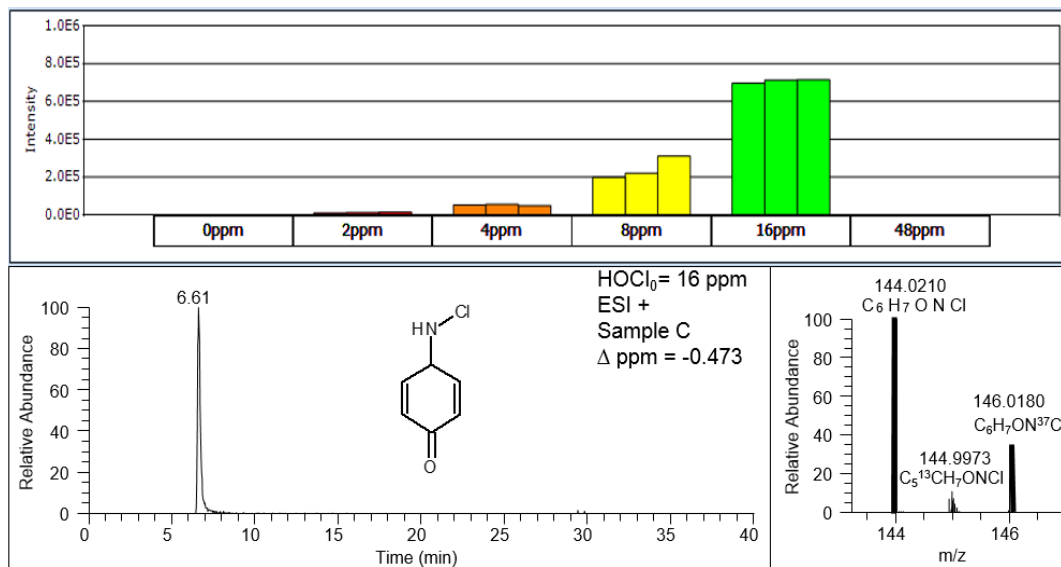


Figure D32: SDM144 had a RT of 6.61 min and MS spectra matched the exact mass of the proposed chemical ($m/z = 144.0210$ for MH^+ , $\Delta m = -0.473$ ppm) and the theoretical abundance (6%) of the ¹³C monoisotopic mass and the theoretical abundance (35%) of the ³⁷Cl monoisotopic mass.

SDM144 was the chlorinated product of SDM108. The mechanism of the chlorination reaction was the same as that leading to the formation of SMX144 from SMX108. In addition, the Sieve integrated intensity patterns were in support of the happening of the reaction.

2.11 SDM269

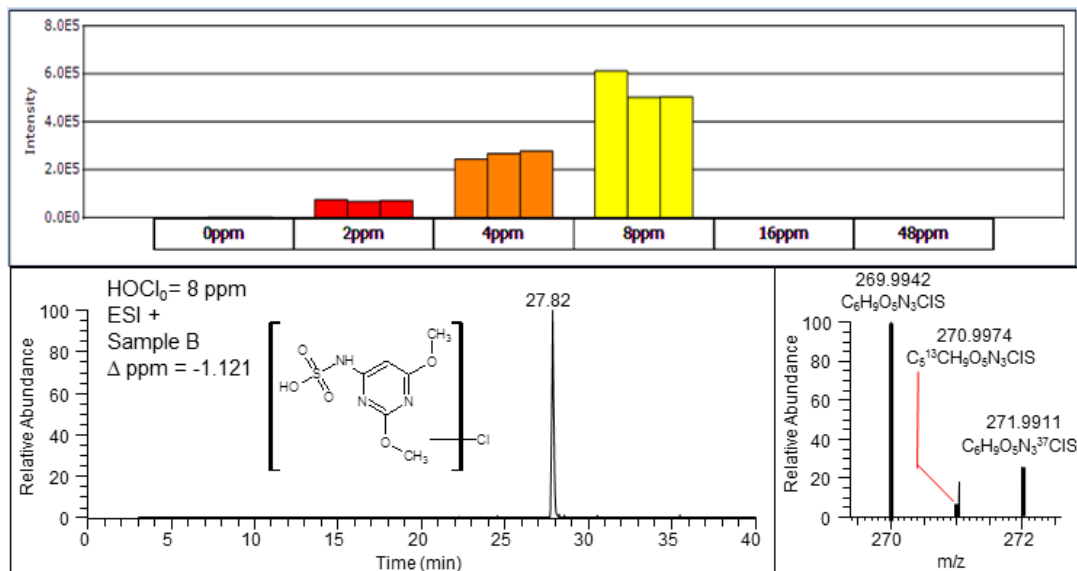


Figure D33: SDM269 had a RT of 27.82 min and MS spectra matched the exact mass of the proposed chemical ($m/z = 269.9942$ for MH^+ , $\Delta m = -1.464 \text{ ppm}$) and the theoretical abundance (6%) of the ^{13}C monoisotopic mass and the theoretical abundance (35%) of the ^{37}Cl monoisotopic mass.

SDM269 was the mono-chlorinated TP of c2, which resulted from a hydrolytic reaction of SDM when S-C bond cleaved.

2.12 SDM327

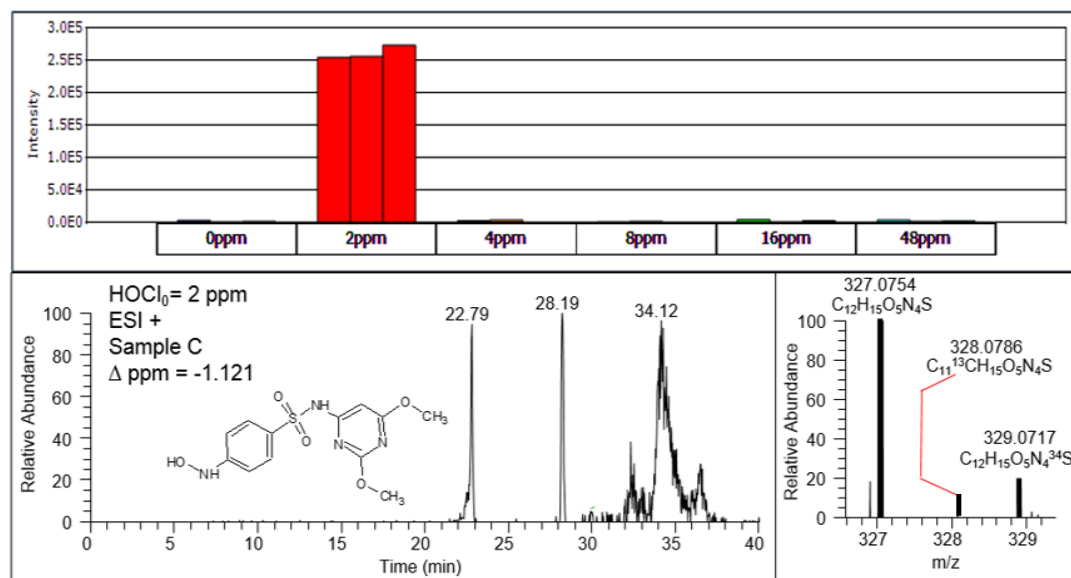


Figure D34: SDM327 had RTs of 22.79 and 28.29 min and MS spectra matched the exact mass of the proposed chemical ($m/z = 327.0754$ for MH^+ , $\Delta m = -1.121$ ppm) and the theoretical abundance (12%) of the ^{13}C monoisotopic mass the theoretical abundance (2%) of the ^{34}S monoisotopic mass.

2.13 SDM330

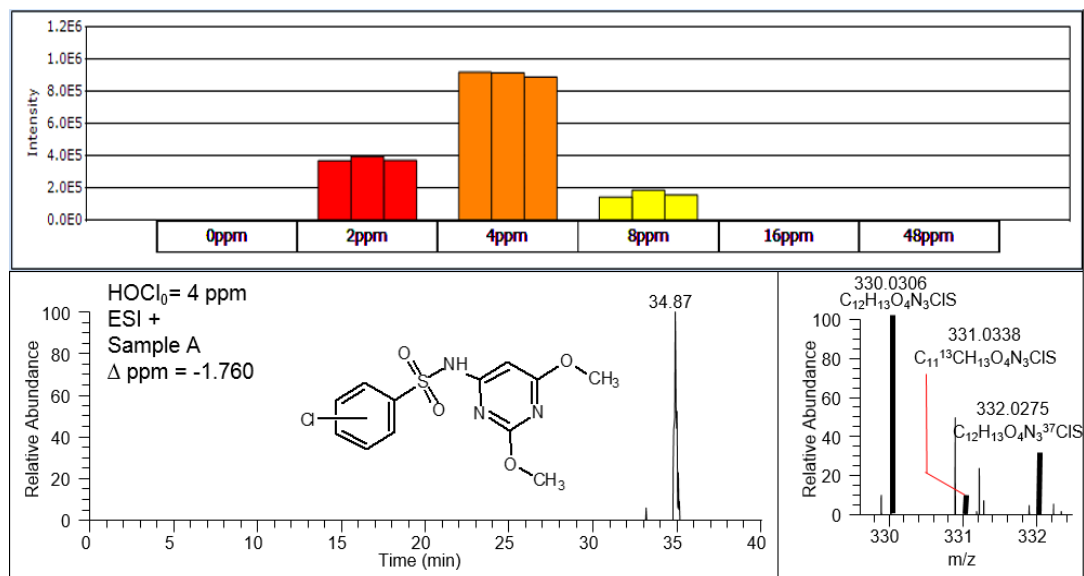


Figure D35: SDM330 had a RT of 34.87 min and MS spectra matched the exact mass of the proposed chemical ($m/z = 330.0304$ for MH^+ , $\Delta m = -1.760$ ppm) and the theoretical abundance (12%) of the ^{13}C monoisotopic mass and the theoretical abundance (35%) of the ^{37}Cl monoisotopic mass.

2.14 SDM247

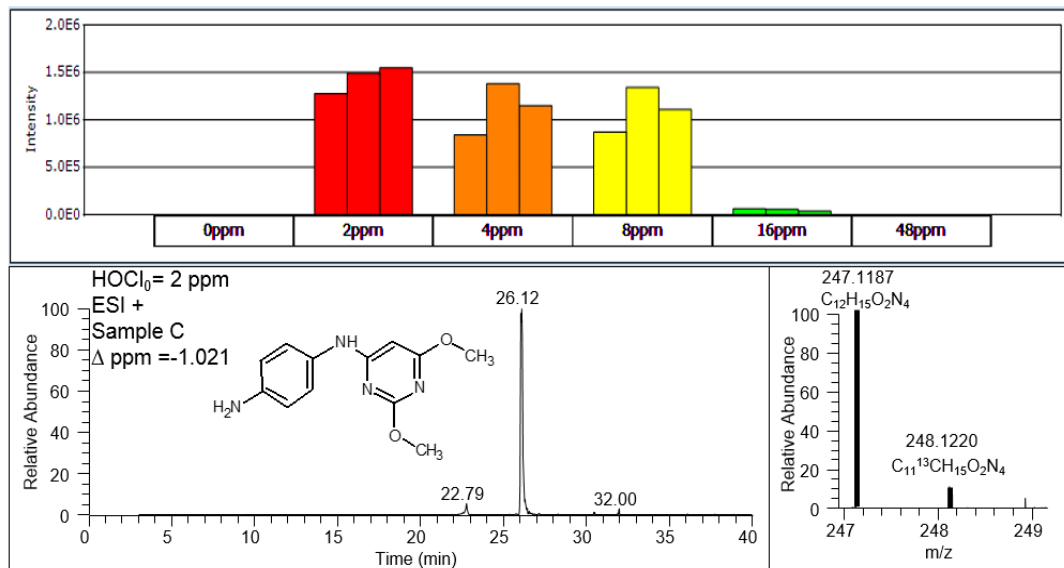


Figure D36: SDM247 had a RT of 26.12 min and MS spectra matched the exact mass of the proposed chemical (m/z = 247.1187 for MH^+ , Δm = -1.021 ppm) and the theoretical abundance (12%) of the ^{13}C monoisotopic mass.

SDM247 was TP of SMX formed from the SO_2 extrusion reactions. The mechanisms were the same as those leading to the formation of SMX190, which was a chemical formed when SMX lost the SO_2 group.

2.15 SDM281

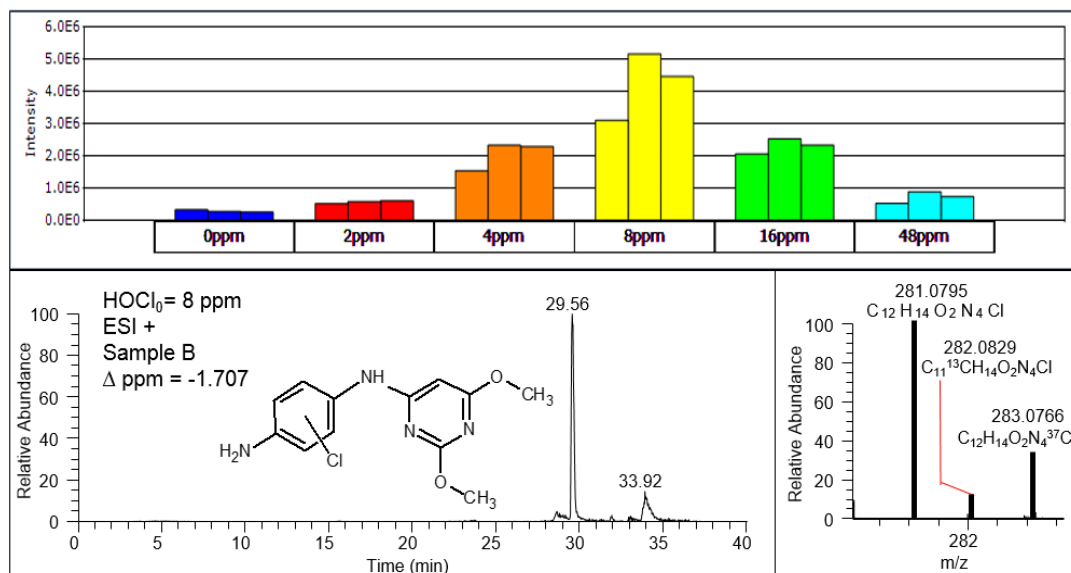


Figure D37: SDM281 had a RT of 29.56 min and MS spectra matched the exact mass of the proposed chemical ($m/z = 281.0795$ for MH^+ , $\Delta m = -1.707$ ppm) and the theoretical abundance (12%) of the ^{13}C monoisotopic mass and the theoretical abundance (35%) of the ^{37}Cl monoisotopic mass.

SDM281 was the mono-chlorinated TP of SDM247. The sieve integrated intensity patterns were in compliance with the proposed reaction. Similar to chlorination of SMX and SDM, the chlorine substitution reaction of SDM247 probably happened at the amino group in the aromatic amine group as well. Correspondingly, the proposed structure was a N-chlorinated product from the chlorinolysis reaction.

2.16 SDM248

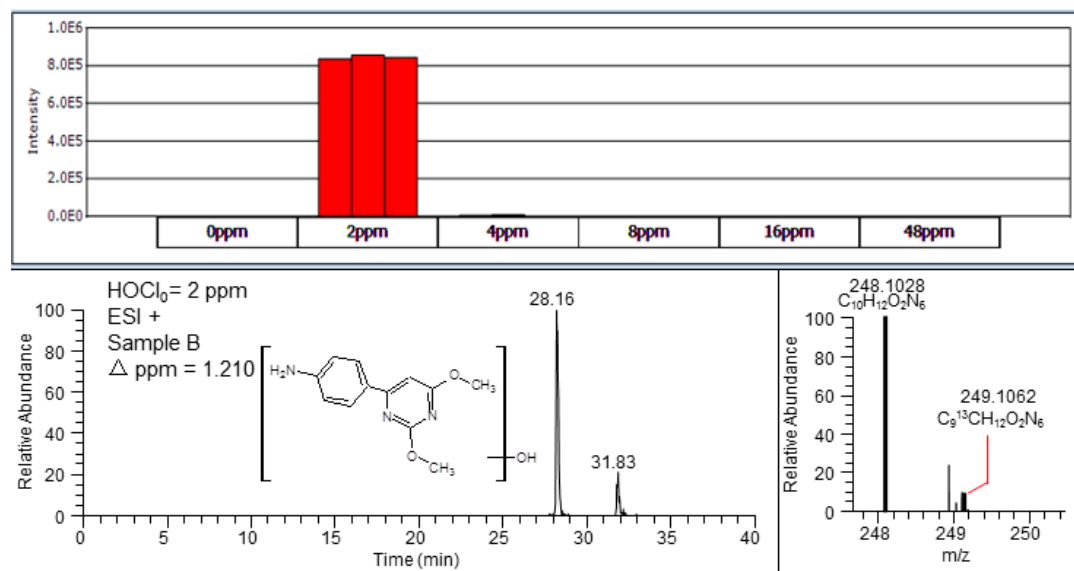


Figure D38: SDM248 had RTs of 28.16 and 31.83 min and MS spectra matched the exact mass of the proposed chemical ($m/z = 248.1028$ for MH^+ , $\Delta m = 1.210$ ppm) and the theoretical abundance (10%) of the ^{13}C monoisotopic mass.

2.17 SDM282

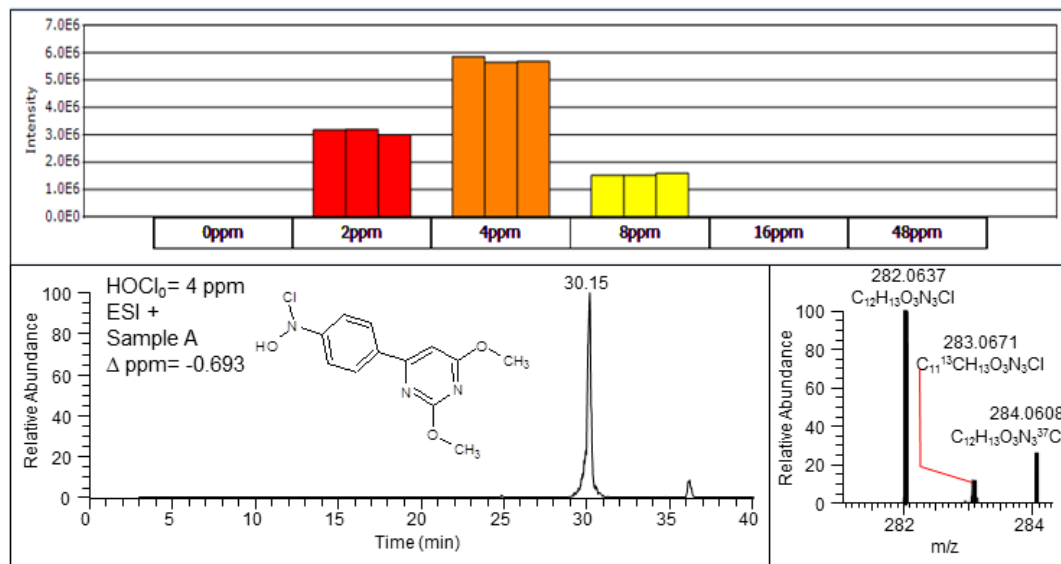


Figure D39: SDM282 had a RT of 30.15 min and MS spectra matched the exact mass of the proposed chemical ($m/z = 282.0637$ for MH^+ , $\Delta m = -0.693$ ppm) and the theoretical abundance (12%) of the ^{13}C monoisotopic mass and the ^{37}Cl monoisotopic mass ($m/z = 284.0608$ for MH^+).

SDM282 was the TP of SDM281 after a successive reaction of losing ammonia group between the aromatic amine and the heterocyclic ring and a hydroxylation reaction. The Sieve patterns were in support of the sequence of the reaction. Due to lack of MS-MS data, the position where hydroxylation happened could not be determined for the time-being.

2.18 SDM410

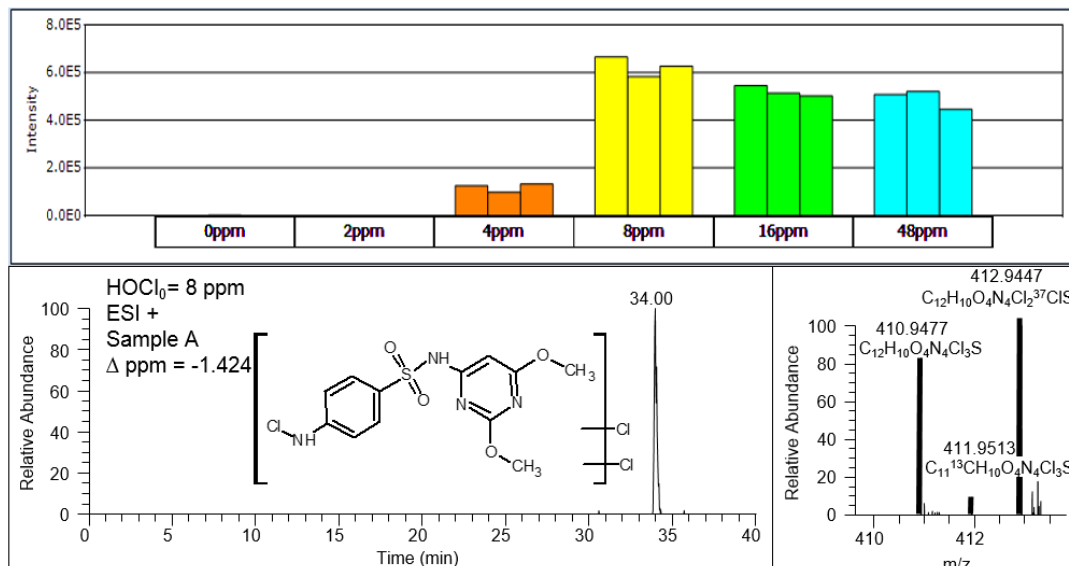


Figure D40: SDM410 had a RT of 34.00 min and MS spectra matched the exact mass of the proposed chemical ($m/z=410.9477$ for MH^+ , $\Delta m = -1.424$ ppm) and the theoretical abundance (12%) of the ^{13}C monoisotopic mass and the theoretical abundance (105%) of the ^{37}Cl monoisotopic mass.

Sieve integrated intensity patterns of SDM410 and SDM281 suggested that SDM410 could be formed from SDM281. According to abundance of the ^{37}Cl monoisotopic mass, SDM410 was formed when SDM281 was substituted with 2 more chlorine atoms.

3.1 STZ289

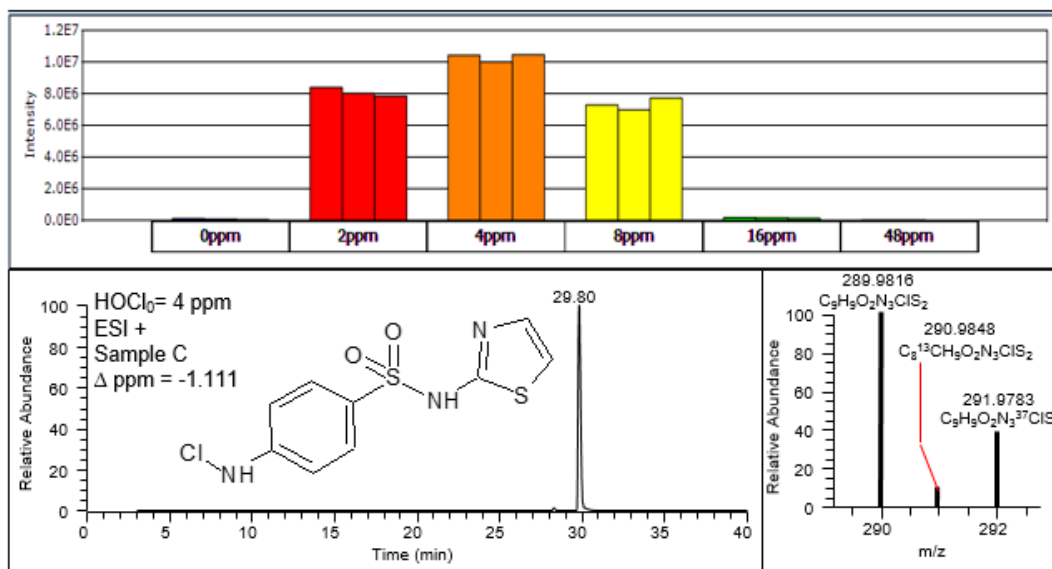


Figure D41: STZ289 had a RT of 29.80 min and MS spectra matched the exact mass of the proposed chemical ($m/z = 288.9816$ for MH^+ , $\Delta m = -1.111$ ppm) and the theoretical abundance (9%) of the ^{13}C monoisotopic mass and the theoretical abundance (40%) of the ^{37}Cl monoisotopic mass.

STZ289 was the mono-N-chlorinated TP of STZ. The reaction mechanism was the same as those that led to the formation of mono-N-chlorinated SMX and mono-N-chlorinated SDM. The sieve integrated intensity graph indicated that STZ289 was mainly formed in under-chlorinated reactions, suggesting that STZ289 was possibly one of the TPs that were formed directly from STZ.

3.2 STZ305

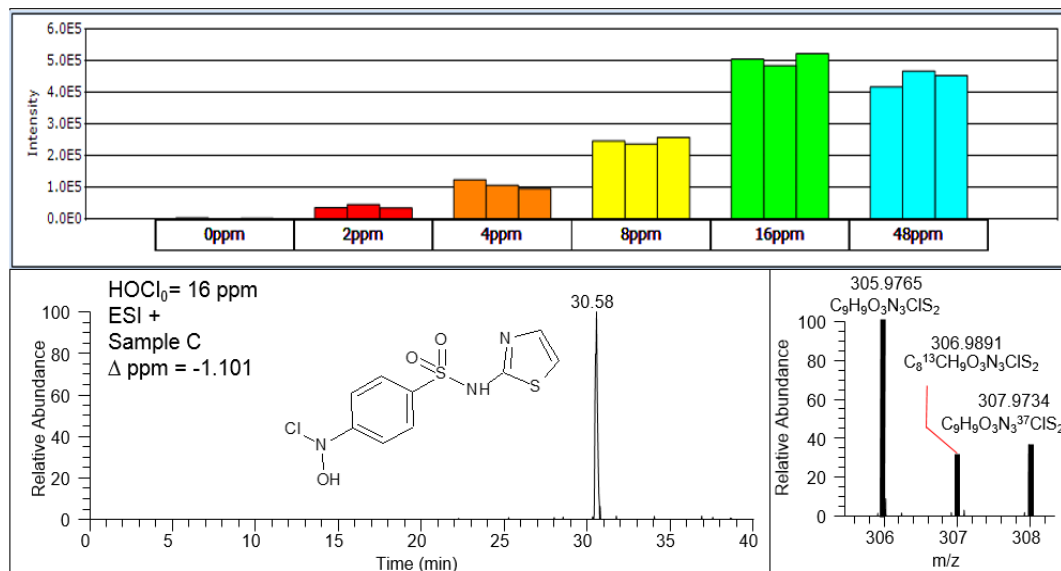


Figure D42: STZ305 had a RT of 30.58 min and MS spectra matched the exact mass of the proposed chemical ($m/z = 305.9765$ for MH^+ , $\Delta m = -1.101 \text{ ppm}$) and the theoretical abundance (9%) of the ^{13}C monoisotopic mass and the theoretical abundance (40%) of the ^{37}Cl monoisotopic mass.

STZ305 resulted from hydroxylation reactions of STZ289. The position where hydroxylation took place remain unknown due to lack of MS-MS data. Having the $-\text{OH}$ moiety substituting the hydrogen atom on the ammonia moiety of the aromatic amine was one possible structure.

3.3 STZ144

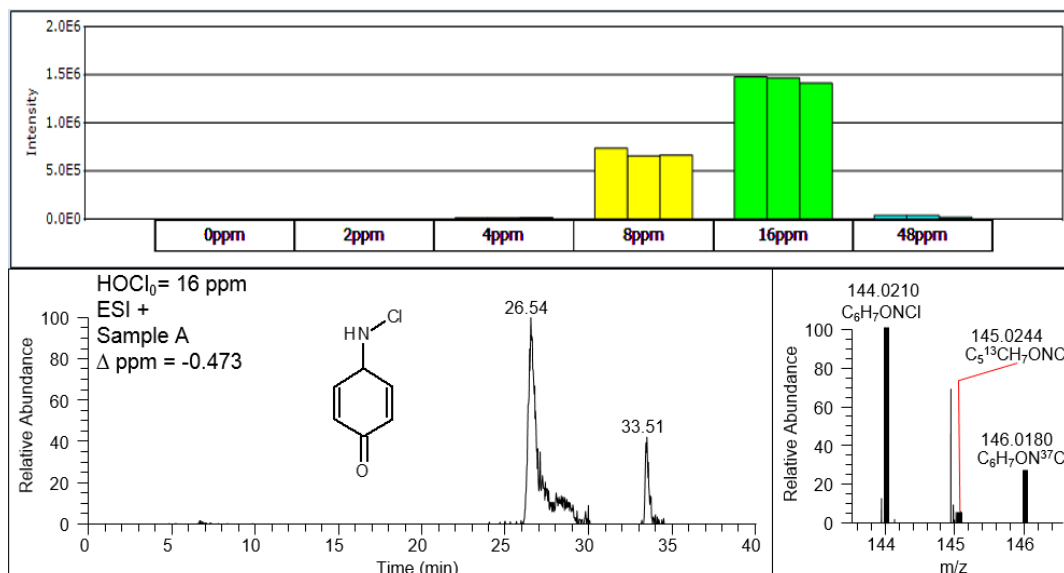


Figure D43: STZ144 had RTs of 26.54 and 33.51 min and MS spectra matched the exact mass of the proposed chemical ($m/z = 144.0210$ for MH^+ , $\Delta m = -0.473$ ppm) and the theoretical abundance (6%) of the ^{13}C monoisotopic mass and the theoretical abundance (35%) of the ^{37}Cl monoisotopic mass.

STZ144 was a mono-chlorinated TP, possibly formed from an intermediate, 4-aminophenol, which was resulted from hydroxylation reactions of aniline. Aniline was proposed to be formed from hydrolytic reaction of STZ when S-C bond cleaved. Formation of aniline from 4-aminophenol was previously discussed in SMX-FAC reactions.

3.4 STZ177

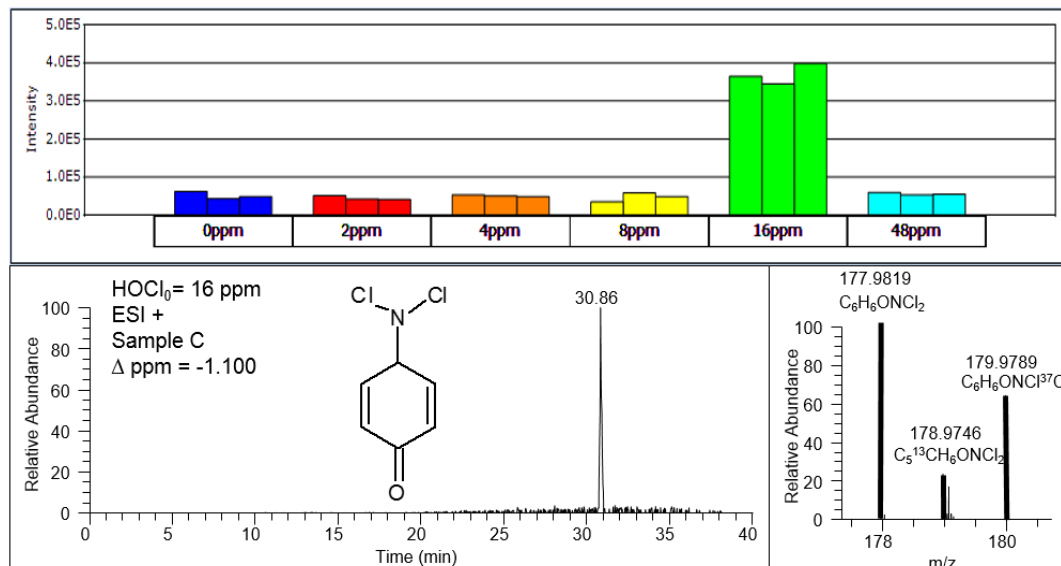


Figure D44: STZ177 had RTs of 30.86 min and MS spectra matched the exact mass of the proposed chemical ($m/z = 177.9819$ for MH^+ , $\Delta m = -1.100$ ppm) and the theoretical abundance (6%) of the ^{13}C monoisotopic mass and the theoretical abundance (70%) of the ^{37}Cl monoisotopic mass.

STZ177 was a dichlorinated product judging from the abundance of the ^{37}Cl monoisotopic mass.

The sieve patterns suggested that STZ177 could possibly be formed from STZ144.

3.5 STZ174

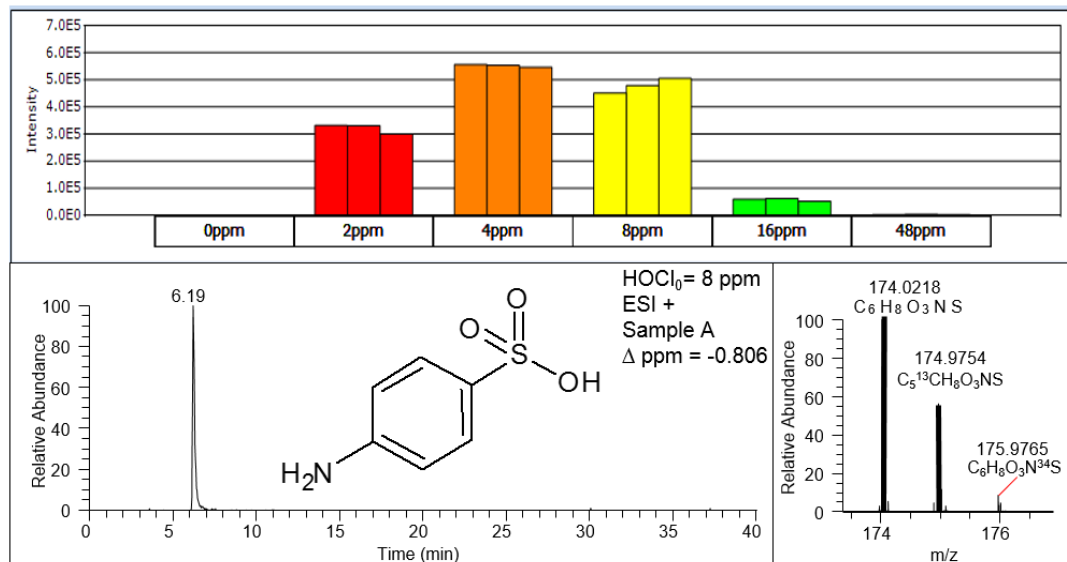


Figure D45: STZ174 had a RT of 6.19 min and MS spectra matched the exact mass of the proposed chemical ($m/z = 174.0218$ for MH^+ , $\Delta m = -0.806$ ppm) and the theoretical abundance (6%) of the ¹³C monoisotopic mass.

STZ174 was a TP resulted from hydrolytic reaction of STZ when the S-N bond cleaved.

Cleavage of S-N was previously discussed in SMX-FAC and STZ-FAC reactions.

3.6 STZ101

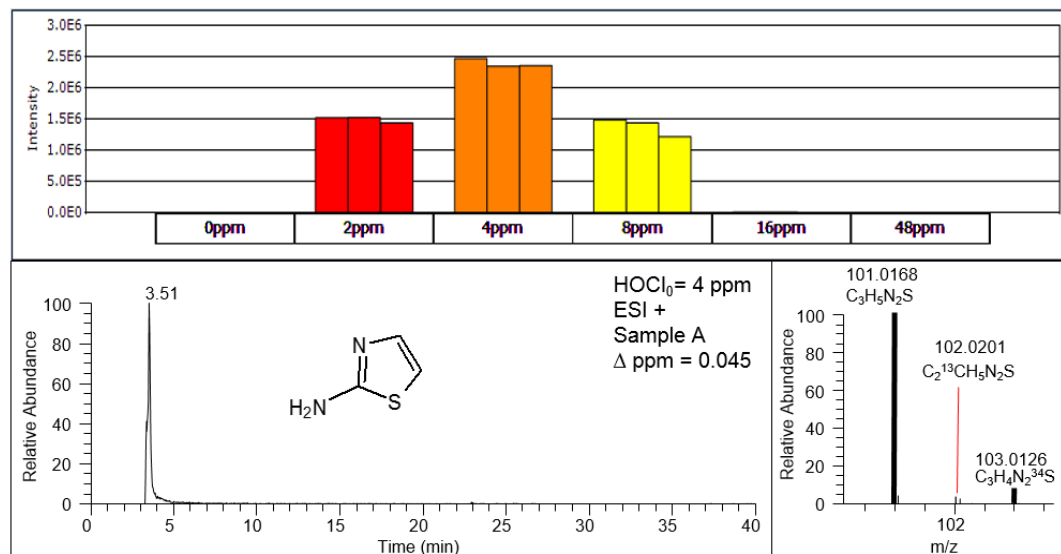


Figure D46: STZ101 had a RT of 3.51 min and MS spectra matched the exact mass of the proposed chemical ($m/z = 101.0168$ for MH^+ , $\Delta m = -0.045$ ppm) and the theoretical abundance (3%) of the ^{13}C monoisotopic mass and the theoretical abundance (2%) of the ^{34}S monoisotopic mass.

STZ101 was possible formed along with the formation of STZ174 when the S-N bond cleaved and hydrolytic reactions took place with STZ. The sieve integrated intensity graphs of STZ101 and STZ174 were similar to each other, confirming the happening of the hydrolytic reaction.

3.7 STZ134

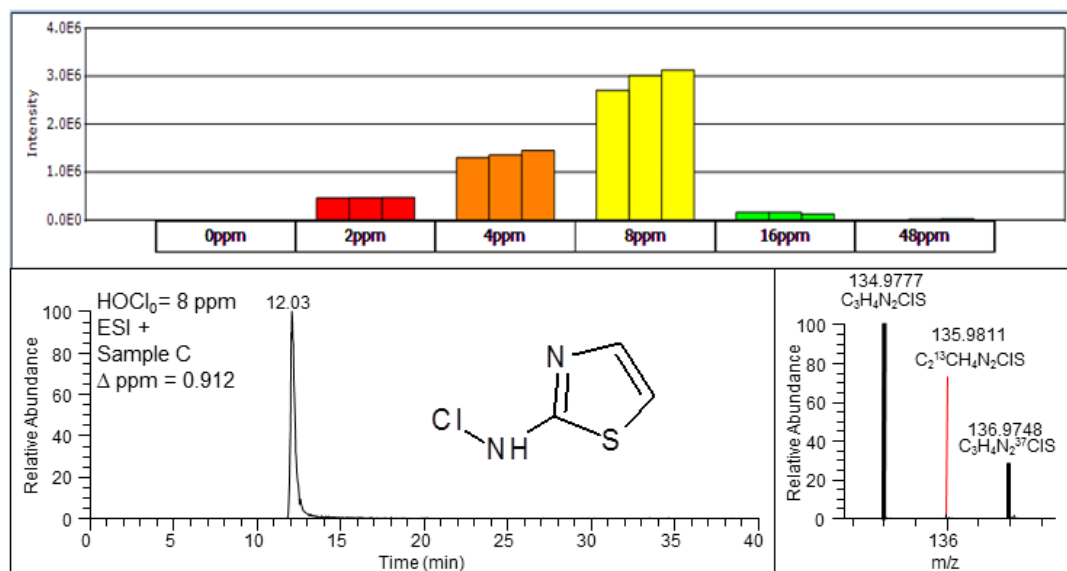


Figure D47: STZ134 had a RT of 12.03 min and MS spectra matched the exact mass of the proposed chemical ($m/z = 134.9777$ for MH^+ , $\Delta m = 0.912 \text{ ppm}$) and the theoretical abundance (3%) of the ^{13}C monoisotopic mass and the theoretical abundance (35%) of the ^{37}Cl monoisotopic mass.

3.8 STZ272

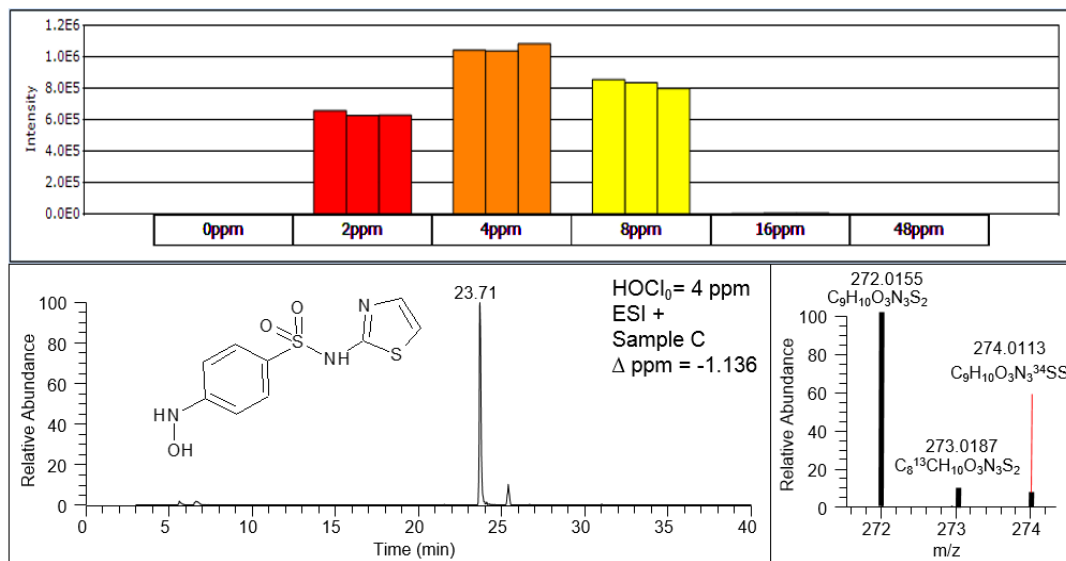


Figure D48: STZ272 had a RT of 23.71 min and MS spectra matched the exact mass of the proposed chemical ($m/z = 272.0155$ for MH^+ , $\Delta m = -1.136$ ppm) and the theoretical abundance (9%) of the ^{13}C monoisotopic mass and the theoretical abundance (4%) of the ^{34}S monoisotopic mass.

STZ272 was formed as a result of STZ undergoing hydroxylation reactions. Position of where hydroxylation reaction took place could not be confirmed yet due to lack of MS-MS data.

However, for the same reasons as we discussed previously why hydroxylation could take place at the ammonia moiety on the aromatic amine portion of SMX and SDM, we proposed that it would be the same case with STZ.

3.9 STZ351

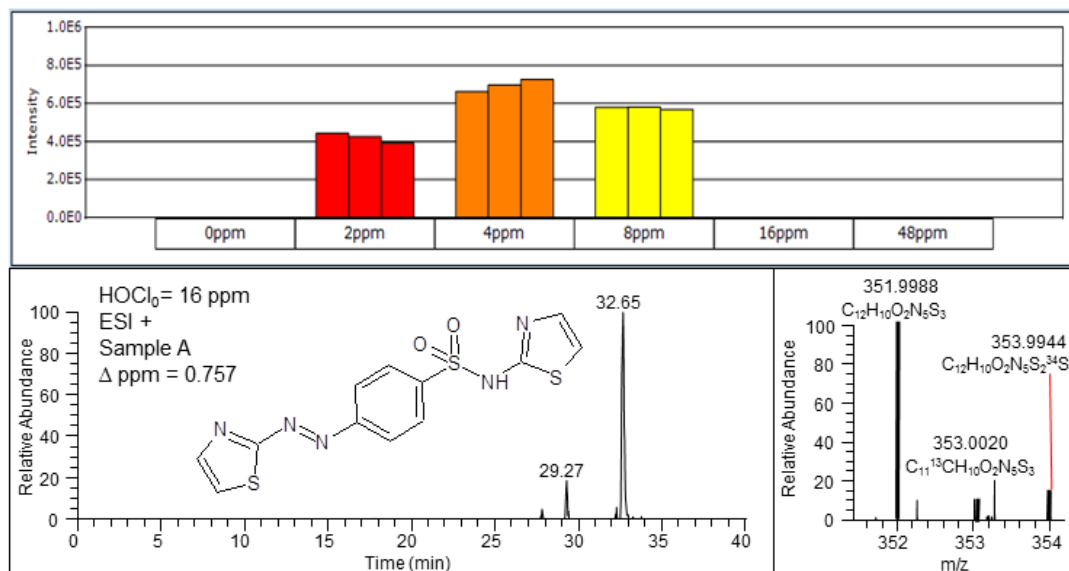


Figure D49: STZ351 had a RT of 32.65 min and MS spectra matched the exact mass of the proposed chemical ($m/z = 351.9988$ for MH^+ , $\Delta m = 0.757$ ppm) and the theoretical abundance (12%) of the ¹³C monoisotopic mass and the theoretical abundance (6%) of the ³⁴S monoisotopic mass.

STZ351 was formed in a coupling reaction of STZ.

3.10 STZ347

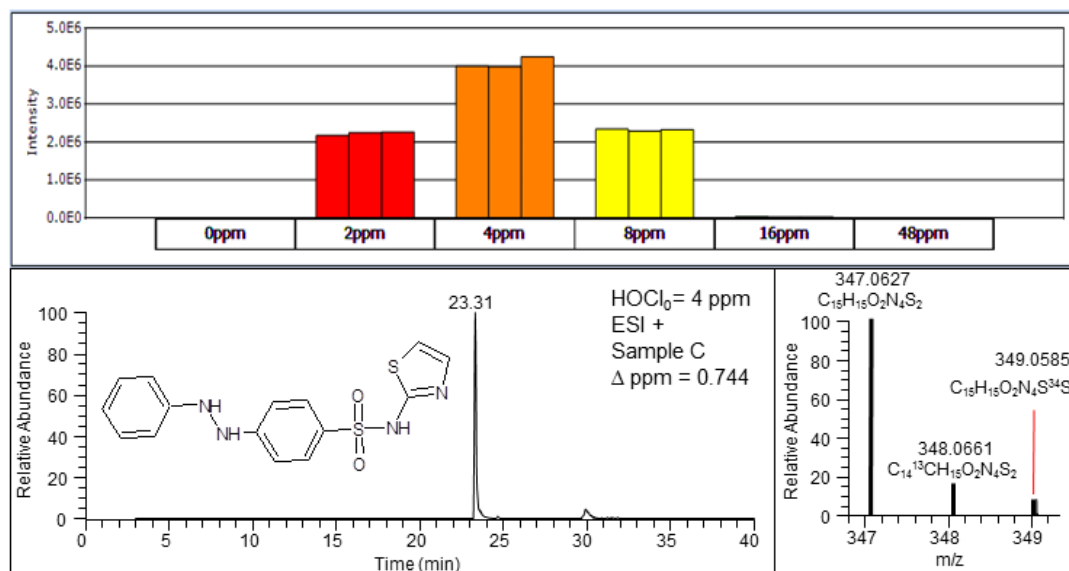


Figure D50: STZ347 had a RT of 23.31 min and MS spectra matched the exact mass of the proposed chemical ($m/z = 347.0627$ for MH^+ , $\Delta m = 0.744 \text{ ppm}$) and the theoretical abundance (15%) of the ^{13}C monoisotopic mass and the theoretical abundance (4%) of the ^{34}S monoisotopic mass.

3.11 STZ381

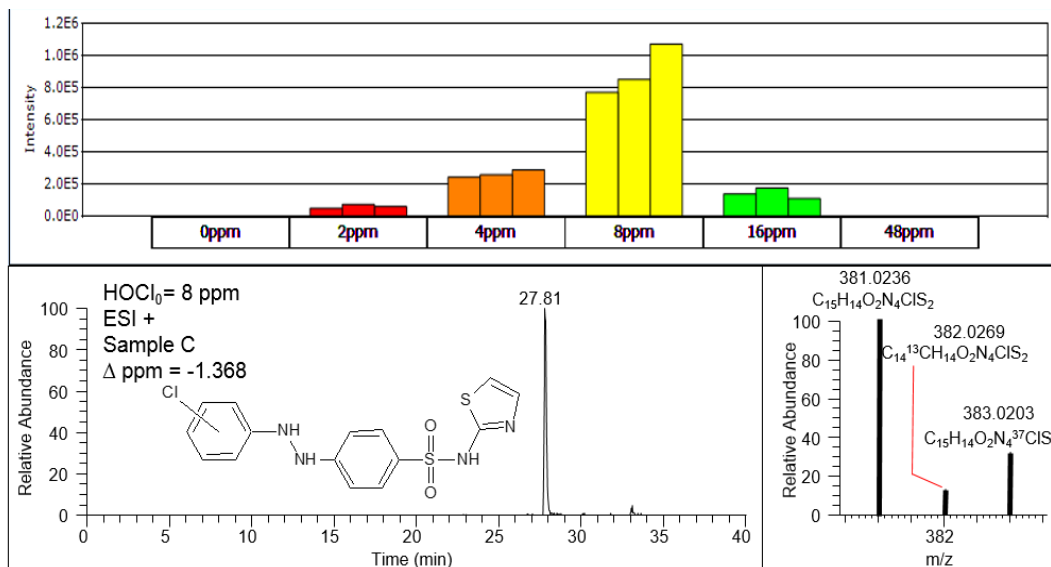


Figure D51: STZ381 had a RT of 27.81 min and MS spectra matched the exact mass of the proposed chemical ($m/z = 381.0236$ for MH^+ , $\Delta m = -1.368$ ppm) and the theoretical abundance (15%) of the ^{13}C monoisotopic mass and the theoretical abundance (35%) of the ^{37}Cl monoisotopic mass.

STZ381 was the mono-chlorinated TP of STZ347. The position where chlorine substitution happened could not be fully confirmed yet, but according to aromatic substitution rules, the chlorine was possibly attached to the *ortho*- or *para*- position of the benzene ring on the aniline part of STZ347.¹⁶

3.12 STZ379

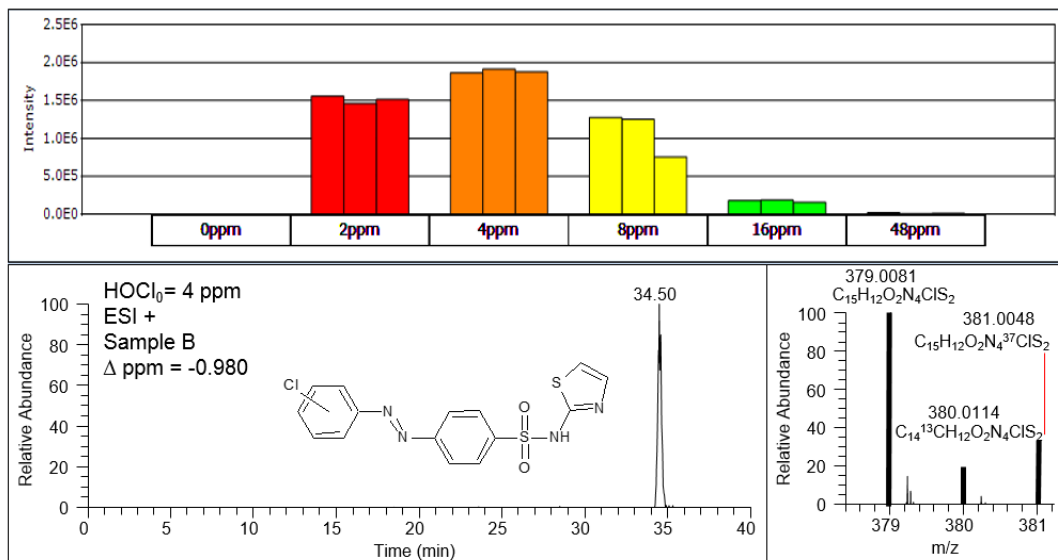


Figure D52: STZ379 had a RT of 34.50 min and MS spectra matched the exact mass of the proposed chemical ($m/z = 379.0081$ for MH^+ , $\Delta m = -0.980$ ppm) and the theoretical abundance (15%) of the ^{13}C monoisotopic mass and the theoretical abundance (35%) of the ^{37}Cl monoisotopic mass.

STZ379 could be TP formed when STZ381 was further oxidized and lost two hydrogen atoms.

Possibly, there were STZ379 formed in this pathway; though the major of STZ379 was formed through a coupling reaction when the nitrogen moieties of a chlorinated aniline and the nitrogen on the aromatic amine portion of STZ combine together. The reaction mechanisms were similar to that leading to the formation of STZ351.

3.13 STZ216

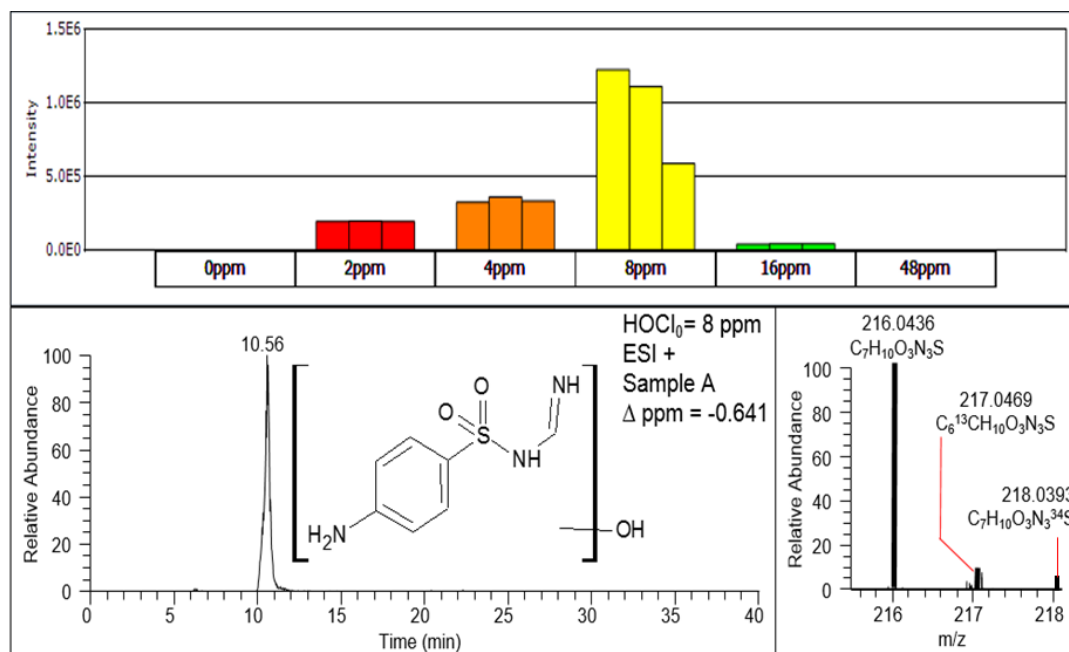


Figure D53: STZ347 had a RT of 19.56 min and MS spectra matched the exact mass of the proposed chemical ($m/z = 216.0436$ for MH^+ , $\Delta m = -0.641$ ppm) and the theoretical abundance (7%) of the ^{13}C monoisotopic mass and the theoretical abundance (2%) of the ^{34}S monoisotopic mass.

3.14 STZ192

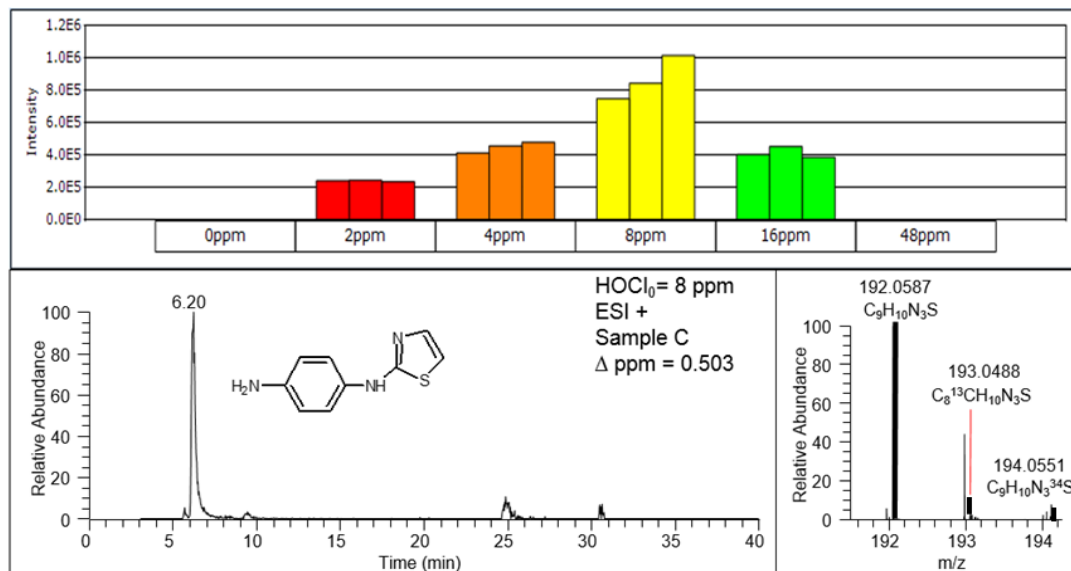


Figure D54: STZ192 had a RT of 6.20 min and MS spectra matched the exact mass of the proposed chemical ($m/z = 192.0587$ for MH^+ , $\Delta m = 0.503 \text{ ppm}$) and the theoretical abundance (9%) of the ¹³C monoisotopic mass and the theoretical abundance (2%) of the ³⁴S monoisotopic mass.

STZ192 was the TP formed when STZ went through a SO₂ extrusion reaction. The mechanisms behind this reaction was the same as those in reactions when SMX and STZ lost the SO₂ group as previously discussed.

3.15 STZ193

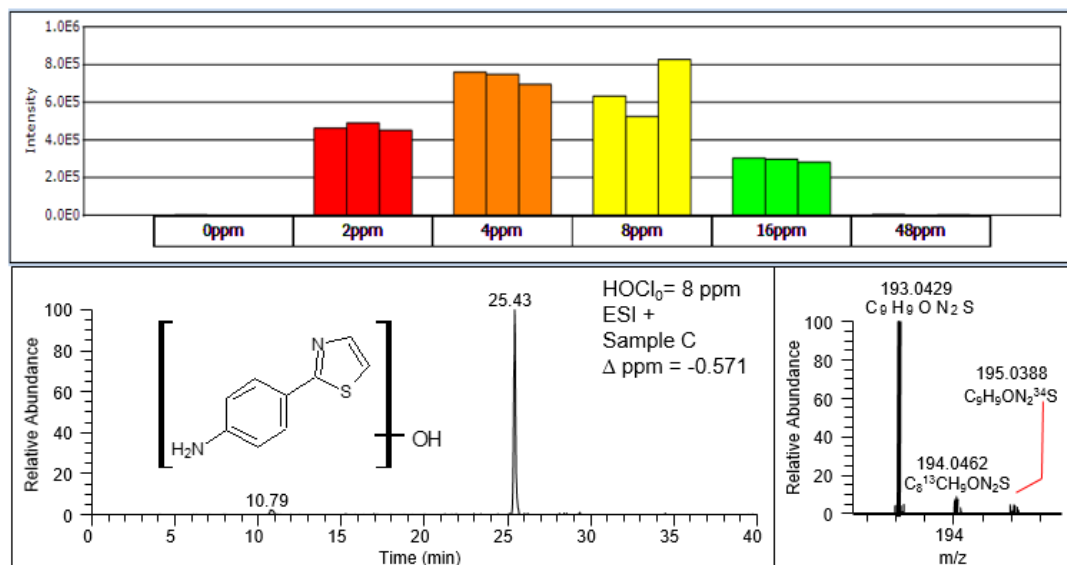


Figure D55: STZ193 had a RT of 25.43 min and MS spectra matched the exact mass of the proposed chemical ($m/z = 193.0429$ for MH^+ , $\Delta m = -0.571$ ppm) and the theoretical abundance (9%) of the ^{13}C monoisotopic mass and the theoretical abundance (12%) of the ^{34}S monoisotopic mass.

Successive reactions including losing ammonia moiety and gaining $-OH$ group through hydroxylation took place with STZ192, leading to the formation of STZ193. The reaction pathway was very similar with that in SDM-FAC reactions, when SDM247 formed SDM248, and when SDM281 formed SDM282.

3.16 STZ224

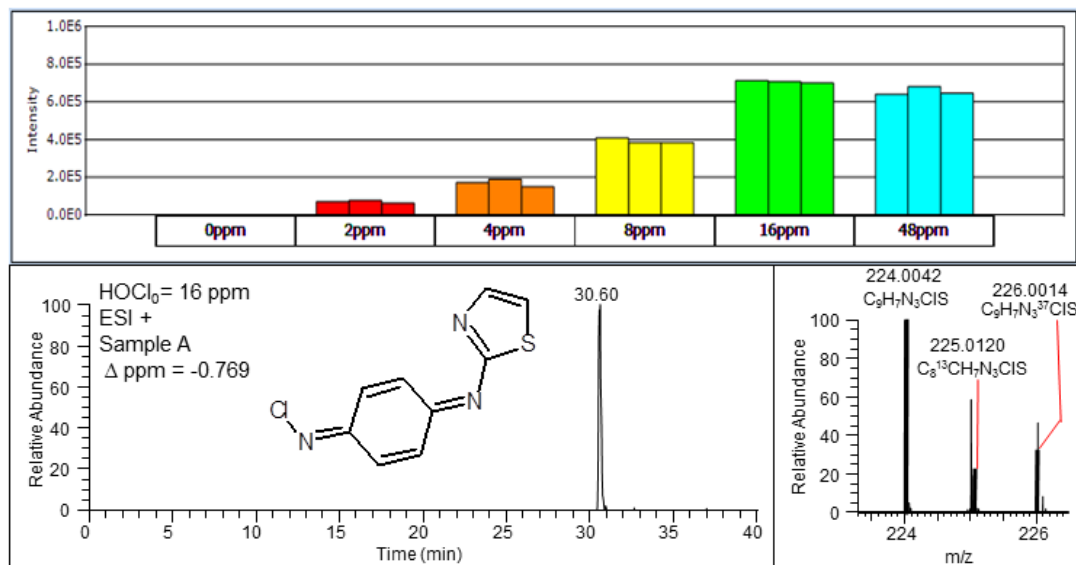


Figure D56: STZ224 had a RT of 30.60 min and MS spectra matched the exact mass of the proposed chemical ($m/z = 224.0042$ for MH^+ , $\Delta m = -0.769$ ppm) and the theoretical abundance (9%) of the ^{13}C monoisotopic mass and the theoretical abundance (35%) of the ^{37}Cl monoisotopic mass.

Formation of STZ224 was similar to formation of SMX222. See description in SMX-FAC for the reaction mechanisms.

REFERENCE

1. Dodd, M. C., Transformation of the Antibacterial Agent Sulfamethoxazole in Reactions with Chlorine: Kinetics, Mechanisms, and Pathways. *Environ Sci Technol* **2004**.
2. Gao, S.; Zhao, Z.; Xu, Y.; Tian, J.; Qi, H.; Lin, W.; Cui, F., Oxidation of sulfamethoxazole (SMX) by chlorine, ozone and permanganate--a comparative study. *J Hazard Mater* **2014**, 274, 258-69.
3. Uetrecht, J. P.; Shear, N. H.; Zahid, N., N-CHLORINATION OF SULFAMETHOXAZOLE AND DAPSONE BY THE MYELOPEROXIDASE SYSTEM. *Drug Metab. Dispos.* **1993**, 21, (5), 830-834.
4. Gassman, P. G.; Campbell, G. A.; Frederick, R. C., Chemistry of nitrenium ions. XXI. Nucleophilic aromatic substitution of anilines via aryl nitrenium ions (anilenium ions). *Journal of the American Chemical Society* **1972**, 94, (11), 3884-3891.
5. Haberfield, P.; Paul, D., The Chlorination of Anilines. Proof of the Existence of an N-Chloro Intermediate. *Journal of the American Chemical Society* **1965**, 87, (23), 5502-5502.
6. Ricken, B.; Fellmann, O.; Kohler, H.-P. E.; Schäffer, A.; Corvini, P. F.-X.; Kolvenbach, B. A., Degradation of sulfonamide antibiotics by Microbacterium sp. strain BR1 – elucidating the downstream pathway. *New Biotechnology* **2015**, (0).
7. Nasuhoglu, D.; Yargeau, V.; Berk, D., Photo-removal of sulfamethoxazole (SMX) by photolytic and photocatalytic processes in a batch reactor under UV-C radiation ($\lambda_{\text{max}}=254\text{ nm}$). *J. Hazard. Mater.* **2011**, 186, (1), 67-75.
8. Hu, L. H.; Flanders, P. M.; Miller, P. L.; Strathmann, T. J., Oxidation of sulfamethoxazole and related antimicrobial agents by TiO₂ photocatalysis. *Water Research* **2007**, 41, (12), 2612-2626.
9. Trovo, A. G.; Nogueira, R. F. P.; Aguera, A.; Sirtori, C.; Fernandez-Alba, A. R., Photodegradation of sulfamethoxazole in various aqueous media: Persistence, toxicity and photoproducts assessment. *Chemosphere* **2009**, 77, (10), 1292-1298.
10. Bonvin, F.; Omlin, J.; Rutler, R.; Schweizer, W. B.; Alaimo, P. J.; Strathmann, T. J.; McNeill, K.; Kohn, T., Direct photolysis of human metabolites of the antibiotic sulfamethoxazole: evidence for abiotic back-transformation. *Environ Sci Technol* **2013**, 47, (13), 6746-55.
11. Majewsky, M.; Wagner, D.; Delay, M.; Brase, S.; Yargeau, V.; Horn, H., Antibacterial Activity of Sulfamethoxazole Transformation Products (TPs): General Relevance for Sulfonamide TPs Modified at the para Position. *Chem. Res. Toxicol.* **2014**, 27, (10), 1821-1828.
12. Timbrell, J., *Principles of biochemical toxicology*. CRC Press: 1999.

13. Lewis, J. C.; Coelho, P. S.; Arnold, F. H., Enzymatic functionalization of carbon-hydrogen bonds. *Chemical Society Reviews* **2011**, 40, (4), 2003-2021.
14. Deborde, M.; von Gunten, U., Reactions of chlorine with inorganic and organic compounds during water treatment-Kinetics and mechanisms: a critical review. *Water Res* **2008**, 42, (1-2), 13-51.
15. Perisa, M.; Babic, S.; Skoric, I.; Fromel, T.; Knepper, T. P., Photodegradation of sulfonamides and their N (4)-acetylated metabolites in water by simulated sunlight irradiation: kinetics and identification of photoproducts. *Environ Sci Pollut Res* **2013**, 20, (12), 8934-8946.
16. Benjamin, M. M.; Lawler, D. F., *Water quality engineering: physical/chemical treatment processes*. John Wiley & Sons: 2013.